TO

H.E.M.

EFFECT OF SUPERPOSED STRESS SYSTEMS ON THE STRENGTH OF GRIP OF BUILT-UP CRANKSHAFT WEBS

BY

ROBERT MUNRO B.SC. A.R.C.S.T. G.I.Mech.E.

Thesis presented for the degree of Ph.D.

at Glasgow University

February 1958

ACKNOWLEDGEMENTS

The author wishes to express his sincere thanks and appreciation to the following.

PROFESSOR A. S. T. THOMSON, D.Sc., Ph.D., A.R.C.S.T., M.I.C.E.,
M.I.Mech.E.,
Head of the Department of Mechanical, Civil and Chemical Engineering
and PROFESSOR A. W. SCOTT, B.Sc., Ph.D., A.R.C.S.T., M.I.Mech.E.,
M.I.Chem.E.,
Professor of Chemical Engineering,

for generous advice, guidance and constructive criticism throughout the period of this research, which forms a small part of the complete programme planned and carried out under their supervision.

MR. W. FERGUSON, B.Sc., M.I.Mech.E.,
Senior Lecturer and Research Leader,

for his most valued practical guidance and research experience so generously given.

DR. C. M. MOIR, B.Sc., Ph.D., M.I.Struct.E., A.M.I.C.E.,
Principal Lecturer in Structural Engineering,

for his interest and generous advice, especially on the theory of plastic thick cylinders, given at all stages in the research.

MR. B. STEWART and THE WORKSHOP STAFF under his supervision, for their cheerful assistance, co-operation and companionship during the building of the test machine.

MR. I. LE MAY, B.Sc., A.R.C.S.T.,

for kind permission to use the results of several tests obtained while he was a Research Student in the College.

GENERAL INDEX

FIGURE INDEX

TABLES

NOMENCLATURE

The following nomenclature is used in the Thesis:

D	Shaft diameter, occasionally sleeve outside diameter.
R	Shaft radius.
d	Distance from load application point to hub or sleeve face; occasionally shaft diameter.
L	Length of grip.
M	Applied Bending Moment - usually at hub face.
M_a	Axial component of friction moment.
M_f	Total friction moment.
M_p	Perpendicular component of friction moment.
M_R	Radial pressure moment.
M_e	Equivalent moment - combined moment and torque.
T	Applied Torque.
T_e	Equivalent torque - combined torque and moment
P	Pressure (general) or Radial stress.
P_s	Shrinkage pressure between shaft and sleeve or web.
P_c	Contact or Crushing pressure in grip.
F	Force (general).
V	Vertical shear force at hub or sleeve face.
f_s	Fatigue endurance stress.
x	Distance along grip measured from grip centre line
θ	Angular displacement
Δ	Shrinkage allowance.
μ	Coefficient of friction.

1. ABSTRACT

The subject of shrinkage fits as applied to marine crankshafts is briefly introduced and discussed. Particular emphasis throughout is placed on the problem of bellmouthing or opening out of crank webs, under the pulsating loading action of service conditions. There follows the presentation of a theoretical analysis to cover the grip strength of a shrinkage assembly subjected to various forms of loading. A new feature - "friction moment strength" - is suggested and shown to be critical to the onset and failure mechanism of bellmouthing. Small scale practical tests and results to illustrate the theory are recorded and discussed. The theory is further developed to cover fluctuating bending moment loading, and some practical fatigue test series are described and results noted and examined.

The design and building of a hydraulic test machine to supply service type loading on a model crank is described in detail, including the work carried out on a simple test rig to check the principles of operation. One test carried out on the machine is recorded and discussed.

General conclusions and discussions complete the report.

2. INTRODUCTION

The experimental investigation described in this thesis forms part of the work being carried out at present at the Royal Technical College, Glasgow, by the authorisation of the British Shipbuilders' Research Association and planned under their direction.

Earlier work at the College(42)* has been confined chiefly to an investigation of the characteristics and strength of the grip in built-up crankshaft webs where the pins and journals are fitted by shrinking. Although this work has been confined to the static effects of shrink fitting, examination of the bores of used Marine Diesel crankwebs indicated that the dynamic effects of service conditions required investigation. The bores examined gave evidence of bellmouthing, resulting in loss of fit and it was agreed that further work should be carried out to determine the progressive effects of service stresses, and in particular bellmouthing.

It was considered that bellmouthing was the result of the superposition of dynamic stresses on web material, which was already in a plastic condition due to the excessive shrink allowances used in current marine engineering practice, resulting in further flow of metal.

Accordingly, a test machine was designed and built which could apply service stress conditions to a model built-up marine single throw crank. The design and building of the machine took place over a period of some two and a half years. Following the development of experimental technique, the modification of several features and the overcoming of the minor setbacks which seem to be inherent with a new project, not much time remained for the derivation of test results for presentation in this report. The results of one test, however, is given which it is hoped will give useful

---

*Numbers thus refer to alphabetical bibliography at end.

guidance for further research.

During the building of the crank testing machine, additional work by way of a complimentary investigation, was carried out on the strength of grip of simple shrink fitted assemblies, subjected to various static and dynamic force actions. The nature of the problem is discussed and analytical forms derived to deal with each type of imposed loading, i.e. bending, twisting, etc., and a combination of these actions.

Experimental data obtained from a series of static and dynamic small-scale tests showed excellent agreement with the analytical forms and would suggest an explanation of the nature and mechanism of bellmouthing.

The analytical investigation and small-scale tests are presented first, followed by the design and erection of the test machine with details of some of the difficulties encountered. As the second section is largely of a descriptive nature a considerable number of diagrams and photographs have been included since it is considered that they speak much more clearly than many words.

3. DISCUSSION

A well designed, well built crankshaft of lasting quality under the most severe conditions is of fundamental importance to the efficient running of an engine. The precision machining and lining-up of the modern crankshaft bear out the importance that engine builders place in the efficiency of this element. It is true to say, however, that even the best machining and most accurate lining-up cannot overcome intrinsic inefficienc of a bad design or inferior material.

It is of interest to note on tracing the evolution of the Marine Engine Crankshaft that although designs have not altered greatly for many years any forward progress has been of a somewhat empirical nature. Some designs have proved more satisfactory than others, although the reasons are not always clear, and these have remained in use; and so it has gone on. Not that progress of this nature does not finally arrive at the best result but obviously, short of chance, much time and energy can be lost on a project to which sound reasoning and well applied research could supply many a short-cu

Industry today is realising more and more the need for improving basic products and processes by research and development and although economically expensive and of a long-term nature the benefits to be derived are unlimited The British Shipbuilding Research Association, one of the many Industrial Research groups formed in the past few years, among their many projects have authorised and directed research on the Strength of Marine Diesel Built-Up Crankshafts, to be carried out at The Royal Technical College, Glasgow.

A considerable amount of research (35) has been carried out to determin the effects of such variables as fit allowance, surface finish and surface treatment on the grip strength of press and shrink fitted assemblies.

Studies on the problem of a press or shrink grip with a fit allowance such that partial plastic flow of the bore material takes place have resulted in many theories being advanced. These theories are mainly highly mathematical with assumptions which, especially for the shrink fit case, are sometimes open to doubt. In many cases reasonable experimental agreement has been found but it would appear that the complete answer has not yet been found, and investigations are still proceeding.

As this report is primarily concerned with the effect of superposed loading on the existing static stress system set up by shrinking it is not intended to review or discuss this work in any detail. It is recognised however to be of fundamental importance in optimum grip design. Any theories advanced in this study on the effect of superposed actions will be shown not to require detailed knowledge of the static stress conditions. Rather, a reasonable estimate of the interface pressure is needed and existing simple theory gives a satisfactory value for this quantity. Emphasis has been placed on the production of a simple and logical design basis for shrink grips.

It is generally agreed(13) that in the light of present day forging and casting technique the built-up or shrunk crankshaft is a more reliable proposition for Marine engines and the longer the shaft the more is this the case. Records show very little data on the theoretical aspect of built-up crankshaft design, Lloyds Rules being the controlling influence in the choice of scantling proportions and fit allowances. Dorey(13) states that scantlings designed according to Lloyds Rules are based on the maximum principal stress for combined bending and twisting with an allowable working stress of 7,500 lb./in^2. Although the fatigue range is not considered the

sizes are based on the maximum value of the equivalent bending moment during each cycle. Torque values are based on indicator diagrams and bending moments calculated from the expression $B.M. = \frac{WL}{8}$.

It is significant however that engine failure records show that crankshafts based on Lloyds Rules rarely fail and any failures that do occur usually take place after many years of service. Despite this low incidence, however, it is considered highly desirable, in view of the serious consequences, to minimise as much as possible the risk of service failures.

In addition the trend of progress is for greater speeds and power which means that engine designers are traversing uncharted areas with many possible hazards if their work is not based on something more than past experience. The need is for sound knowledge based on experience, research and a complete understanding of the underlying principles.

Dorey(13) maintains that the main factors contributing towards the failure of shafts can be divided into two types:-

(a) Loading in excess of design considerations
    1. Torsional oscillations.
    2. Mal-alignment due to excessive bearing wear.
    3. Axial vibrations.

(b) Material failings
    1. Defective forgings.
    2. Bad shrink fits.

The fact that little is known about the condition for breakdown of a built-up crank web grip makes the assessment of the first type (a) rather difficult since design considerations are indeterminates. It is known, however, that grips do occasionally fail after a period of service which

would suggest either a progressive grip weakening, or an increased loading cycle due to some factor such as (a)2. Bearing wear is known to produce greater bending and vibration stresses which, with failure, would suggest a weakening of the shaft if their possible origin and development were not recognised.

The possibility of progressive weakening of the grip is borne out by the bellmouthing found in the webs of a marine crank dismantled after many years' service.(42) Current marine practice is known to favour shrinkage allowances which produce yield of the web material around the bore. It has been suggested that such bellmouthing is due to the action of high bending moments on a web grip which is in a state of plastic flow due to this excessive shrinkage allowance. Dorey has indicated that in the absence of torsional vibration stresses, bending fatigue stresses constitute the most serious type of loading. The directional effect of the reported bellmouthi also gave further evidence of the apparent deleterious effect of high bending loads on the partially plastic web material.

A shrink fit is normally designed on a torsion strength basis. Slip has been attributed in the past to an excessive torque on a grip which has perhaps been weakened in service by such effects as bellmouthing, oil penetration, fretting, etc. The effect of bending moment or combined bending moment and torque on a grip is a problem which has received scant attention. It will be shown later that bending stresses would appear to constitute an additional load on the friction grip presenting a hazard which has hitherto been unseen or overlooked.

Grip length, too, has considerable bearing on grip strength and this is a factor which must be seriously examined as the need for reduced shaft lengths, arising from increased power requirements, becomes essential.

Dorey(13) has investigated some theoretical aspects of grip length and web thickness round the bore. The section in this report on fatigue was carried out to find an experimental value of grip length/shaft diameter, rat which was as likely to produce fatigue of the shaft material as loosening of the grip. Some interesting results were obtained which again emphasised the importance of friction grip strength when a built-up assembly is subjected to bending.

Fretting corrosion has been mentioned as likely to cause weakening of the grip. This effect is well known as producing a severe shortening of the fatigue life of press and shrink-fitted assemblies and it is not uncommonly found in Marine cranks.(42) Its occurrence was one which was looked for closely in all the dynamic work carried out.

The fatigue aspect of fitted assemblies has been widely covered by many researchers. Some particular features of the problem are discussed later and it is not proposed to examine them any further now.

Bad shrink fits can arise from a variety of causes, not the least of which is the technique adopted when heating. It is known that flame heating at the bore can give rise to temperature gradients which produce thermal stresses in excess of the material yield stress. The advantages of a furnace with its slow and uniform heating are obvious but all shops do not possess such equipment, at least of such capacity to take a crank web. It has been suggested(42) that flame heating from the outside of the web, if flame heating is inevitable, would help to reduce these thermal stresses, although making for a longer time to reach fitting temperature. Shop practice today does not normally exercise any particular care to ensure that the coefficient of friction of the grip is as high as possible. The "shop dry" condition produced by wiping with a cloth cannot achieve the same

gripping effect as a grip specially dried, cleaned and free from film when fitted.

Although surface finish is not, within the limits of normal machine shop practice, critical to friction coefficient it is recognised that a close approach to perfect roundness and parallelism is an essential requirement of a successful grip.(42)

It is perhaps unfair to label a particular shrink fit as "bad" when it fails. The fact that it has been subjected to loads which cause failure is not necessarily a reflection of its poor quality but more likely on the poor quality of the design. Bad workmanship is something which can indeed be corrected but poor design gives inherent weaknesses which only progress can eliminate. Thus it is hoped in the limited scope of this report to shed some light on the voids which exist in present day shrinkage design knowledge. A simplification of theory and an improvement of technique is what is aimed at without reducing, but rather increasing the confidence that all concerned will place on the quality of the built-up assembly.

4. ANALYTICAL INVESTIGATION

4.1 INTRODUCTION

It was reasoned that bellmouthing of crank webs was the result of high bending stresses on a material which, by virtue of shrinkage stresses, was in a plastic state. Accordingly it was considered of some importance that the mechanism of moment transfer from a shaft to a shrunk-on member should be clearly understood, together with the nature of the resultant stress system arising from the combination of shrinkage and bending effects.

It at once became evident from the extent of the published research that the subject has not received much attention and a fundamental approach has, of necessity, been adopted.

Initially the problem was made as simple as possible by considering the effects of a pure bending moment on a simple muff coupling, i.e. two shafts joined by a shrunk-on sleeve with a small gap left between the shaft ends to prevent any abutment (see fig. 1A). This type of assembly can be readily produced as a specimen for experimental work and provides two shrink-fit grip

Later, in the light of the initial experimental results, it was found expedient to consider the effects of shear and twisting combined with bending on the grip strength.

It may be argued that at times in the theoretical approach some effects have been over-simplified. Mention is made where simplification has taken place with the possible subsequent errors involved. In general, the derivation of readily applicable design expressions was the ultimate aim of the investigation.

4.2 DERIVATION OF EXPRESSION FOR THE TRANSFER OF A MOMENT FROM A SHAFT TO A SLEEVE

When a moment is applied to a component assembly of shaft and sleeve as shown in fig. 1A it is obvious that the moment transfer from shaft to sleeve must take place at the grip surface. It is proposed to show that this moment transfer is achieved by two means, for convenience termed: Radial Pressure Distribution Effect and Friction Effect.

4.3 RADIAL PRESSURE DISTRIBUTION

The following theory has been derived to give the same result as expressed in A.S.M.E. Handbook of Metals Engineering Design (PAGE 181) on the subject of the holding ability of a press or shrink fit in transverse loading. Details of the derivation of formulae were not given although reference was made to the work of Wood[(45)] on the crushing stress in crankpi fits. This paper was unfortunately not readily available, hence although a similar result is obtained the assumptions may be somewhat different.

It is assumed that when a moment is transferred from a shaft to a shrunk-on sleeve the transfer is obtained by a redistribution of radial pressure, i.e. the pressure distribution on the grip surface produced by the moment can be summed algebraically with the shrink fit radial pressure. The shaft within the grip is assumed to behave as a rigid member giving the type of pressure distribution as shown in figs. 1A and 1B . In actual fact the shaft deforms inside the grip and affects the pressure distribution to an increasing extent as ratio of the length of grip to the shaft diameter increases. However, for lengths of grip which are not much greater than th shaft diameter the assumption can be taken as being accurate enough.

The general case of an applied bending moment and vertical shear force at the sleeve face is considered, the effects being treated separately but

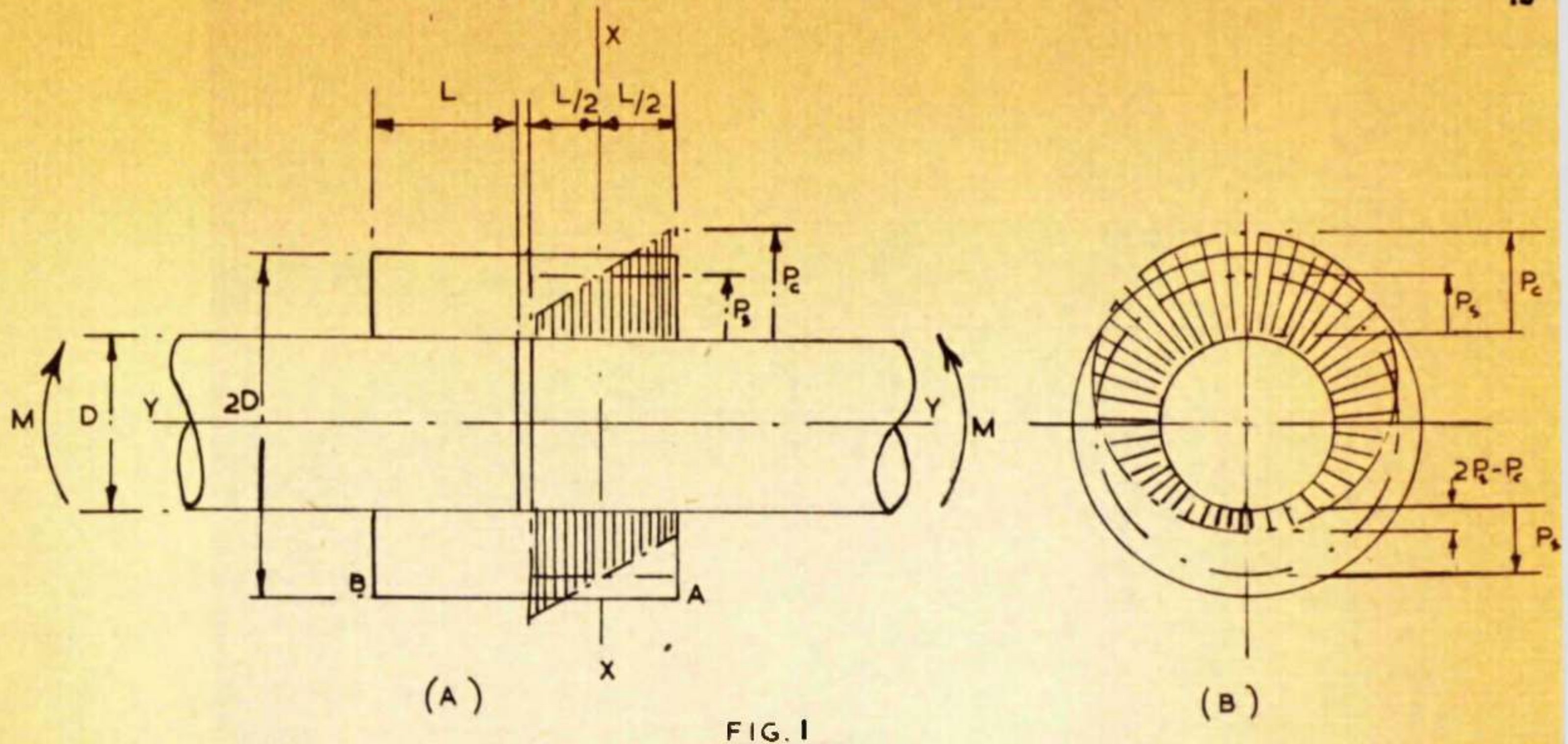

FIG. 1

MOMENT TRANSFER THEORY

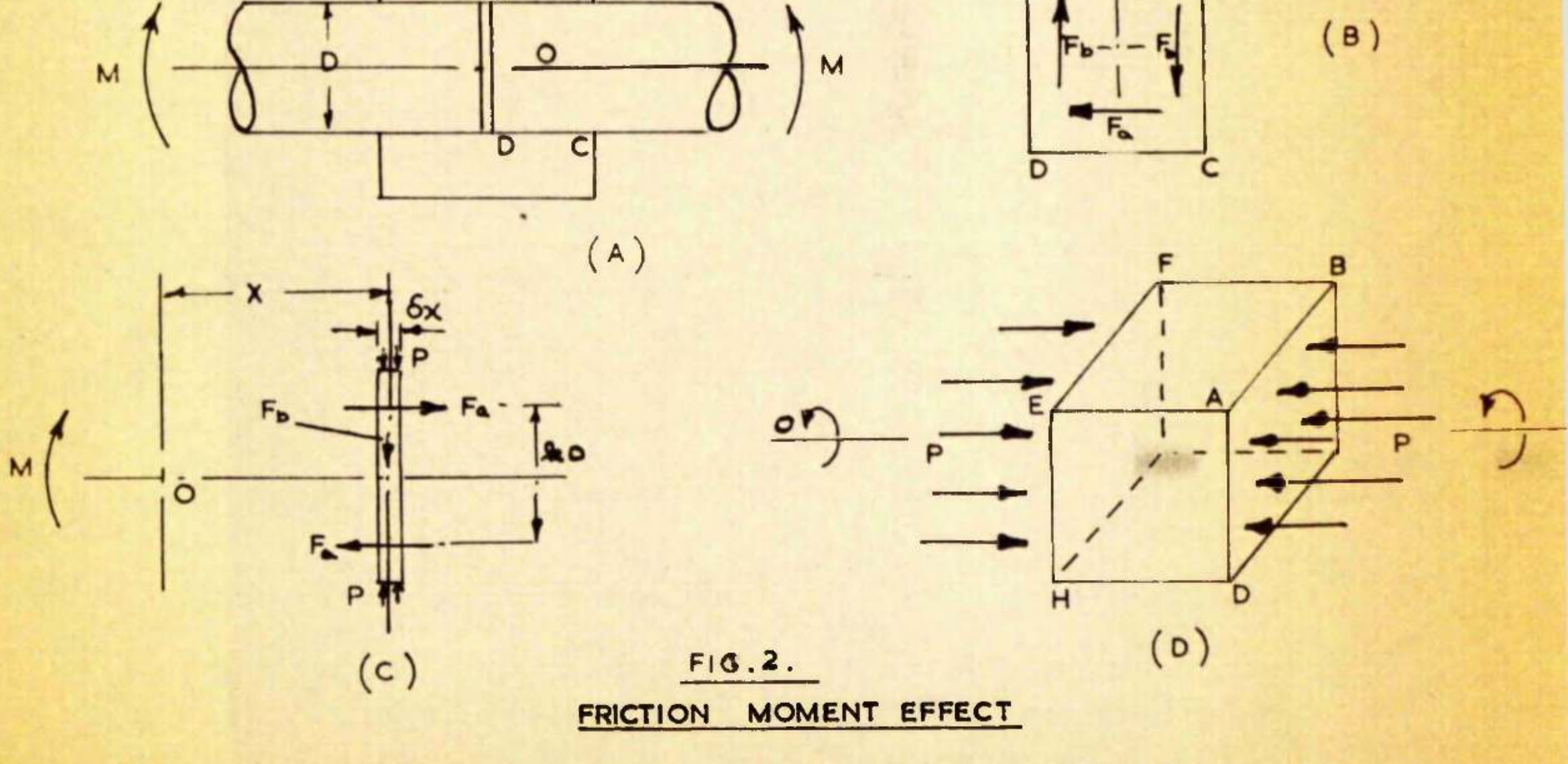

FIG. 2.

FRICTION MOMENT EFFECT

combined later.

Referring to fig. 1 the following nomenclature is used:-

M = Applied Bending Moment.

V = Vertical shearing force at hub face AA, and is such that as the face AA is approached from the shaft side, M is increasing.

P_c = Maximum crushing or contact pressure between shaft and sleeve.

P_s = Shrink-fit pressure.

L = Length of sleeve grip on each end of shaft.

D = Diameter of shaft.

4.3(a) BENDING MOMENT (M) EFFECT

It is assumed that the bending moment M is transferred to the sleeve by a redistribution of the shrink pressure P_s giving a maximum value P_c with a variation over the length ± L/2 given by:

$$P_x = P_s + (P_c - P_s)\frac{x}{L/2}$$

$$= P_s + (P_c - P_s)\frac{2x}{L}$$

Assume the pressure P_c takes up the form given in fig. 1B, i.e. a cosine distribution round the shaft.

$$P_{x,\theta} = P_s + (P_c - P_s)\frac{2x}{L}\cos\theta$$

Consider an elementary strip δx of the shaft:

F_x Nett vertical force on the strip is given by:-

$$\int_0^{2\pi} P_{x\theta}\, R\cos\theta\, dx\, d\theta$$

$$F_x = \int_0^{2\pi}\left[P_s + (P_c - P_s)\frac{2x}{L}\cos\theta\right]R\cos\theta\, dx\, d\theta$$

$$= R\,dx\int_0^{2\pi}\left[P_s\cos\theta\, d\theta + (P_c - P_s)\frac{2x}{L}\cos^2\theta\right]d\theta$$

Since $\int_0^{2\pi} P_s \cos\theta \, d\theta = 0$

$$F_x = R\,dx\,(P_c - P_s)\frac{2x}{L}\int_0^{2\pi}\cos^2\theta\,d\theta$$

$$= \frac{2Rx}{L}\,dx\,(P_c - P_s)\left[\theta/2 + \frac{\sin 2\theta}{4}\right]_0^{2\pi}$$

$$= \frac{2\pi R x}{L}\,(P_c - P_s)\,dx$$

(M_R) MOMENT produced by force F_x over length L given by

$$M_R = \int_{-L/2}^{+L/2} F_x x$$

$$\text{i.e. } M_R = \frac{2\pi R}{L}(P_c - P_s)\int_{-L/2}^{+L/2} x^2\,dx$$

$$= \frac{2\pi R}{L}(P_c - P_s)\left[x^3/3\right]_{-L/2}^{+L/2}$$

$$= \frac{\pi D L^2}{12}(P_c - P_s) \qquad \ldots\ldots (1)$$

From (1)

$$P_c = \frac{12 M_R}{\pi D L^2} + P_s \qquad \ldots\ldots (2)$$

4.3(b) <u>VERTICAL SHEAR (V) EFFECT</u>

Vertical shear force V at hub face will produce a direct and a moment effect on the pressure distribution.

(1) **Direct Effect** (P_V)

Assume once again a cosine distribution round the shaft

Nett force on strip δx given by

$$F_x = V \times \frac{\delta x}{L}$$

As before

$$P_{x,\theta} = P_s + (P_V - P_s)\cos\theta$$

Nett force on strip δx :-

$$F_x = \int_0^{2\pi} P_{x,\theta}\, R\,dx\cos\theta\,d\theta$$

[illegible]

[illegible]

[illegible] (9) [illegible]

[illegible]

As before gives $F_x = \pi R (P_V - P_S)\,\delta x$

Hence $$V \times \frac{\delta x}{L} = \pi R (P_V - P_S)\,\delta x$$

or $$P_V - P_S = {}^{2V}/_{\pi D L}$$

$$P_V = P_S + {}^{2V}/_{\pi D L} \qquad \text{.... (3)}$$

(2) Bending Effect (P_M) due to V

Moment due to V $= V \times {}^{L}/_{2}$

Hence as before from (1)

$$P_M = P_S + \frac{12\,VL/2}{\pi D L^2}$$

$$= P_S + {}^{6V}/_{\pi D L} \qquad \text{.... (4)}$$

4.3(c) COMBINED EFFECT

The combined effect of equations (2), (3) and (4) gives P for the resultant radial pressure at hub face

$$\underset{\text{(at hub face AA)}}{P} = P_S + {}^{12M}/_{\pi D L^2} + {}^{2V}/_{\pi D L} + {}^{6V}/_{\pi D L}$$

$$= P_S + {}^{4}/_{\pi D L^2}\left[3M + 2VL\right] \qquad \text{.... (5)}$$

$$\underset{\text{(at shaft end)}}{P} = P_S + {}^{12M}/_{\pi D L^2} - {}^{2V}/_{\pi D L} + {}^{6V}/_{\pi D L}$$

$$= P_S + {}^{4}/_{\pi D L^2}\left[3M + VL\right] \qquad \text{.... (6)}$$

This is a similar result to that shown in A.S.M.E. Handbook, page 181, for press fitted assemblies.

The above type of expression arising from a redistribution of radial pressure, according to all published work that could be found on the subject,

is regarded as fully covering the problem of moment and vertical shear transfer. However, another moment transfer effect is now suggested arising from the friction grip between shaft and sleeve.

4.4 FRICTION MOMENT

When a bending moment is applied to a shaft and sleeve they tend to strain together because of the friction force which exists at the grip. This introduces a shear stress along the grip. The exact nature and development of this stress is not clear but it is evident that should such a friction moment transfer exist there will be a limiting value. Beyond this limiting value of bending moment slip will take place and no further moment can be transferred by the friction grip.

An alternative way of looking at the problem is to consider the section of the shaft A B C D gripped in the sleeve (fig. 2.) to rotate about its centre O, when a bending moment is applied. This is a similar assumption to that made when considering the pressure distribution moment in 4.3 where the gripped length of shaft was considered to act as a rigid member. Consider any point on the shaft such as A. As the section ABCD rotates A has two component movements, axially and at right angles to the axial direction. It is suggested that it is this latter movement component which produces the radial pressure distribution effect 4.3 while the axial movement component is resisted by the friction grip. This does not give a completely true picture of the friction moment since it will be shown later that there is also a friction force resisting the other component movement, but serves to illustrate to some degree the possible existence of such a friction moment action.

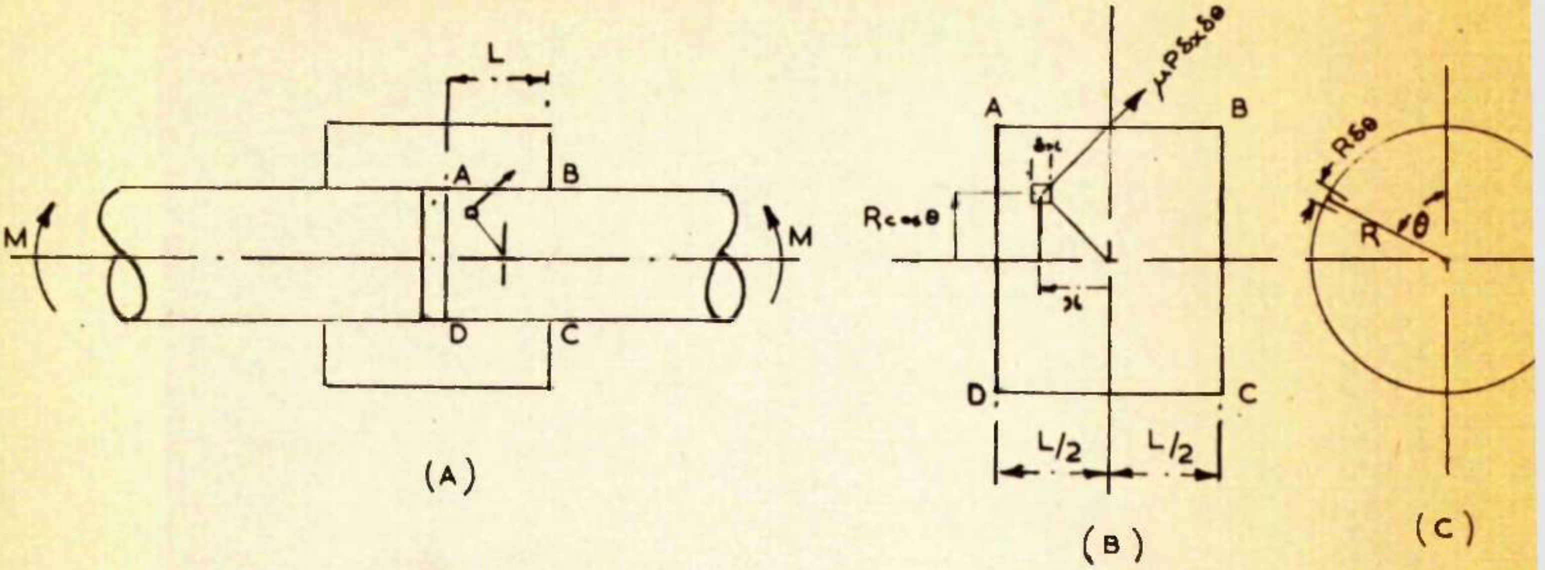

(A) (B) (C)

FIG. 3.

FRICTION MOMENT EFFECT ~ STRINGENT TREATMENT

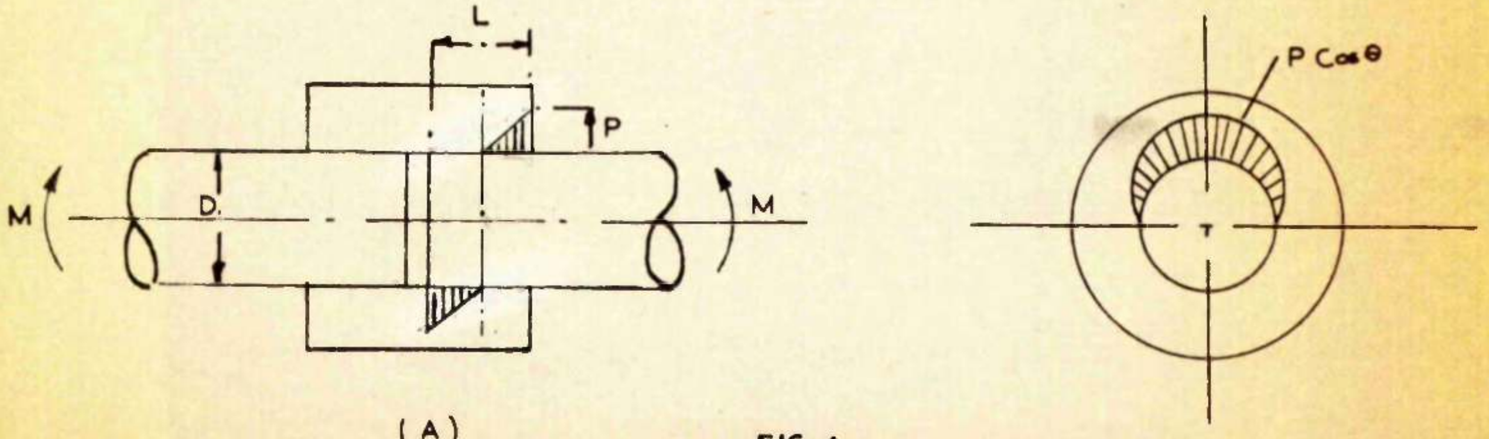

(A) (B)

FIG. 4

MOMENT TRANSFER ~ NO-FIT CASE

Since the component movements are interdependant it is realised that should the resistance to one component movement be much greater than the other the tendency will be for the forces involved in the greater resistance to carry most of the applied moment.

By considering the strength of a sleeve in resisting forces applied in various directions it is seen that the friction forces could readily carry most of the applied moment till slip occurs. It will be shown later that the test results would appear to confirm this observation.

An original derivation for the friction moment follows with further explanation of the principles involved.

4.4(a) Before considering the case of the shaft and sleeve it is perhaps of advantage to consider the case of a square block with a pressure P on two opposite faces ABCD and EFGH. If the block is rotated about the axis OO a friction force resists the movement. This friction moment can be divided into two components, one produced by the axial component of force F_a and the other by the component of force F_b at right angles to F_a.

4.4(b) Now consider a shaft and sleeve as shown in fig.2C.

Taking an elementary strip δx at distance x from the centre O about which the section ABCD tends to rotate due to moment M_1 see fig.2.

The moment of the friction force on element δx can be divided into two components due to forces at right angles.

(1) Due to axial component, moment = $F_a \times KR$

(2) Due to perpendicular component,

$$\text{moment} = F_b \times x$$

These two components will be considered separately.

(1) Axial

Consider as before a strip δx.

As previously

$$P(x,\theta) = P_s + (P_c - P_s)\frac{2x}{L}\cos\theta$$

At slip, moment of friction force on top half of ring is:

$$\underset{(\frac{1}{2}\text{ RING})}{M(a,\delta x)} = \int_{-\pi/2}^{+\pi/2} P(x,\theta)\,\mu\,R\,\delta x\,R\cos\theta\,d\theta$$

$$= R^2\mu\,\delta x\int_{-\pi/2}^{+\pi/2}\left[P_s + (P_c - P_s)\frac{2x}{L}\cos\theta\right]\cos\theta\,d\theta$$

$$= R^2\mu\,\delta x\left[\int_{-\pi/2}^{\pi/2} P_s\cos\theta\,d\theta + (P_c - P_s)\frac{2x}{L}\int_{-\pi/2}^{\pi/2}\cos^2\theta\,d\theta\right]$$

$$= R^2\mu\,\delta x\left\{P_s(\sin\theta)_{-\pi/2}^{\pi/2} + (P_c - P_s)\frac{2x}{L}\left[\tfrac{1}{2}\left(\theta + \frac{\sin 2\theta}{2}\right)\right]_{-\pi/2}^{+\pi/2}\right\}$$

$$= R^2\mu\,\delta x\left[2P_s + (P_c - P_s)\pi\frac{x}{L}\right]$$

Over length L i.e. $\pm L/2$ half moment is given by:

$$\tfrac{1}{2}M_a = \int_{-L/2}^{+L/2} R^2\mu\,\delta x\left[2P_s + (P_c - P_s)\pi x/L\right]dx$$

$$= 2R^2\mu P_s L + \mu R^2/L\,\pi(P_c - P_s)\left[x^2/2\right]_{-L/2}^{+L/2}$$

$$= 2R^2P_sL\mu + 0$$

$$= 2R^2P_sL\mu$$

Total moment (both halves)

$$M_a = 2 \times 2R^2P_sL\mu$$

$$= D^2P_sL\mu \qquad \ldots\ldots (7)$$

(2) Perpendicular Component (M_p)

Consider strip δx as before.

$$P(x,\theta) = P_s + (P_c - P_s)2x/L\cos\theta$$

Nett side force on $\delta x = \int_0^{\pi} P_{(x\theta)} \sin\theta \, R \, d\theta = F_{(\delta x)}$

$$F_{(\delta x)} = R\,\delta x \int_0^{\pi} \left(P_s + [P_c - P_s] \tfrac{2x}{L} \cos\theta \right) \sin\theta \, d\theta$$

$$= R\,\delta x \left[P_s(-\cos\theta) \right]_0^{\pi} + R\left[P_c - P_s\right] {}^{x}/_{L} \left[-\cos 2\theta \right]_0^{\pi} \delta x$$

$$= \left[2RP_s + 0 \right] \delta x$$

$$= P_s D \,\delta x$$

Friction force $= F_{(\delta x)} \mu$

$$= P_s D \mu \,\delta x$$

Moment for one side of length L:

$$= \int_{-L/2}^{+L/2} P_s D \mu x \,\delta x$$

$$= \frac{P_s D \mu L^2}{4}$$

TOTAL MOMENT (M_p) $= 2 \times \frac{P_s D \mu L^2}{4}$

$$= \frac{P_s D \mu L^2}{2} \qquad \text{.... (8)}$$

Total friction moment from equations (7) and (8)

$$M_f = M_a + M_p$$

$$= D^2 P_s L \mu + \frac{P_s D L^2}{2} \mu$$

$$= D P_s L \mu \left(D + L/2 \right) \qquad \text{.... (9)}$$

It is realised that the expression (9) is not strictly correct since the two component moment actions (7) and (8) have not been summed as vectors. Accordingly, a more stringent solution of the problem is presented (4.6).

It will be seen that this solution requires more extensive calculation and for all practical design purposes the expression (9) is quite accurate and much more convenient to use.

4.5 COMBINED RADIAL PRESSURE AND FRICTION EFFECTS

Combining the two moments from Articles 4.3 and 4.4 for the Total Moment on the sleeve:

Total Moment = Radial Pressure Moment + Friction Moment

$$M = M_R + M_f$$

$$= \frac{\pi D L^2}{12}(P_L - P_s) + P_s D \mu L (D + L/2) \qquad \ldots\ldots (10)$$

[illegible]

[illegible]

[illegible]

[illegible]

[illegible]

[illegible]

[illegible]

[illegible] ....

4.6 STRENGTH OF GRIP DUE TO FRICTION FORCES OF A FITTED SHAFT MEMBER SUBJECTED TO A MOMENT ACTION - STRINGENT TREATMENT

Referring to fig.3 consider the elemental area $\delta x\, R\, \delta\theta$ which is on the mating surface of shaft and sleeve and subjected to the uniform pressure P due to the shrink fit.

If it is accepted that for small lengths of grip L (small being defined as not greater than $L/D = 1$) the shaft section ABCD tends to rotate about centre O and that there is a limiting value of moment when the mating surfaces well slip, an expression can be derived for this limit condition.

Friction force on element

$$= P\mu R\,\delta\theta\,\delta x$$

Moment arm

$$= \sqrt{x^2 + R^2\cos^2\theta}$$

Friction moment for element

$$= P\mu R\sqrt{x^2 + R^2\cos^2\theta}\quad \delta\theta\,\delta x$$

For complete section ABCD

$$\text{Friction Moment} = \int_0^{L/2}\int_0^{\pi/2} P\mu R\sqrt{x^2+R^2\cos^2\theta}\; d\theta\, dx \times \overset{\text{(SIDES)}}{2} \times \overset{\text{(QUADRANTS)}}{4}$$

$$= 8P\mu R\int_0^{L/2}\int_0^{\pi/2}\sqrt{x^2+R^2\cos^2\theta}\; d\theta\, dx \qquad \ldots\ldots (11)$$

This can be written

$$8P\mu R\int_0^{L/2}\int_0^{\pi/2}\sqrt{x^2+R^2[1-\sin^2\theta]}\; d\theta\, dx$$

$$= 8P\mu R\int_0^{L/2}\int_0^{\pi/2}\sqrt{x^2+R^2}\;\sqrt{\left(1-\frac{R^2}{x^2+R^2}\sin^2\theta\right)}\; d\theta\, dx$$

$$= 8P\mu R\int_0^{L/2}\int_0^{\pi/2}\sqrt{x^2+R^2}\;\sqrt{(1-k^2\sin^2\theta}\; d\theta\, dx$$

$$\text{WHERE } k^2 = R^2/x^2+R^2$$

since $\frac{R^2}{x^2+R^2}$ is always less than 1.

This can be written:

$$8P_{\mu}R\int_{0}^{L/2}\int_{0}^{\pi/2}\sqrt{x^2+R^2}\sqrt{1-\sin^2\phi\sin^2\theta}\;d\theta\,dx \qquad \ldots\ldots (12)$$

$$\sin\phi = k.$$

The elliptic integral

$$\int_{0}^{\pi/2}\sqrt{1-\sin^2\phi\sin^2\theta}\;d\theta$$

can be solved for various values of ϕ i.e.

$$\int_{0}^{\pi/2}\sqrt{1-\sin^2\phi\sin^2\theta}\;d\theta$$

can be expressed as a function of x i.e. $f(x)$

The integral $8P_{\mu}R\int_{0}^{L/2}\sqrt{x^2+R^2}\;f(x)\,dx$

is solved by tabulation of various values for increments in $x = 0$ to $x = L/2$ and integration by Simpson's Rule.

Tables of values for $\int_{0}^{\pi/2}\sqrt{1-\sin^2\phi\sin^2\theta}\;d\theta$ are available(15) and the Friction Moment may be evaluated for particular values of L and D.

The Friction Moment equation as derived in both art. 4.4 and 4.6 can be expressed thus:-

F.M. = E x P_{μ} where E is some constant depending on L and D.

Assuming values for L and D, E can be evaluated from the expressions (8) and (12) and the values compared.

Table I gives E values for three lengths of L, D being constant and equal to $1\frac{1}{2}$".

TABLE I

L	$E = DL[D+L/2]$ .. ART 4.4	E .. ART 4.6	% DIFFERENCE
0·5	1·31	1·19	9
0·665	1·83	1·65	9½
1·0	3·0	2·68	10

The percentage difference for the range of grip lengths in the test series which exhibit slip (i.e. Friction Moment effects) is not greater than 10%. It is considered that for most design purposes the expression (8) is adequate and much more readily applied. It will be proposed later that (8) does in fact give a more reliable value of Friction Moment.

4.7 THEORY FOR NO-FIT SLEEVE-SHAFT ASSEMBLY

The special case, where there is no fit allowance for the assembly and the sleeve is just a slight push fit on the shaft, will now be considered.

Since there is no shrink pressure P_s, the contact stress distribution on the application of a bending moment will be similar to that shown in fig. 4. A cosine distribution of pressure round the shaft and a linear variation over the grip length is assumed. A similar analysis to the shrinkage case is made.

(a) Friction Effect

(1) Axial Component

Similarly to art. 4.4(b)1 -

$$M_a = \int_{-L/2}^{+L/2}\int_{-\pi/2}^{+\pi/2} \mu R\cos\theta \, R \, P_{(x,\theta)} \, d\theta \, dx$$

In this case $P_{(x,\theta)} = P_x \cos\theta$

Hence:

$$M_a = \int_{-L/2}^{+L/2}\int_{-\pi/2}^{+\pi/2} \mu R^2 \cos^2\theta \, P_x \, d\theta \, dx$$

$$= \int_{-L/2}^{+L/2} \frac{P_x \mu R^2 \pi}{2} dx$$

Also in this case $P_x = P_c \frac{x}{L/2} = 2P_c \frac{x}{L}$

Then:

$$M_a = \int_{-L/2}^{+L/2} \frac{2P_c \mu R^2 \pi}{2} \frac{x}{L} dx$$

$$= \frac{P_c \mu R^2 \pi L}{4} \qquad \text{......} \; (13)$$

(2) Perpendicular Component

Similarly as for art. 4.4(b)2 -

Side thrust on elemental strip

$$F_{(\delta x)} = \int_0^{\pi/2} P_x \cos\theta \sin\theta \, R \, d\theta \, \delta x$$

$$\text{i.e. } P_{(x,\theta)} = P_x \cos\theta$$

Hence:

$$F_{(\delta x)} = \frac{R P_x}{2} \delta x$$

Friction moment due to $F_{(\delta x)}$ on strip δx

$$M_{P(\delta x)} = \frac{R P_x}{2} \delta x \times \mu \times x$$

Hence Moment/side = $\frac{1}{2}M_P = \int_{-L/2}^{+L/2} \mu \frac{R P_x}{2} x \, \delta x$

$$P_x = 2 P_c \, x/L$$

Thus $\frac{1}{2}M_P = \int_{-L/2}^{+L/2} \mu R P_c \frac{x^2}{L} \, dx$

$$= \frac{P_c R L^2}{12} \mu$$

Then $M_P = \dfrac{P_c R L^2}{6} \mu$ ...... (14

The Combined Friction Moment

$$= M_a + M_P$$

$$= \mu \frac{P_c R L}{12} \left[3\pi R + 2L \right]$$

$$= \mu \frac{P_c D L}{24} \left[\frac{3\pi D}{2} + 2L \right]$$ ...... (15

(b) <u>Radial Pressure Distribution Moment</u>

The Radial Pressure Moment can be derived in a similar manner to equation (1), art. 4.3. In this case there is no shrinkage pressure

$$M_R = \int_{-L/2}^{+L/2} \int_{-\pi/2}^{+\pi/2} R P_x \cos\theta \cos\theta\, x\, d\theta\, dx$$

$$= \int_{-L/2}^{+L/2} \int_{-\pi/2}^{+\pi/2} R P_c \frac{x^2}{L} \cos^2\theta\, d\theta\, dx$$

$$= \frac{\pi D L^2}{24} P_c \qquad \ldots\ldots (16)$$

(c) <u>Combined Effect</u>

The complete expression for the no-fit moment strength is:

$$M = \frac{\pi D L^2}{24} P_c + \mu \frac{P_c D L}{24} \left(\frac{3\pi D}{2} + 2L \right)$$

$$= \frac{P_c D L}{24} \left[\pi L + \mu \left(\frac{3\pi D}{2} + 2L \right) \right] \qquad \ldots\ldots (17)$$

It is assumed in this case that slip takes place continuously as the load is applied, i.e. the friction moment does not predominate. Hence there is no point where a break in the curve will occur due to breakdown of the friction grip. However, this expression will give a value for the contact pressure at which yield of the assembly occurs if some arbitrary value of μ is chosen and the value of M is taken from an actual test.

4.8 BENDING AND SHEAR EFFECTS

Although the effect of combined bending and shear force on a shrinkage grip was considered in art. 4.3(b), the shear force effect was not included when deriving any subsequent expression which involved friction moment considerations (Arts. 4.4 to 4.7).

It was shown (art. 4.3(b)) that the net pressure (P_v) on a grip due to shrinkage stresses (Ps) and vertical shear force V, without considering bending, is given by:

$$Pv = Ps \pm \frac{2V}{DL} \qquad \ldots\ldots (3)$$

the sign denotes the side of grip.

The bending moment on the grip due to V is $VL/2$.

Hence, with a moment M and a shear force V, equation 10 becomes:

$$M + VL/2 = \pi \frac{DL^2}{12} (Pc - Ps) + PsD\mu L \, (D + L/2) \qquad \ldots\ldots (18)$$

Pc, the contact stress calculated from this expression, is modified by $\pm 2V/DL$ due to the direct load effect of V.

4.9 BENDING, SHEAR AND TWISTING

The normal design criterion of a shrinkage grip is usually taken as its ability to withstand torsion. The design expression is:

$$T = \frac{P_s \mu D^2 L}{2} \qquad \text{......} \; (19)$$

It has been shown, however, that the bending moment strength of a grip is also dependent on the frictional grip. It would appear reasonable that the combined effect of bending and twisting would have the result of reducing the component strengths of the grip. The grip strength is taken as its ability to withstand bending or torsion without slipping.

Ideally, the component forces due to combined bending and twisting on the grip should be summed vectorily to obtain a true value for the grip strength. The mathematics of this problem are considerable and, combined with the lack of any real knowledge of the force actions arising under torsion, it is proposed to substitute the following approximation.

The component actions M and T are summed in the form:

$$Q = \sqrt{M^2 + T^2} \qquad \text{......} \; (20)$$

When designing a grip, should the value of T predominate, the suggested best form for no slip is:

$$Q = \sqrt{M^2 + T^2} = \frac{P_s \mu D^2 L}{2} \qquad \text{......} \; (21)$$

When M predominates the suggested form is:

$$Q = \sqrt{M^2 + T^2} = P_s \mu D L (D + L/2) \qquad \text{......} \; (22)$$

For normal crankshaft proportions there is no significant difference in the above two forms and it is not considered important which is used despite the predominance of bending or torsion. The important point is that the component actions must be summed as in equation (20).

[illegible]

[illegible]

...... [illegible]

[illegible]

[illegible]

[illegible]

...... [illegible]

[illegible]

...... [illegible]

[illegible]

...... [illegible]

[illegible]

4.10 FRICTION MOMENT - Photoelastic Study Note.

It is perhaps of interest at this stage, following the derivation of expressions involving such a feature as a Friction Moment, to examine some previous research and, in particular, to quote an extract from a photoelastic study(31). This study was on a somewhat similar set-up for which the preceding theory was derived. A photo-elastic comparison was made on a one-piece and a three-piece built-up shaft and sleeve assembly subjected to bending.

The following was observed:

> "When the bending moment was also applied, marked differences occurred in the fringe patterns. The one-piece model showed pronounced stress concentrations at upper and lower corners but these were absent or very much diminished on the tension side of the axle in the three-piece model.
>
> Further experiments involving a loading and an unloading cycle showed marked frictional effects which could not have occurred unless slip had taken place between the press fitted surfaces. This was to be expected, as the sharp corner would be a point of extreme stress concentration in the one-piece model, whereas in the three-piece model the upper limit of the shear stress between the press fitted members is that corresponding to the frictional grip; once this limit is reached further loading must cause slip."

Although the model tested in this study is not the same as present case of two shafts joined by a sleeve, it is significant that the frictional effects were observed and that the author believed that a condition of slip would be reached.

5. SMALL SCALE STATIC TESTS - EXPERIMENTAL

Most of the small scale tests carried out were designed to produce results for comparison with the theoretical analysis. The tests cover a range of specimen and type of loading and are sub-divided into various series.

5.1 SERIES A - Static Bend Tests - Pure Bending.

This first general series of tests was carried out on assemblies consisting of two shaft lengths joined by a shrink-fitted sleeve or muff coupling (see fig. 5).

The tests covered a range of sleeve lengths and shrink-fit allowances with a constant shaft to sleeve diameter ratio of 2.

Three arbitrary sleeve length/shaft diameter (L/D) ratios were chosen giving Series IA L/D = .45, Series IIA L/D = .71, and Series IIIA L/D = 1.1. Since Lloyd's Rules for a built-up marine crankshaft give an L/D ratio of approximately .625, this range would appear suitable for comparison.

In each Series three fit allowances were employed with a split shaft assembly:

(1) .001 in/in diam. giving a fully elastic grip.

(2) .002 in/in diam. giving a partially plastic grip.

(3) .004 in/in diam. giving a more plastic grip.

Also for each Series a specimen was prepared with a fit allowance of .002 in/in diam. and a straight through shaft, i.e. the sleeve did not join two shafts, but was shrunk on to one solid length.

In Series IA and IIA a test was carried out with an assembly which had no fit allowance. In this case the two shaft lengths were joined by a sleeve which was a very light push fit on the shaft ends giving specimens

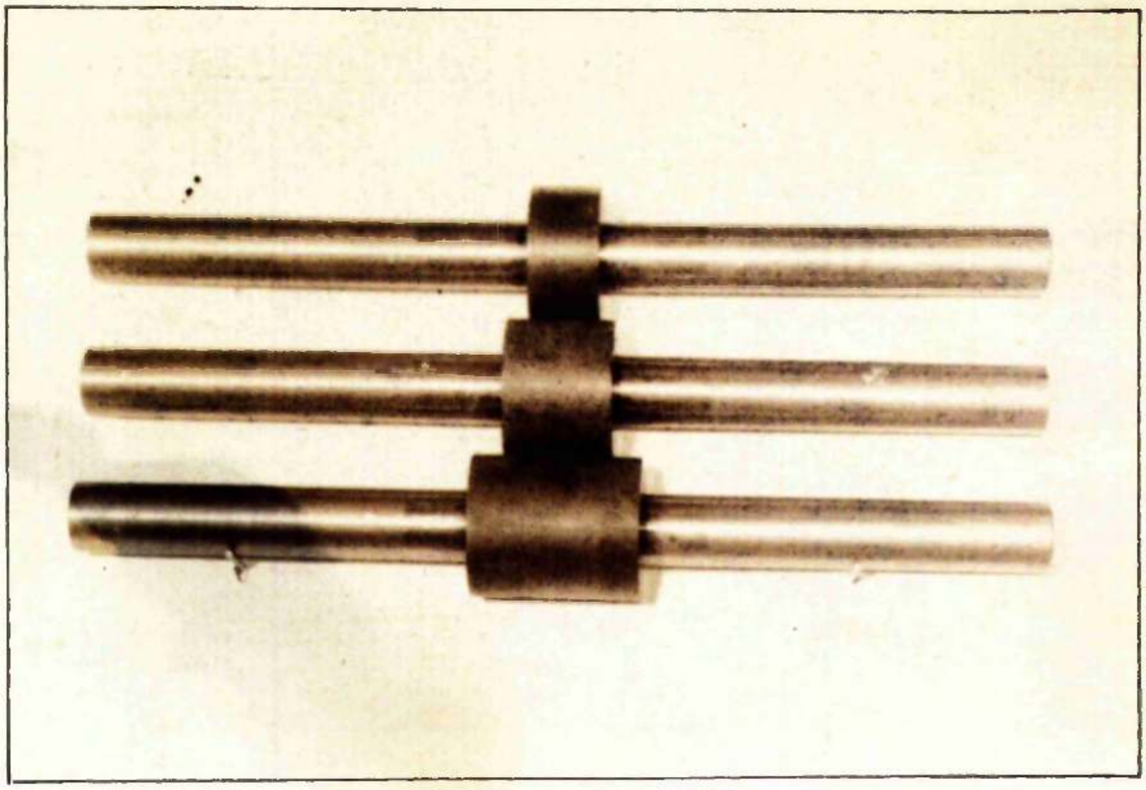

FIG. 5.
STATIC BEND TEST SPECIMENS
SERIES 'A'

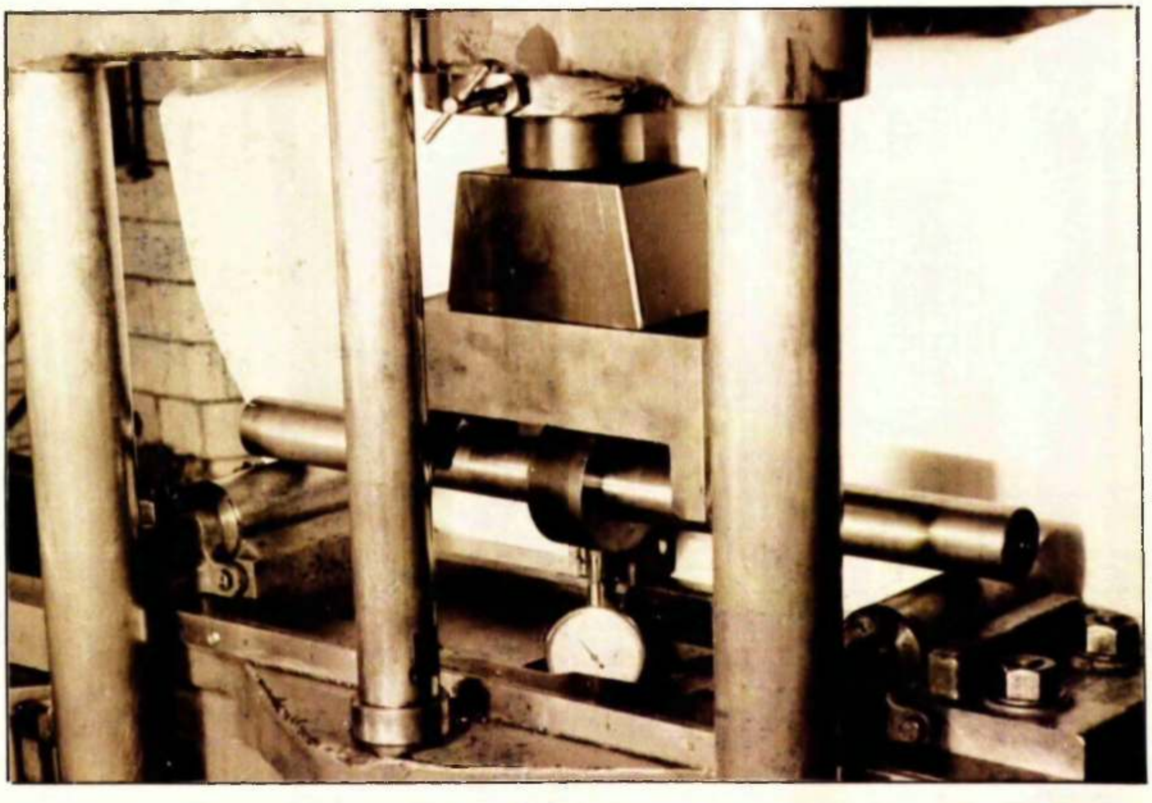

FIG. 6.
STATIC BEND TEST ARRANGEMENT
SERIES A & C

which could be used to check the No-fit Theory of art. 4.7. For purposes of comparison a solid shaft with no sleeve was also prepared and tested.

Details of the shaft and sleeve material were obtained by preparing and testing a standard tensile specimen.

5.2 BEND SPECIMEN PREPARATION

For the split shaft tests a specimen consisted of two 10 inch lengths of 1½ inch diameter mild steel joined by means of a shrunk-on mild steel sleeve with a 1/8 inch gap left between the shaft ends. The sleeve bores were drilled, bored and finish honed to ±.0001 inch size and parallelism. The shaft was prepared in a 20 inch length. The length was turned between centres to size with a grinding allowance left on the central 5 inch section on which the sleeve would be shrunk. This section was then ground between centres to ±.0001 inch size and parallelism and parted off into two equal lengths.

The ends of the sleeves were initially not specially prepared but latterly, arising from the chance appearance of Lüders lines, they were groun and lapped to give a smooth matt finish.

When shrinking the sleeves were placed in an electric furnace at 500°C for one hour. The two lengths of shaft were fitted with adjustable collars at such a distance from the shaft ends that a gap remained between them when they were in the sleeve.

The .004 in/in diam. fit series required a shrinking temperature of 600°C. Just prior to shrinking the shaft ends were wiped with a cloth soaked in Sperm oil to give a lubricated fit.

The solid shaft specimens were prepared in a similar fashion except that the shaft did not require parting off into two pieces.

The no-fit specimens were assembled by pushing the shaft ends into the sleeve to the required measured depth. A check on the grip length was made again when the specimen was in the machine ready for testing in case the shaft ends had moved in handling.

5.3 TEST PROCEDURE

All tests were carried out on an Avery 30 ton Testing machine. The loading arrangement is shown in fig. 6. The shaft was placed on an 18 inch span as for a normal transverse bend test and load was applied through a solid, shaped block bridging the central sleeve section. This arrangement gives a pure bending moment over the grip length.

The central deflection was measured by means of a Mercier clock gauge with a travel of ½ inch and .001 inch scale divisions.

Loading increments of .1 ton were applied to the specimen until a condition of yield was reached. The straining rate was kept low and approximately the same for all tests.

In latter tests of Series IA, IIA and IIIA the sleeve forces were kept under constant observation during test for the appearance and progress of Lüders lines (see fig.20).

5.4 SERIES B - Static Bend Tests - Loading Direction Varied.

This short series was conducted to determine the effect of varying the direction of the applied pure bending moment on similar specimens to the previous series.

The three split-shaft type assemblies tested had fit allowances of .001 .002 and .004 in/in diameter with a constant sleeve length/shaft diameter ratio of 0.71 and sleeve/shaft diameter ratio of 2 : 1.

TEST SPECIMENS

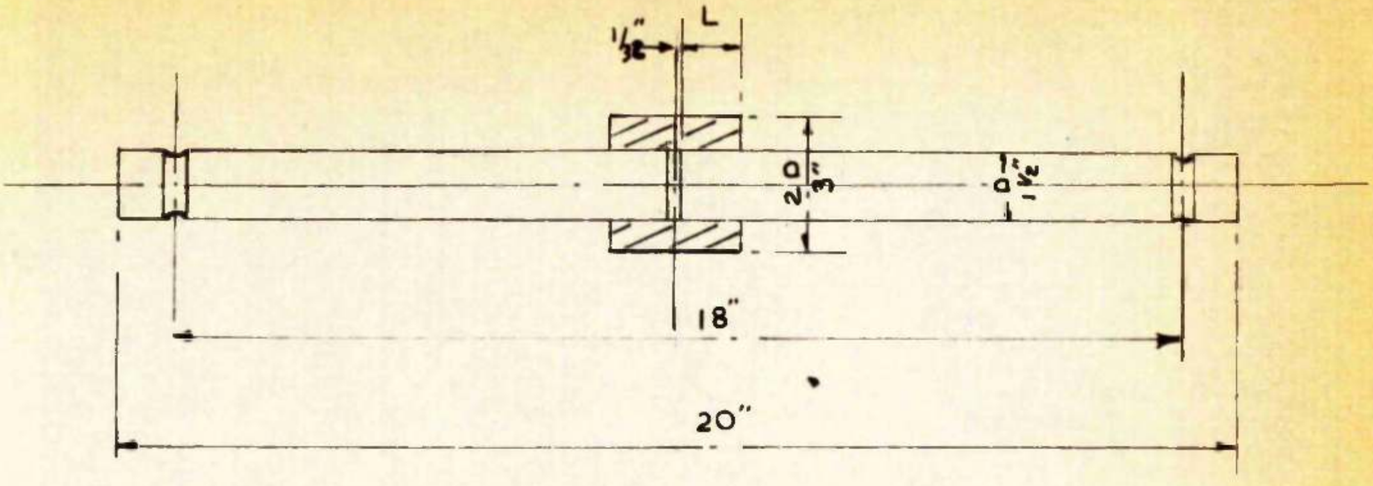

(A) SERIES 'B' SPECIMENS – ROTATED PURE BENDING

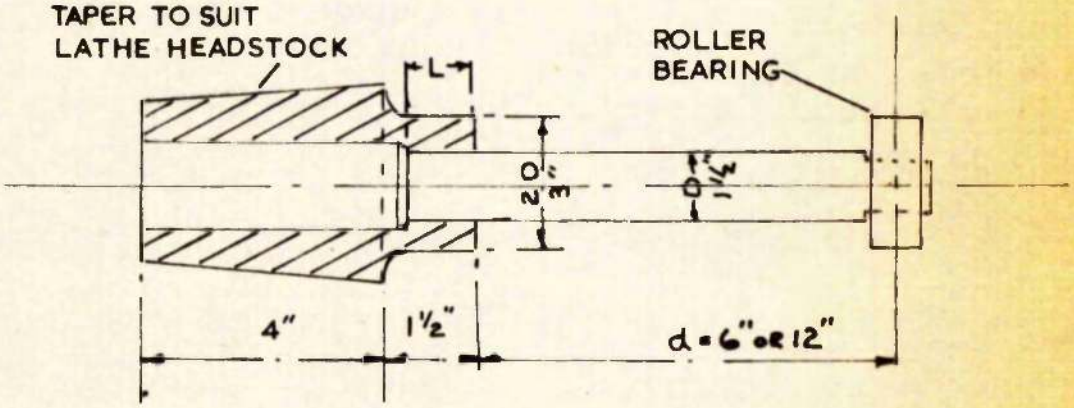

(B) SERIES 'D' SPECIMENS ~ BENDING & DIRECT LOADING

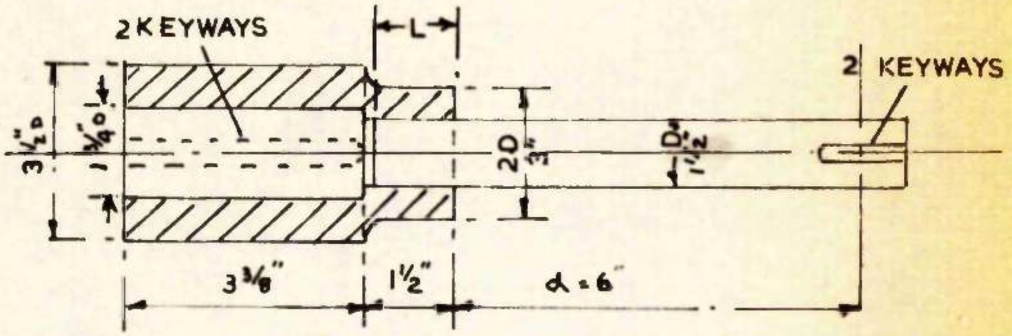

(C) SERIES 'E' SPECIMENS – BENDING. DIRECT & TORSIONAL LOADING

FIG. 7.

The specimens were prepared in exactly the same manner as before except that grooves were machined in the shaft ends to locate on the rollers of the 30 ton Avery testing machine (see fig. 7A).

As before a pure bending moment was applied to the specimen and the central deflection noted for load increments of 0.1 Ton. At each load step the specimen was turned through 360° by increments of 30° and the deflection noted for each angular position. The load was removed at each angular step to permit rotation of the assembly and re-applied when the new position was reached. The grooves in the shaft ends keep the assembly position constant during rotation thus maintaining exactly the point of application of the central dial gauge. This ensured good repeatability throughout the test.

5.5 SERIES C - Static Bend Tests - Varying Sleeve/Shaft Diameter.

This brief series was to determine the effect on the assembly strength of varying the sleeve/shaft diameter (D/d) ratio. Two specimens were used, one with a solid shaft, the other with a split shaft assembly. Both specimens had a fit allowance of .0015 in/in diameter and a sleeve length/shaft diameter ratio (L/D) of 0.67.

The sleeves initially were prepared to give a D/d ratio of about 4 : 1. After testing in a similar manner to Series A, measuring the central deflection for increasing bending moments in one plane only, a portion was machined off the sleeve diameter giving another (D/d) ratio. The specimen was then tested again and in this way, by machining successive portions off the sleeve, a complete test series down to a D/d ratio of 1.33 : 1 was conducted for both specimens.

The maximum load for the series was such that the elastic limit for bending stresses in the shaft was not exceeded.

5.6 SERIES D - Static Bending and Direct Loading Tests.

This series illustrated the effect of direct load in an assembly subjected to bending. As in the Series B tests the loading was rotated.

The specimens were somewhat different from the previous series and are shown in fig. 7B. They consisted of a shaft shrunk into a parallel section of a sleeve or hub which also had a tapered portion of external diameter. The shrinking process was carried out in the same manner as for the specimens of previous tests.

A lathe was adapted for use as a testing machine. The tapered portion of the specimen sleeve fitted exactly the lathe headstock in place of the headstock centre and was held rigidly in position by four clamps. A spherical roller bearing was force fitted to the free shaft end of the specimen and a load applied through this point by means of a lever arm, a hanger and weights. Varying the position of the roller bearing alters the ratio of direct load to bending moment. Only two positions were used in the tests giving moment arms of 6 inches and 12 inches.

The pivot point for the lever was built up from, and could be moved along, the lathe bed. (FIG. 8)

Deflection readings were taken by means of a Mercer dial gauge placed at a point near the end of the shaft. The lathe headstock was marked out in 30° divisions fixing the angular plane of the loading. For load increments of 10 or 20 lb. on the lever arm hanger deflection readings were noted at planes of 30° spacing through 360°. For two ratios of direct load to bending moment, tests were carried out on specimens with a fit allowance of .001 in/in diameter and L/D ratios of 0.4 and 0.71, and specimens with a fit allowance of .002 in/in diameter and an L/D ratio of 0.71 - six tests in all.

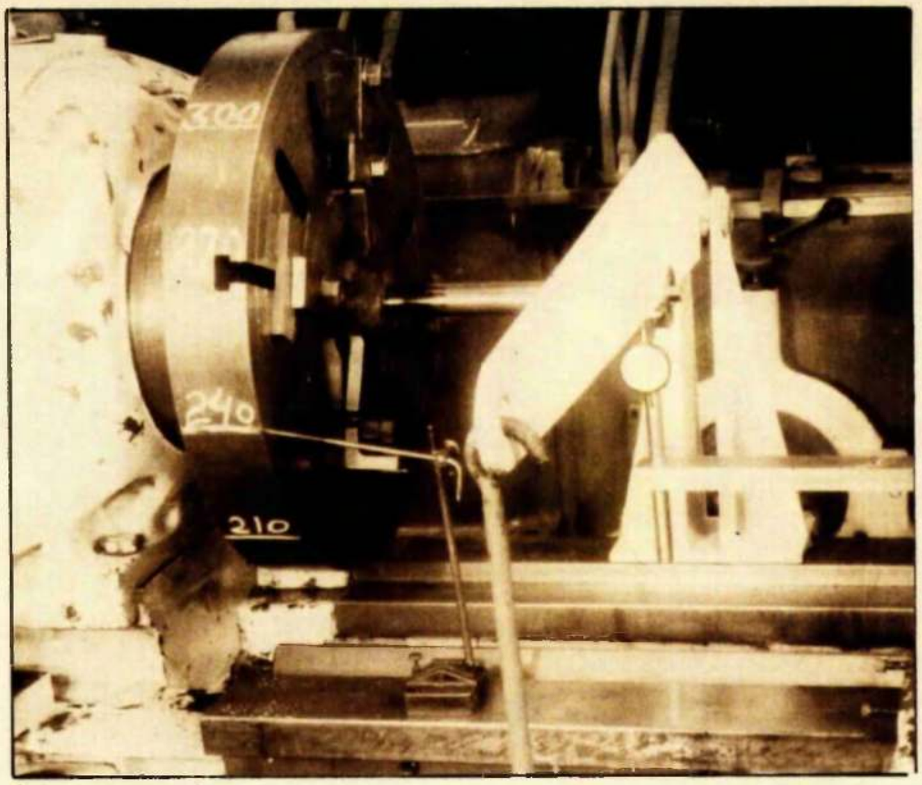

FIG.8.
SERIES 'D' TEST ARRANGEMENT

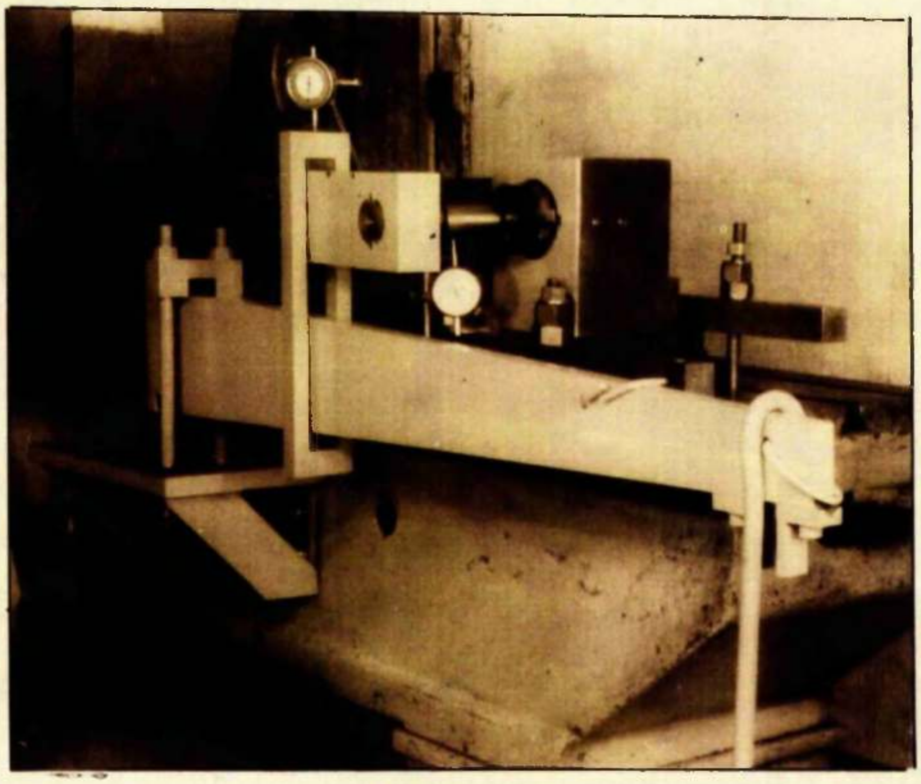

FIG.9.
SERIES 'E' TEST ARRANGEMENT

5.7 SERIES E - Bending, Direct and Torsional Loading.

This final static test series was devised to impose in static form the same types of loading (not necessarily in the same ratios of magnitude) encountered by a crankshaft pin and web assembly in service. The theoretica analysis had shown the possible harmful effect that combined torsional and bending loading would have in the individual torsional and bending strengths since both were dependent on friction. It was hoped to examine this by comparison with some of the previous bending tests.

The specimen used in the series is shown in fig.7C. A shaft is shrunk into a hub which beyond the shrinkage length has a section with enlarged internal and external diameters and two keyways cut along its length on the outer surface. Two further keyways are machined at the end of the shaft. The shrinkage process was carried out as previously described for the Series test specimens.

The specimen was held in a large block mounted on an old planing machine being restrained torsionally by the two keys in the hub. (See fig.9) A lever arm keyed to the end of the shaft had several notches cut along its length to fit the knife-edge of a carrier which supported another large lever arm. This arm pivoted at one end about a fulcrum point fixed to the machine bed and carried a hanger for weights at the other.

Bending, direct and torsional loads were thus applied to the shrinkage grip by adding weights to the hanger. The ratio of torsional to bending and direct load can be varied by altering the position of the lever carrier on the notches of the torque arm.

Deflection readings were recorded by dial gauges placed under the shaft 4 in. from the hub face and at a point on the torque arm 6 in. from the shaft

centre line. The operation of this latter gauge was found not to be satisfactory as torsional deflections produced a change in the point of its application. The values obtained from this source were not recorded.

Deflections were noted for 20 lb increments on the hanger until torsional slip or obvious bending failure occurred.

Tests were carried out on specimens with a fit allowance of .001 in/in. diameter and L/D ratios of 0.71 and 0.4, and on specimens with a fit of .002 in/in. diameter and an L/D ratio of 0.71. A range of three torque/ bending moment ratios was employed for each type of specimen.

5.8 RESULTS AND DISCUSSION

5.9 A SERIES IA, IIA AND IIIA

The full range of tests is recorded in figs. 11 , 12 , and 13 , the series being classified according to L/D ratio.

To aid a general discussion, fig. 10 has been prepared giving curves for an unsleeved shaft, a shaft with no fit allowance and one with .001 in/in diameter fit allowance, both for an L/D ratio of .71.

Considering the curve for .001 in/in. diameter fit allowance it is observed that a linear variation takes place until point A is reached. Further loading produces further linear variation but with a reduced slope until point B is reached, when a yield condition becomes evident and shortly no further load can be sustained.

It was previously suggested that although moment transfer by radial pressure and friction may act together, one may carry a major portion of the applied moment. It is suggested in this case that the friction forces predominate and the radial pressure does not become significant until the friction forces become limiting and carry no further moment.

The point A would appear to give the value of moment when slip of the friction forces takes place. From A to B the additional moment is transferred purely* by radial pressure according to equation (1) art. 4.3, the relationship being elastic, since the shrinkage pressure has not overstrained the sleeve. At B the sleeve begins to yield at the bore due to the excess radial or contact pressure. Increased loading produces further yielding of the sleeve until a point is reached where the shaft also begins to yield. Thereafter both yield actions take place until complete failure occurs.

The assumption that the friction forces carry practically the full moment up to the point of slip will now be examined.

---

*Not quite accurate - See later ... Pages 48 and 49

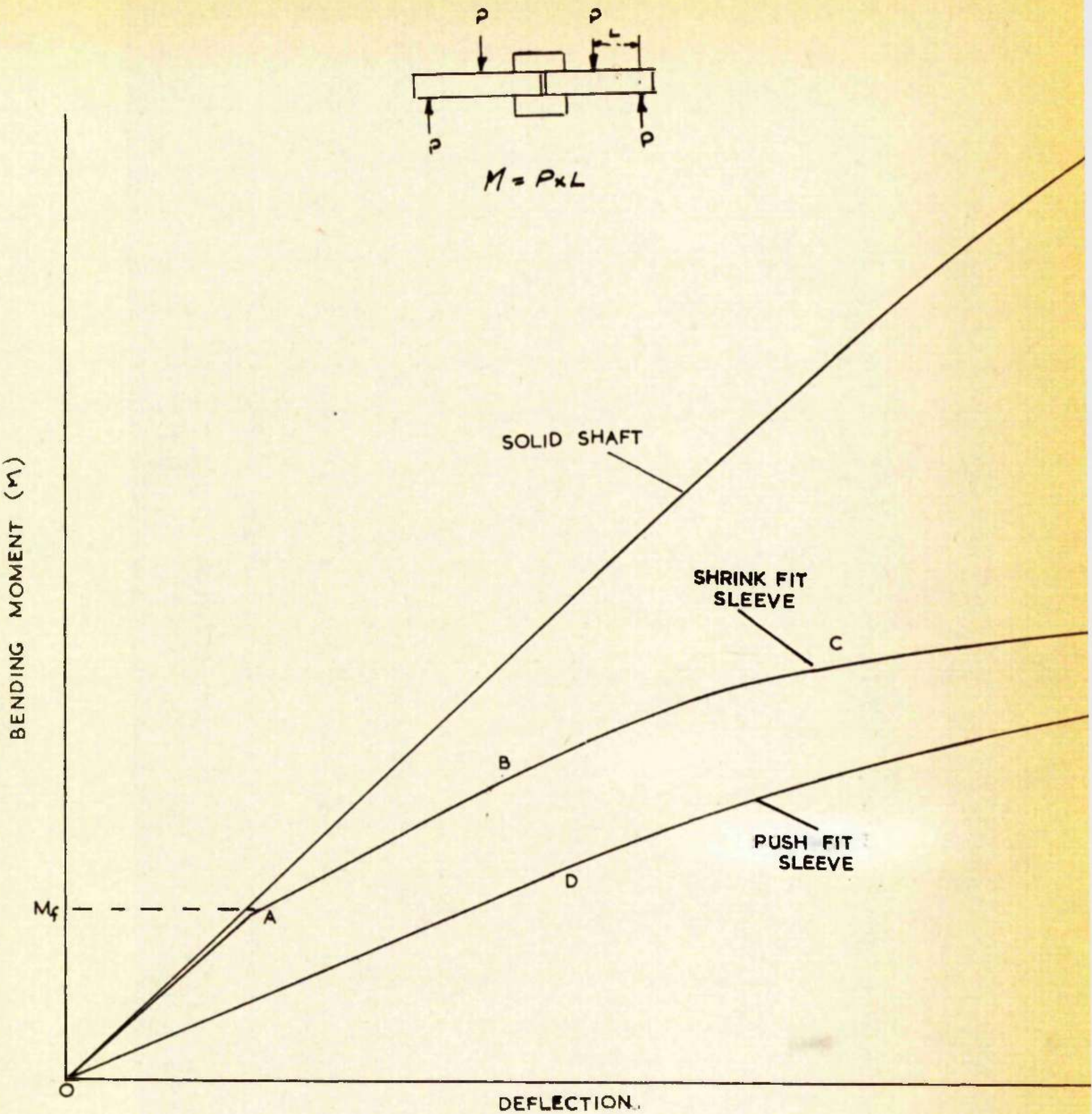

FIG. 10. BEND TEST ILLUSTRATION

In all calculations based on the Friction Moment Theory (44) the first form derived is used. The other form (11) although a more correct theoretical approach is considered difficult to use. The assumption that all the moment up to slip is carried by the friction forces is perhaps not quite accurate since slight flexture of the shaft within the grip will give rise to some radial pressure effects which the stringent form does not cover. The inherent error of the first form seems to compensate for this effect and gives more realistic results. The differences, however, are small and it is mainly the simplicity of the first form which merits its use.

Values for μ, the coefficient of friction, have been calculated from equation (9) using the full moment at the point of slip and are shown in Table 2, together with μ values obtained by pulling out the shafts after testing. It is realised that the results for μ from the pull-out tests may be low where slip has occurred in the bending test, but since no slip took place in any of the L/D = 1.13 tests, the figures obtained from these assemblies perhaps represent the condition at bending slip more accurately.

There is marked agreement with the compared results for μ as Table shows, which covers L/D ratios of .45, .71 and 1.13, and fit allowances of .001", .002" and .004" per inch diameter. The high value of μ for the .004"/inch fit can be partly explained by the high temperature required in th shrinkage process. It is thought that the lubricating sperm oil was burnt off as soon as it touched the sleeve, which had been heated to 600°C, giving in effect an unlubricated fit. The remaining μ values are consistent with previously recorded figures for lubricated shrink fits(42).

It is understandable that both sides of the grip do not necessarily slip at precisely the same load with the result that the change-over point

STATIC BEND TESTS 'A' SE

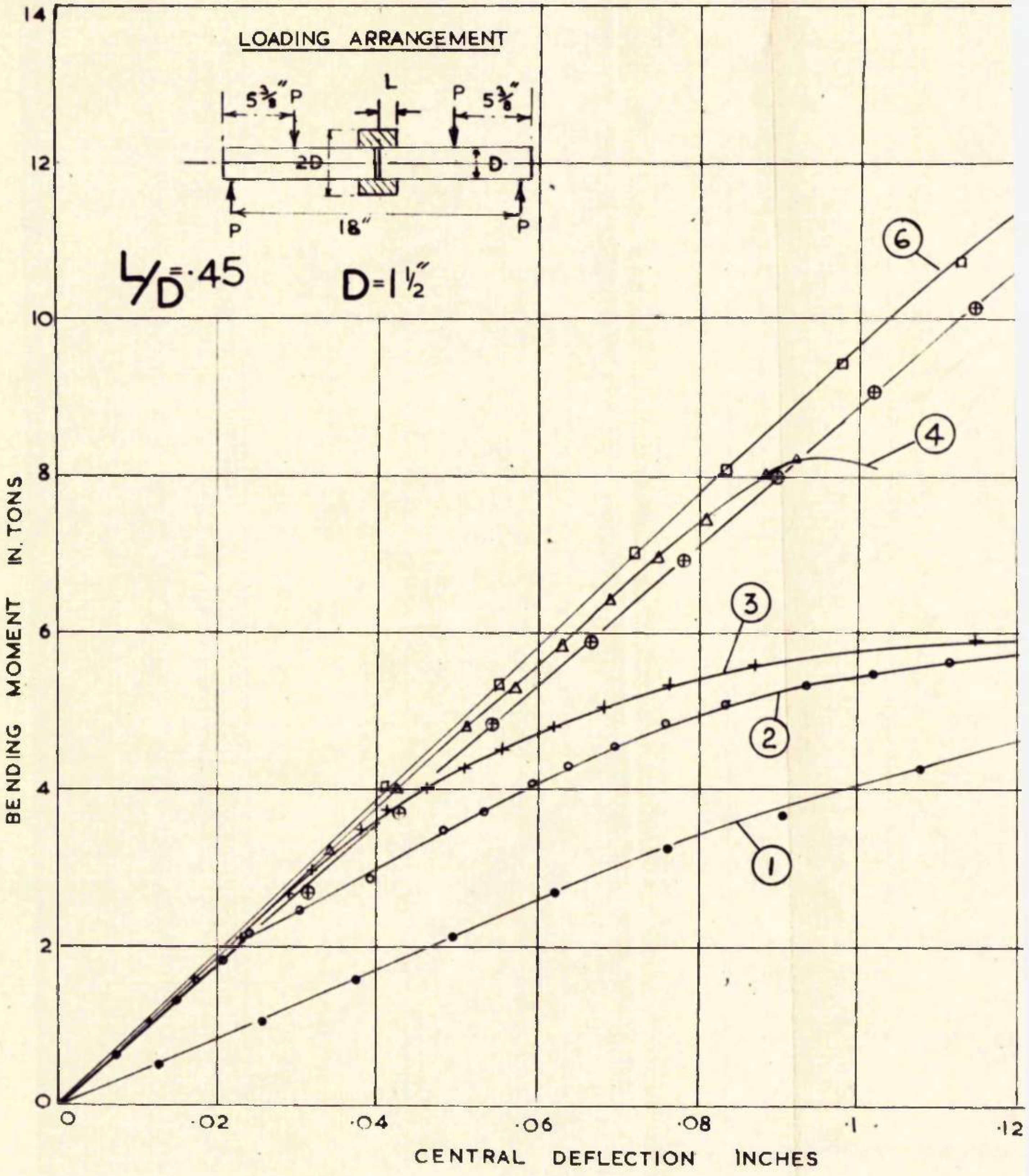

FIG.11. SERIES IA.

① • NO SHRINK ALLOWANCE
② ∘ FIT ·001"/INCH DIAMETER
③ + FIT ·002"/INCH DIAMETER
④ △ FIT ·004"/INCH DIAMET
⑤ ⊕ SOLID SHAFT NO SLEEV
⑥ ⊡ SOLID SHAFT FIT·002"/I

STATIC BEND TESTS 'A' S

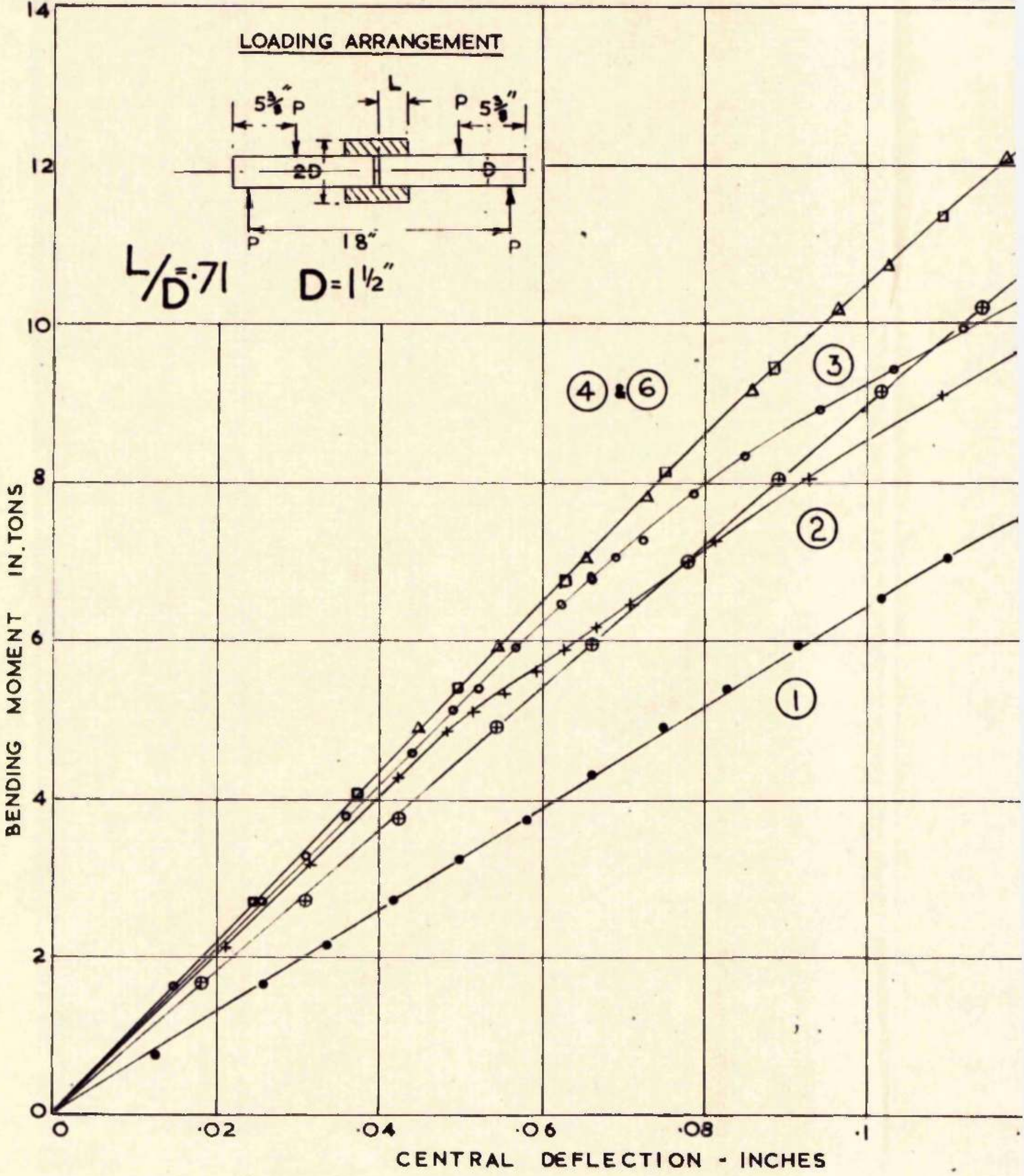

FIG.12. SERIES IIA

① • NO SHRINK ALLOWANCE
② + FIT ·001/INCH DIAMETER
③ ∘ FIT ·002"/INCH DIAMETER
④ △ FIT·004"/ INCH DIAMETE
⑤ ⊕ SOLID SHAFT NO SLEEV
⑥ ⊡ SOLID SHAFT FIT ·002"/

SERIES 'A' STATIC BEND TESTS

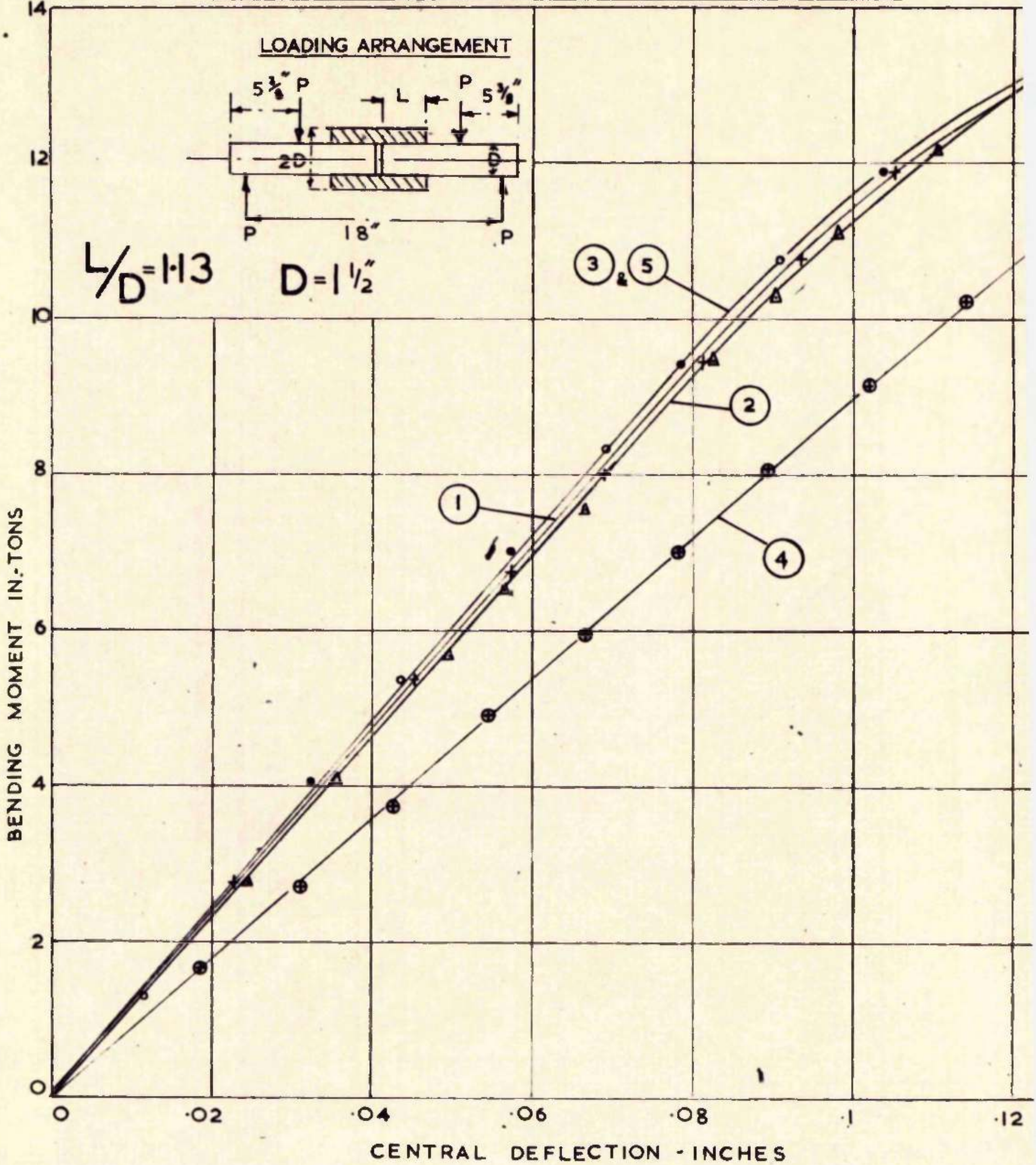

FIG.13. SERIES IIIA

① + FIT ·001"/INCH DIAMETER ④ ⊕ SOLID SHAFT NO SLE

② Δ FIT ·002"/INCH DIAMETER ⑤ • SOLID SHAFT FIT·002

③ ∘ FIT ·004"/INCH DIAMETER

from friction to radial pressure grip may not be clearly defined. This is particularly evident in Series I, fig. 11, curve 4, for L/D = .45 and fit = .004"/inch where following the initial slip at 7.5 in Ton a second sudden slip occurred. After this second slip the assembly could not even maintain the slip load and no further readings could be taken. This failure was particularly interesting and is dealt with more fully in the section dealing with the appearance of Lüders lines (page 65).

In general it is noticeable in the tests where the sleeve is overstrained by the shrinkage allowance (.002" and .004" per inch fits) that onc slip has taken place further load cannot be carried elastically and yielding occurs. This further confirms the idea that the radial pressure does not become prominent till after slip, since a sleeve already plastic would immediately yield further with continued loading.

The derived theory for combined friction and pressure moments has been applied to the cases of the fit and no-fit tests where sleeve yield has taken place, i.e. points B and D respectively in fig. 10.

From equation (17), P_o, the contact pressure between shaft and sleeve at yield in the two no-fit tests, is found to be 18.7 T/in^2 (L/D = .45) and 19.4 T/in^2 (L/D = .71). These figures are derived with an assumed value of friction coefficient $\mu = .2$ which is regarded as normal for a sperm oil lubricated fit.

The calculation of the contact pressure at yield for the two shrink test (No. 2 graphs - Series I and II) which had a fit allowance of .001" per inch diameter and did not produce yield of the sleeve under the shrinkage stresses is somewhat more complicated. In these cases it is assumed that after friction slip has taken place all the <u>additional</u> moment is taken by a radial pressure effect up to a point where the shrinkage pressure (P_s) is completely

TABLE. 2.

(STATIC BEND TESTS SERIES I, II & III)

SHRINK FIT IN/IN. DIA.	SHRINK PRESSURE TON/IN²	L/D	BM AT SLIP IN. TON.	μ CALCULATED	μ FROM PUSH OUT TESTS	REMARKS
·001	5	·45	2·1	·226	–	
		·71	48	296	–	
		1·13	–	–	·218	
·002	9	·45	3·0	·18	·125-·187 *	
		·71	6·2	·213	–	
		1·13	–	–	·1	FALSE READING LIKELY SINCE ASSEMBLY MUCH STRAINED
·004	11	·45	7·0	·344	–	
		·71	–	–	–	
		1·13	–	–	·324	

* CHECK READING TAKEN AFTER LOW READING FROM L/D = 1·13 TEST

relieved at the two corners of the grip, i.e. up to a point where there is still some shrinkage pressure over the full grip length to redistribute, equation$^{(2)}$ can be applied. Further loading is taken by the mechanism of the no-fit case (equation 17) until yield of the sleeve. No definite bre is evident in the deflection curve due to this latter change in form of moment transfer since the assembly strength is not greatly affected by the change. This is made more obvious when the slopes of the no-fit and fit after slip graphs are compared, i.e. O to D and A to B in fig.10. If it is accepted that the deflection in each case is proportional approximately to P_c, the contact stress, it can be shown from the derived theory that when M, the applied moment, is expressed in the form $M = kP_c$, the constant k for both cases is nearly the same.

Applying this analysis, the equations quoted give contact pressures at yield of 16.2 T/in.^{2} (L/D = .45) and 14.7 T/in.^{2} (L/D = .71). Examples of the calculations leading to these results are shown in an Appendix.

Examining the four results quoted it is seen that the contact pressures in the no-fit cases are close to the crushing stress of 20 T/in. for the sleeve material, while the other two fall well short of this figure The crushing stress, however, is not necessarily regarded as the yield criterion, especially in the case of the shrinkage tests where the complex associated stress system is likely to produce stresses exceeding yield at a grip contact pressure of less than 20 T/in.^{2}

The lack of further experimental results precludes any definite conclusions being drawn on the analyses. As a general comment, however, the no-fit results would appear to be particularly significant despite the fact that an arbitrary value of μ is involved.

It is noticeable that the moment producing yield in the no-fit specim

varies as L^2 which does agree with the usually accepted simple form $M = \frac{DP_cL^2}{24}$. The value of P_c, however, from this form would be about 35 T/in^2 which is considered unrealistic.

The Series III tests (L/D = 1.13) indicate that with this ratio no slip occurs and it is seen that there is little, if any, difference in streng with variation of fit allowance. It is felt with L/D = 1.13 there is considerable flexture of the shaft within the sleeve and the full length of grip is never really employed since the shaft yields before the grip.

In the complete A Series, comparing the assembly strengths with that of a solid unsleeved shaft, it is seen that with L/D = .45 there is little difference until slip is reached. With L/D = .71 the assembly is stronger in each case until slip occurs but with L/D = 1.13 no slip takes place and the built-up specimen is always stronger.

The solid unsleeved shaft bend test apparently shows an unusually high yield stress of 30 Tons/in^2 for the shaft material. A tensile test gave the value of 20Tons/in^2. This feature was not investigated further although it is apparently not unusual to get such high yield stresses in bend tests of this nature.

Series A has been discussed more fully than the succeeding Series as many of the points covered apply to all the tests and are not repeated later. This is particularly true of the feature of "friction moment" which required a full explanation illustrated by these first test results.

5.10 SERIES B

The three tests of this Series show the effect on a shrink fitted grip of a pure bending moment applied, in turn, at 30° planes round the specimen. Fig. illustrates the results and should be compared with the complementary non-rotated loading Series IIA, fig. 12 .

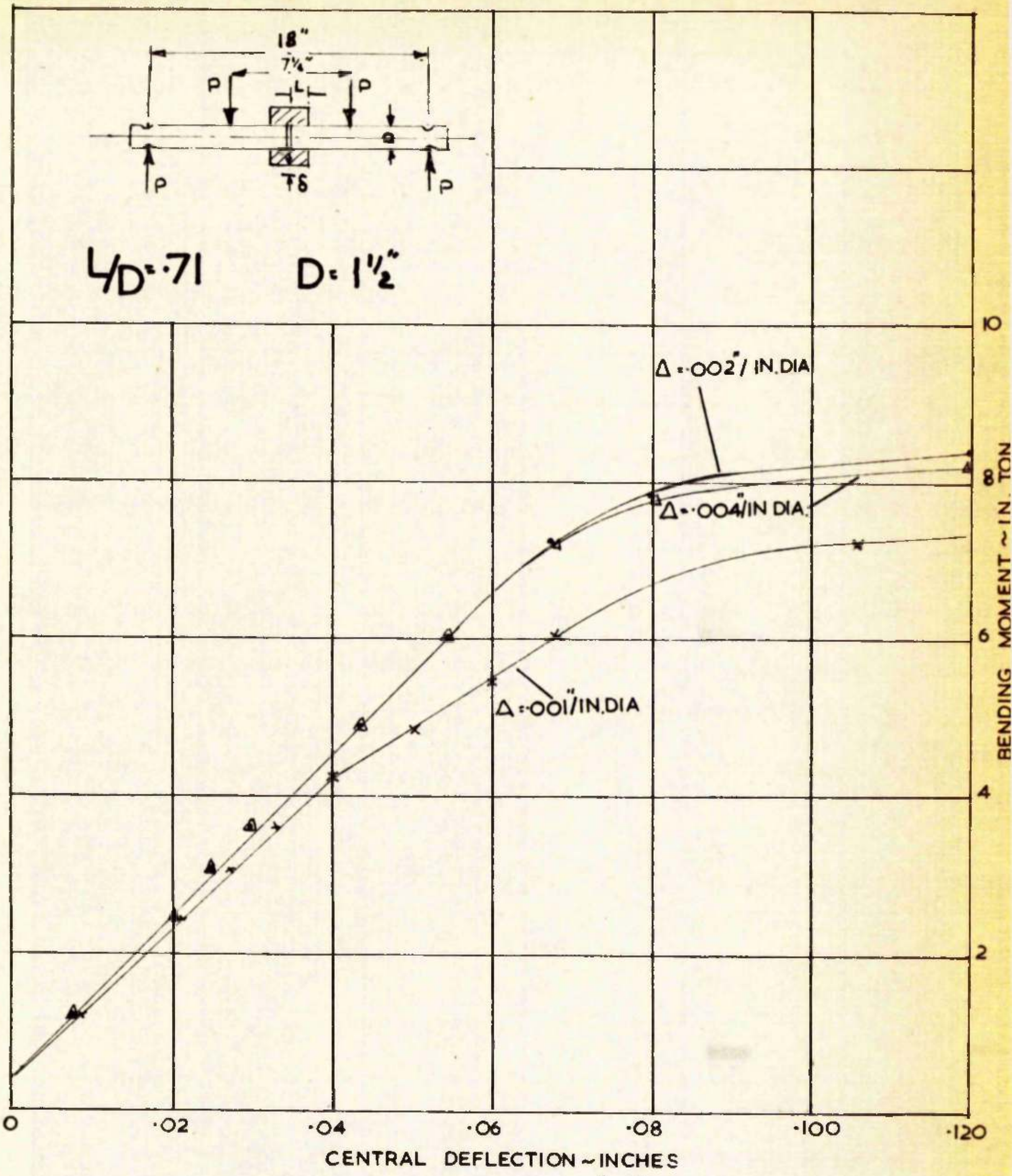

FIG.14. SERIES 'B'

ROTATED PURE BENDING

The general form of the graphs does not differ and what was said about the Series A tests holds here also. The most apparent difference in the tw series is the abrupt loss in strength, once failure has commenced, which takes place in the rotated loading cases. In addition to this more abrupt change to failure the ultimate strength of the assembly is considerably reduced.

The values of bending moment at which friction slip occurs do not vary ostensibly for similar specimens in the two series. The .001 in/in. diameter fit test once again shows the proportional form after slip, leadin to failure when the sleeve bore material becomes plastic. The two other tests show, as before, that a sleeve which has reached a state of yield due to a shrinkage allowance, cannot withstand further moment once friction sli has taken place. This is made more obvious than previously, however, by th more rapid failure already noted. These features are of definite significance when dynamic loading is considered.

It is understandable that rotated loading will produce more rapid failure than the non-rotated case. The rotated loading induces overstrain of the complete sleeve bore at the load which initiates yield at one point only in the non-rotated series. Hence the overstrain at a lower value of load is made much more complete in the rotated cases.

It is noticeable that slip occurs in the .004 in/in. diameter fit test which did not take place in the non-rotated series. This could well be explained by the fact that seizure may have taken place in the A Series .004 in/in. fit specimen, preventing friction slip and presenting in effect a solid assembly.

5.11 SERIES C

The results of this small series of tests are shown in Table 3 and presented in graphical form in fig. 15.

It is at once obvious that the sleeve diameter is not a critical facto in assembly strength. Practically no change in stiffness is evident as the sleeve shaft diameter ratio is reduced from 3.92 to 2.33. Further reduction to a D/d ratio of 2 : 1 produces a more abrupt change in stiffness but little further change in stiffness is noticeable as the ratio is still further reduced. It is thus interesting to note that over the complete range of sleeve diameters tested, assembly stiffnesses fall into two distinct groups, one for $D/d \geq 2.33$ and the other $D/d \leq 2$. This is borne out by both solid and split shaft assemblies.

It is once again noticeable that where friction slip has not occurred there is practically no difference between the solid and split shaft load/deflection curves. For the range of load covered only two tests ($D/d = 1.5 : 1$ and $D/d = 1.33 : 1$) exhibited friction moment slip.

As a general comment, it would appear from strength considerations that there is nothing to be gained by having a sleeve/shaft diameter ratio much in excess of 2.33 : 1. For all further tests, however, the ratio was standardised at 2 : 1, a commonly used value in crankshaft manufacture.

5.12 SERIES D

The full range of tests is recorded in the graphs of fig. 16 . Although the specimens were subjected to rotated loading, only results for deflections in one plane have been plotted. The results for the other plan showed no significant differences.

The deflection characteristics follow the pattern set by the previous tests with a few minor differences. From a comparison of specimen pairs,

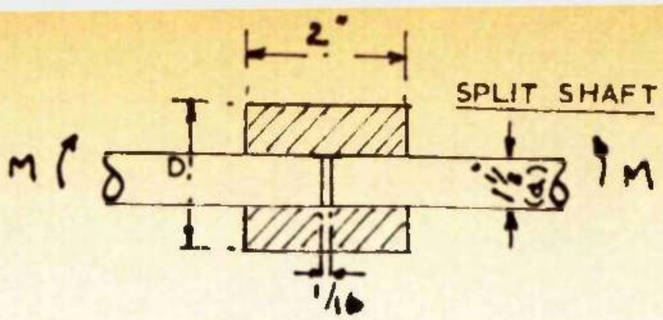

SLEEVE DIAMETER	→	5⅞"	5"	4½"	4"	3½"	3"	2½"	2¼"	2"
D/d RATIO	→	3·92	3·33	3	2·66	2·33	2	1·67	1·5	1·33
BENDING MOMENT IN. TONS	TYPE OF SHAFT	CENTRAL DEFLECTION ·0001 IN								
·3	A	20	19	19	17	20	23	16	20	26
	B	15	14	19	11	20	28	16	17	21
·6	A	46	46	44	44	45	52	52	49	59
	B	44	42	44	37	49	60	49	52	48
·9	A	74	72	70	71	75	85	85	86	91
	B	69	68	71	66	75	85	76	91	89
1·2	A	103	101	99	98	104	117	111	120	125
	B	95	94	96	94	107	123	105	131	134
1·5	A	133	130	128	131	134	147	148	146	151
	B	124	126	125	123	134	151	139	172	188
1·8	A	159	158	154	161	164	180	182	181	181
	B	156	153	154	155	167	182	172	217	241
2·1	A	187	186	181	190	200	216	212	215	212
	B	182	180	182	181	200	212	199	258	301
2·4	A	219	216	209	221	227	247	247	242	243
	B	208	209	214	221	221	243	237	317	367

A – SOLID SHAFT
B – SPLIT SHAFT

FIT ·0015 IN/IN DIA

TABLE 3

(STATIC BEND TESTS SERIES 'C')
VARYING SLEEVE DIAMETER

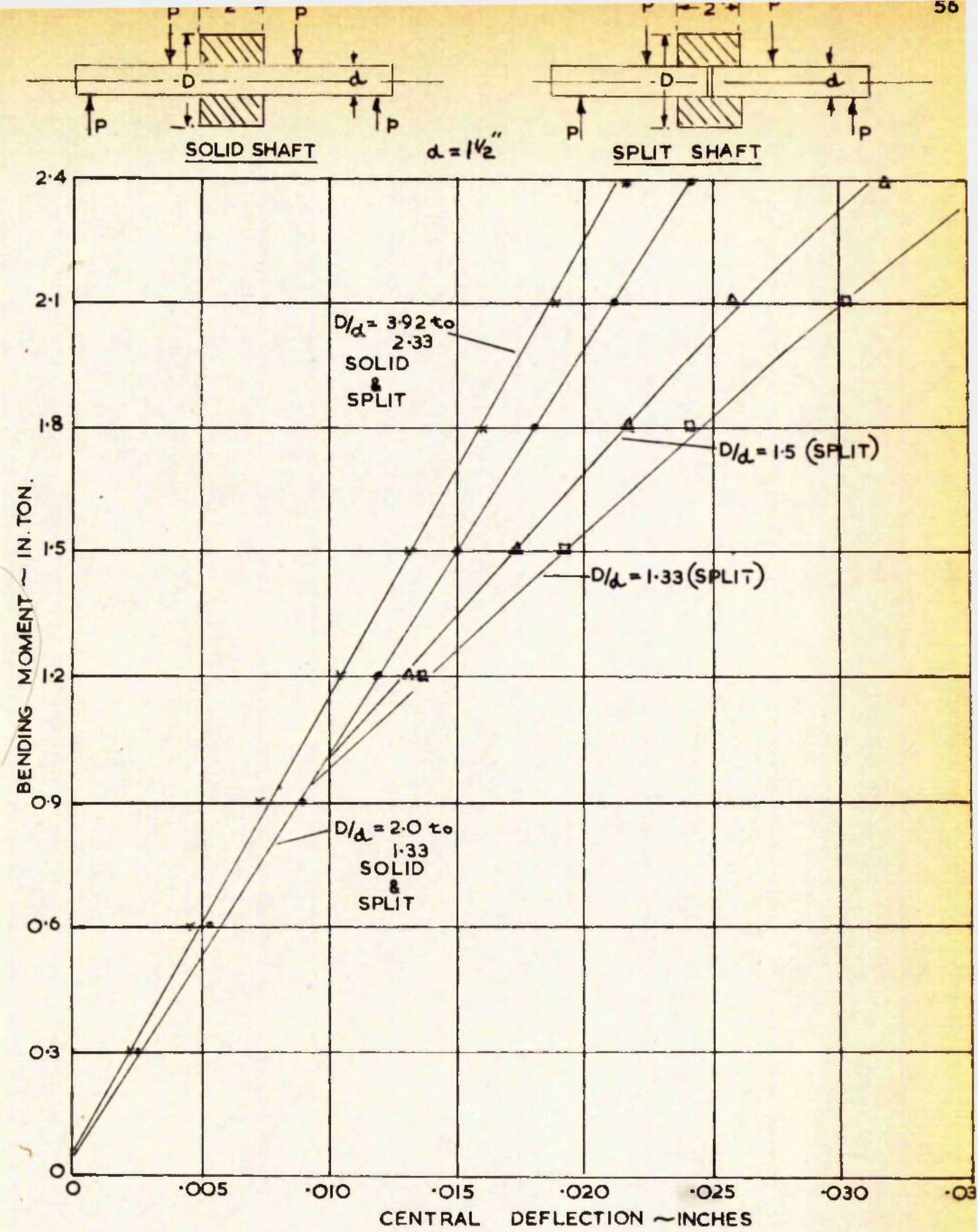

FIG.15

SERIES 'C' STATIC BEND TESTS
(VARYING SLEEVE DIAMETER)

with one moment arm twice the other (i.e. direct loads in ratio 2: 1), it is seen that the direct load, as might be expected from theory, has no appreciable effect on the point of friction moment slip.

Friction coefficient values for all the slip points (i.e. where proportionality ceases) have been calculated and are presented in Table . For this type of lubricated grip the values, lying as in previous tests between .2 and .3, are considered quite reasonable.

The tests do show, however, that an increase in direct load causes a reduction in the ultimate strength of the grip. This effect is most noticeable in the tests where L/D = .71 and would appear to be the natural outcome of increased radial pressure on the grip. Although a comparison with previous series of actual deflections cannot be made the values of bending moment slip (as shown previously) and ultimate grip failure can be compared, since they depend solely on the grip itself, i.e. length and fit allowance. This comparison shows that the combined effect of rotational and direct load produces complete grip breakdown at a lower value of bending moment than any previous test.

As in previous tests a watch was kept for the initial appearance of Lüders lines. Although the exact load value at which they originated was rather obscure, once again in no case did they appear before slip was reached.

5.13 SERIES E

The results are presented in graphical form in figs. 17 , 18 and 19 , and some features of the analytical tie-up are summarised in Table 5 .

The stiffness characteristics follow the same general pattern set by the previous series. The break-off point of friction moment slip is obvious in nearly every case. In some tests complete torsional failure

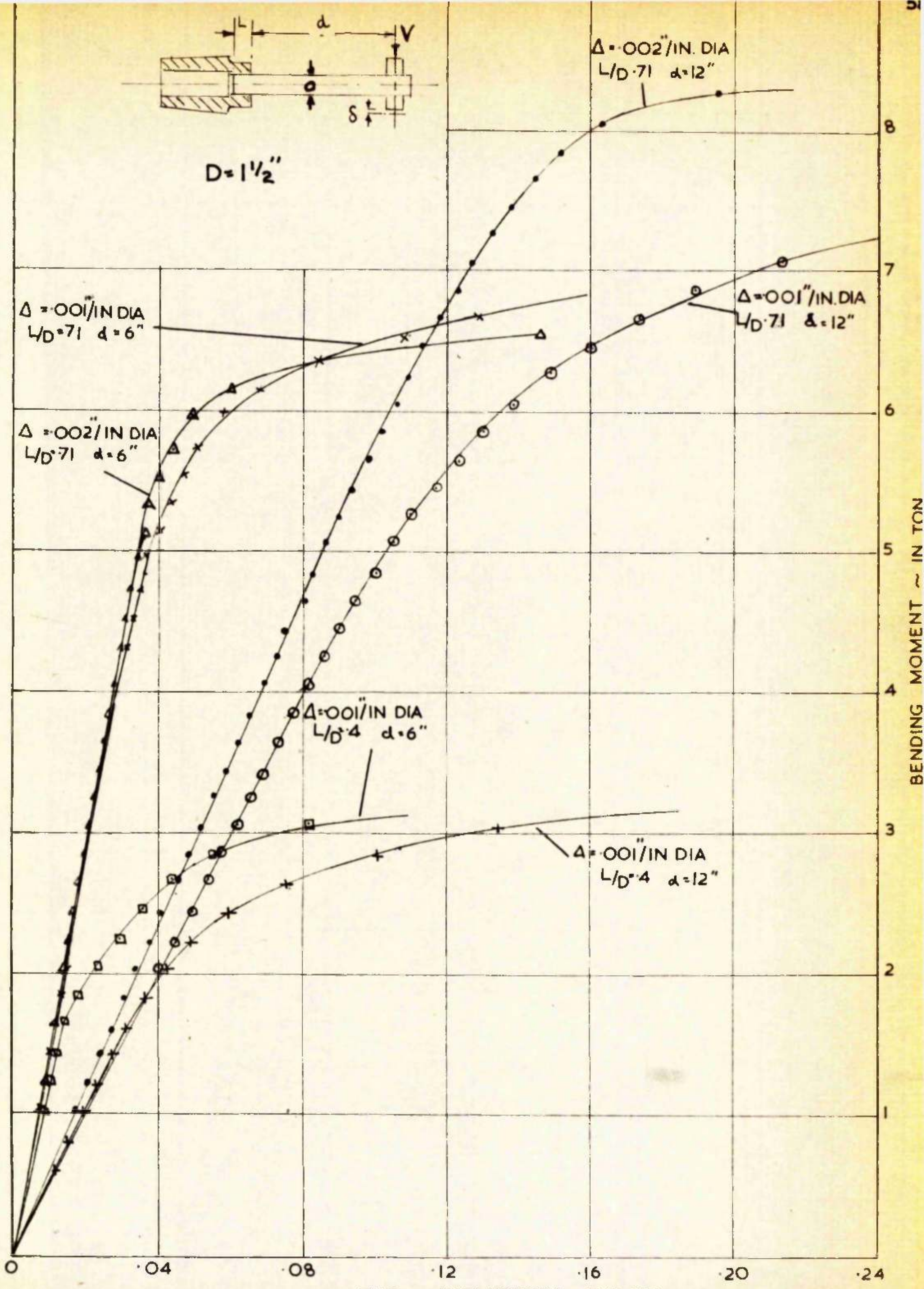

FIG. 16. SERIES 'D' BENDING & DIRECT ROTATED LOADING

TABLE 4

SERIES 'D' FRICTION COEFFICIENTS

L/D	MOMENT ARM d''	FIT Δ IN/INDIA.	P_s TON/IN^2	M IN TON	$M_s = M + VL/2$ IN TON	μ *
·4	6	·001	5	1·65	1·73	·212
4	12	·001	5	1·75	1·79	·216
·71	6	·001	5	3·8	4·14	·255
·71	12	·001	5	4·0	4·16	·256
·71	6	·002	9	5·3	5·6	·191
·71	12	·002	9	5·5	5·7	·195

* $M_s = \mu P D L (D + L/2)$

took place after friction moment slip and in one case before slip. This latter test may readily have failed simultaneously by moment and torsional slip.

The outstanding feature of the results is that the superposed torque, as predicted in the analytical investigation, causes a reduction in the value of moment where friction slip takes place. The series L/D = .71 and fit = .002 in/in. diameter show this point quite clearly with the moment at slip being reduced as the torque/bending moment ratio is increased The other tests, although not presenting such strong evidence, nevertheless show the same tendency.

Table 5 has been drawn up for the points where friction moment slip and torsional failure have occurred. Friction coefficients have been calculate for points of friction moment slip using the combined moment and torque values with bending as the failure criterion, i.e. equation 22 has been applied. Where torsional failure has taken place coefficients have been derived for combined moment and torque values with torque the critical factor, i.e. equation 21 has been applied. The value of moment for this latter calculation is taken as that at friction moment slip and not that at torsional failure. This is only an approximation since the friction moment at torque failure is rather indefinite, being shared at this stage by both friction and radial pressure effects according to equation 10 art. 4.5 . The friction values in all cases show excellent agreement and give strong support for the applied theory.

The series is perhaps not full enough to be conclusive but certainly does indicate that a grip's strength is shared between bending and torsional loading. This fact is of prime importance in crankshaft grip design and would indeed suggest the need for some revision of the accepted present-day design criteria.

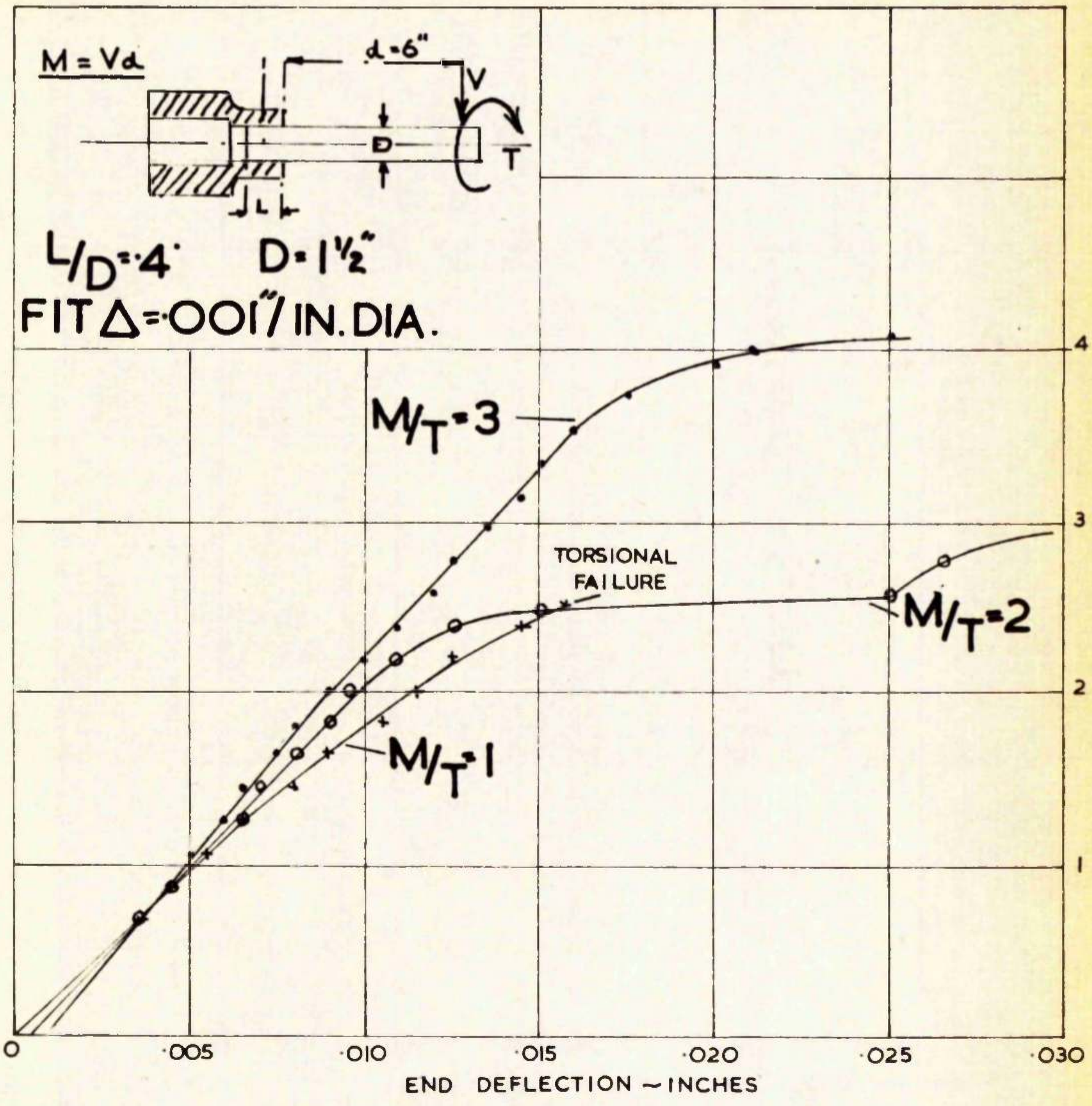

FIG. 17

SERIES 'E' ~ COMBINED BENDING, DIRECT & TORSION

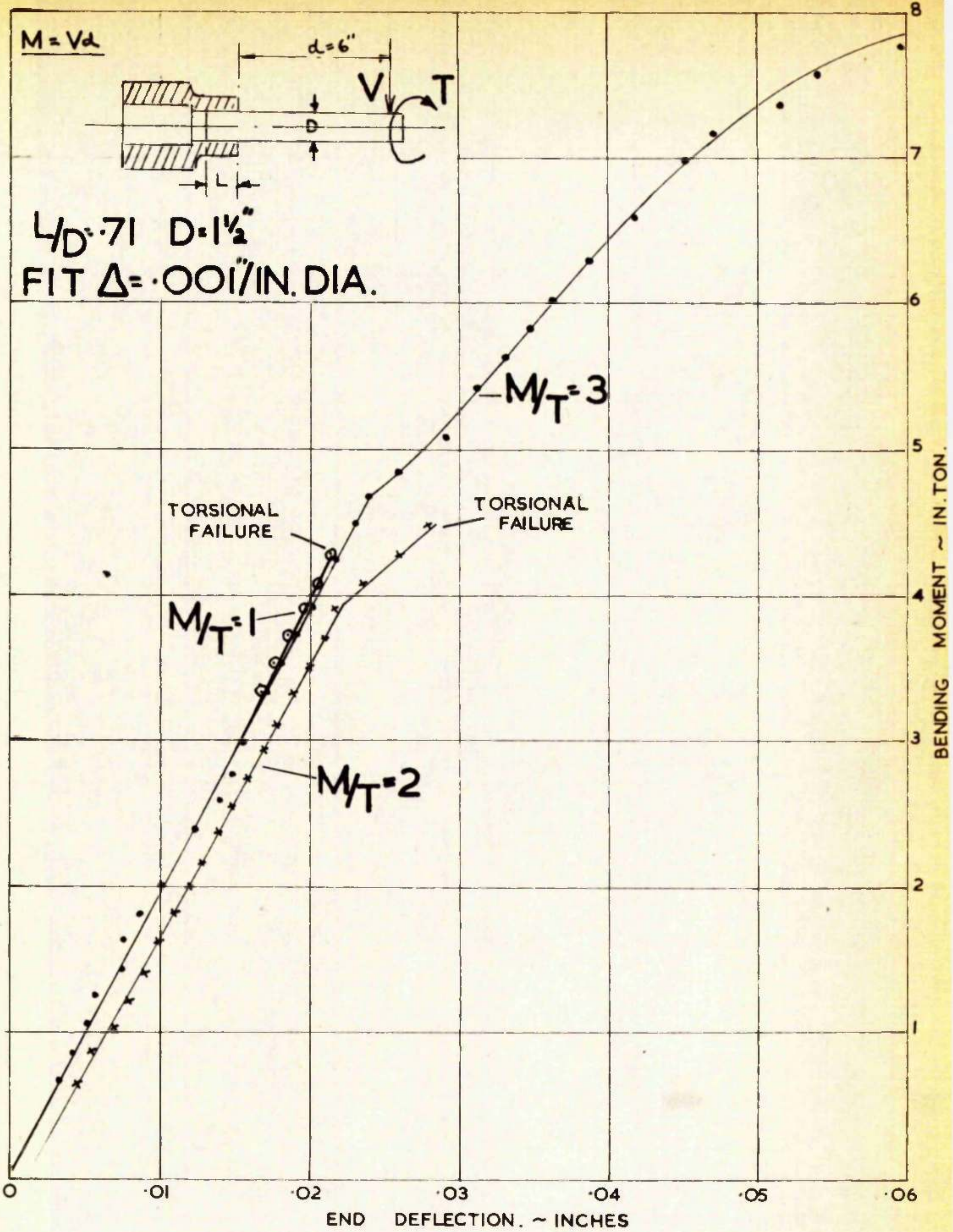

FIG. 18.

SERIES 'E' ~ COMBINED BENDING DIRECT & TORSION

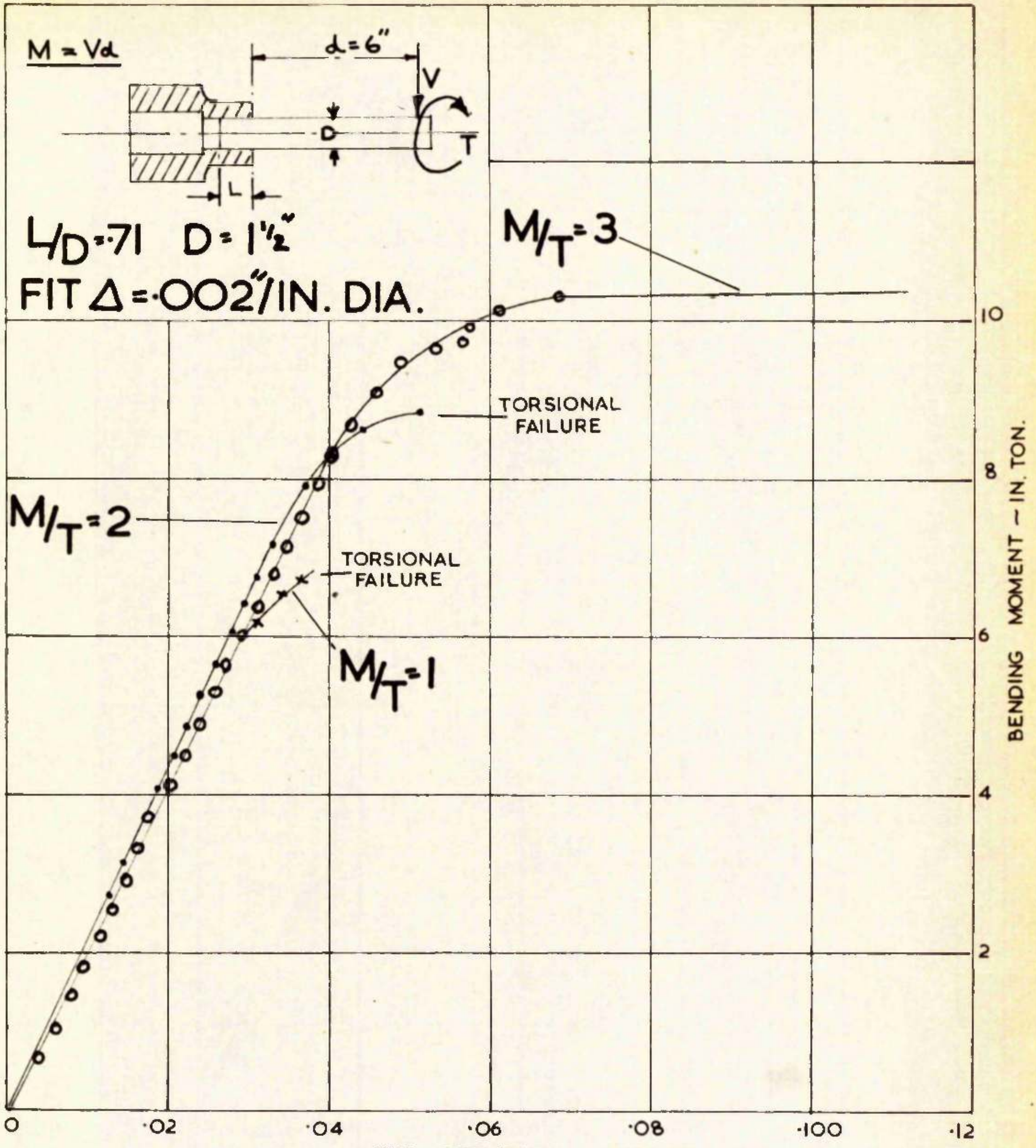

FIG. 19.

SERIES 'E' ~ COMINED BENDING, DIRECT & TORSION

TABLE 5

SERIES 'E' FRICTION COEFFICIENTS ~ COMBINED BENDING & TORSION

L/D	FIT Δ	P	M/T	BENDING SLIP					TORSIONAL SLIP				
	IN/IN.D.	TON/IN^2		M IN TON	$M_s = (M + VL/2)$ IN TON	T IN TON	$M_e = \sqrt{M^2+T^2}$ IN TON	① μ	M IN TON	$M_s = (M + VL/2)$ IN TON	T IN TON	$M_e = \sqrt{M^2+T^2}$ IN TON	② μ
·4	·001	5	3	2·0	2·1	·66	2·2	·272	–	–	–	–	–
			2	2·0	2·1	1·33	2·48	·306	–	–	–	–	–
			1	1·3	1·37	1·3	1·9	·236	1·3	1·37	2·5	2·84	·268
·71	·001	5	3	4·7	4·94	1·59	5·18	·318	–	–	–	–	–
			2	3·9	4·1	2·6	4·85	·298	3·9	4·1	3·0	5·07	·27
			1	–	–	–	–	–	4·3	4·5	4·3	6·22	·33
·71	·002	9	3	8·0	8·4	2·66	8·82	·30	–	–	–	–	–
			2	7·0	7·35	4·66	8·7	·297	7·0	7·35	5·9	9·44	·282
			1	6·0	6·3	6·0	8·7	·297	6·0	6·3	6·7	9·2	·275

① $M_e = \mu P_s D L (D + L/2)$

② $T_e = \mu P_s \frac{\pi D^2 L}{2}$

5.14 LUDER'S LINES

After the completion of the first series of static bend tests, an examination of the end faces of one of the sleeves revealed a set of lines emanating from that part of the bore which had been most highly stressed (see fig. 20). The pattern of the lines indicated that they were Lüder's lines that had been made much more evident by the cracking and flaking off of the oxide layer on the sleeve, formed during the heating and cooling of the shrinking process.

The lines represent thin wedges of plastic material produced by overstrain of the bore, and this progress across the sleeve face gives an indication of the depth of overstrain.

Although the first specimen examined with Lüders lines was not specially prepared, all the sleeve faces of succeeding specimens were ground and lapped to give a smooth mat surface. It was found that if the end surfaces were rubbed with a cloth soaked in sperm oil during cooling, it produced a black oxide coating which showed up the lines admirably. The sleeve was normally heated up to 500°C. The technique of oxide coatings is fully discussed in Handbook of Experimental Stress Analysis,(20) p. 643.

During the tests, an attempt was made to observe the initiation of the lines and the corresponding load. This proved to be more difficult than was anticipated, and no results are presented in view of their doubtful reliability.

One feature, however, which is worthy of note is that at no time were lines observed prior to a load corresponding to slip of the friction grip.

This would seem to further substantiate the view that the radial pressure in the sleeve did not become significant till after friction slip. This was

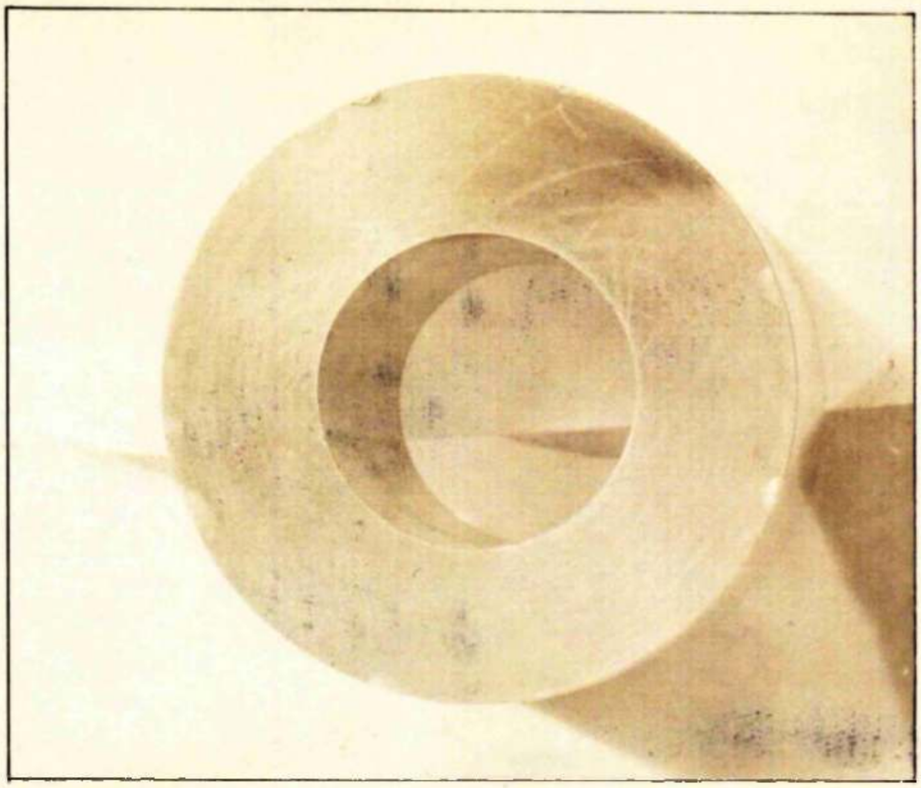

FIG. 20.
LÜDERS LINES ~ AS FIRST OBSERVED

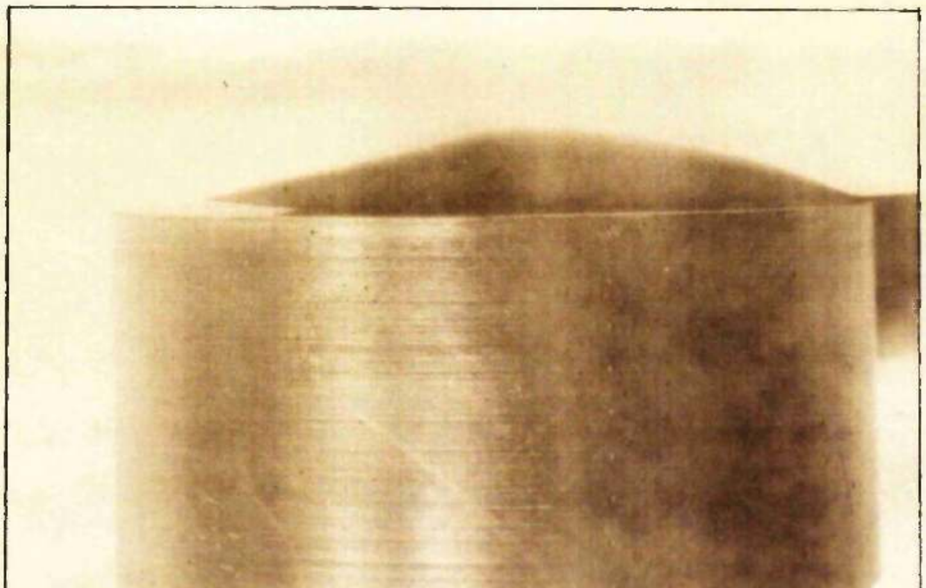

FIG. 21.
LÜDERS LINES ~ ON EXTERNAL DIAMETER

clearly illustrated in one particular case - Series I, .004"/inch fit allowance. This assembly sustained a very high load until slip took place, when no further load could be applied. The slip was sudden and as it took place the Lüders lines shot out from the bore to the outside of the sleeve (see fig. 23). This would appear to be caused by a sudden reduction in μ, following the initial slip, causing a sudden transfer of moment from friction grip to radial pressure distribution. This effect is similar to the high μ values obtained when seizure of a grip occurs during push-out tests. Once the first slip is obtained, the load required for successive movement is much lower. This was indeed the effect produced when the specimen under discussion was disassembled by pulling apart and pushing out the remaining shaft.

The progress of the lines is not gradual, but proceeds in a series of definite jumps. As the line shoots out, the original part becomes wider giving the complete line a tapered thickness. The shape traced out by the ends of the lines gives an approximate cosine distribution round the bore which is thought to justify the assumption for the radial distribution in the theoretical analysis.

Figs. 22 & 23 show the line patterns at different loads. These lines have been made more prominent by rubbing the surface lightly with very fine emery cloth. This tends to remove the loose oxide and polish the surface of the metal. It is also seen that the lines are raised up from the surface, this being very evident where two lines cross, and the polishing reveals the high points without disturbing the oxide layer.

Fig. 21 , although not very clear, shows the progress of the lines axially along the outside surface after considerable overstrain.

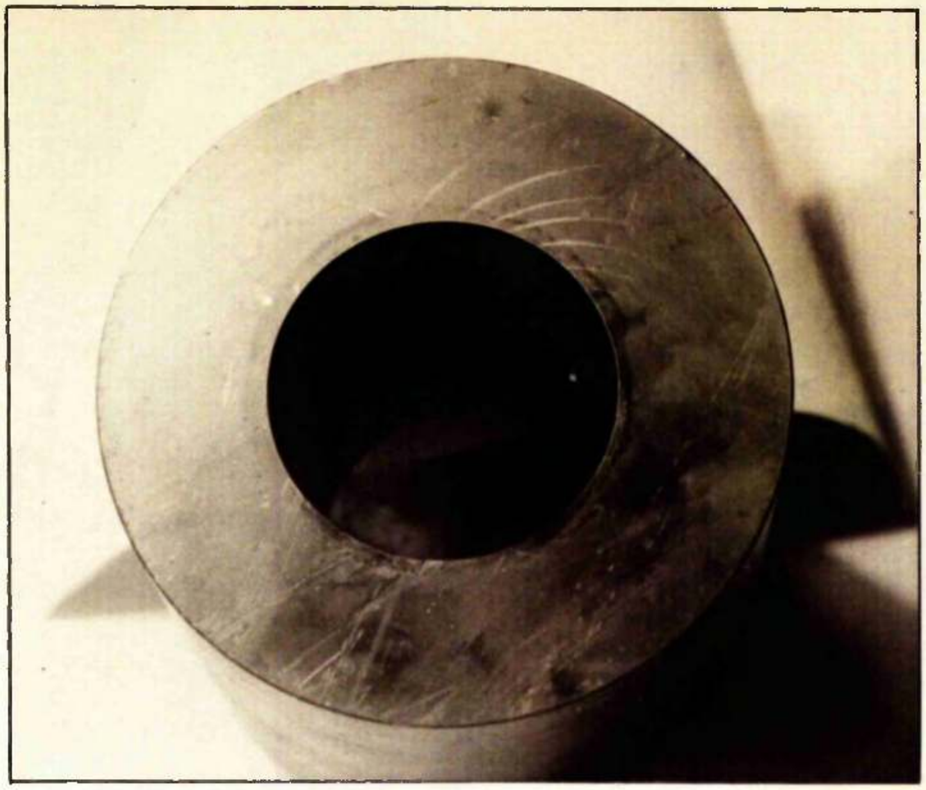

FIG. 22.

LÜDERS LINES ~ SEMI-PLASTIC

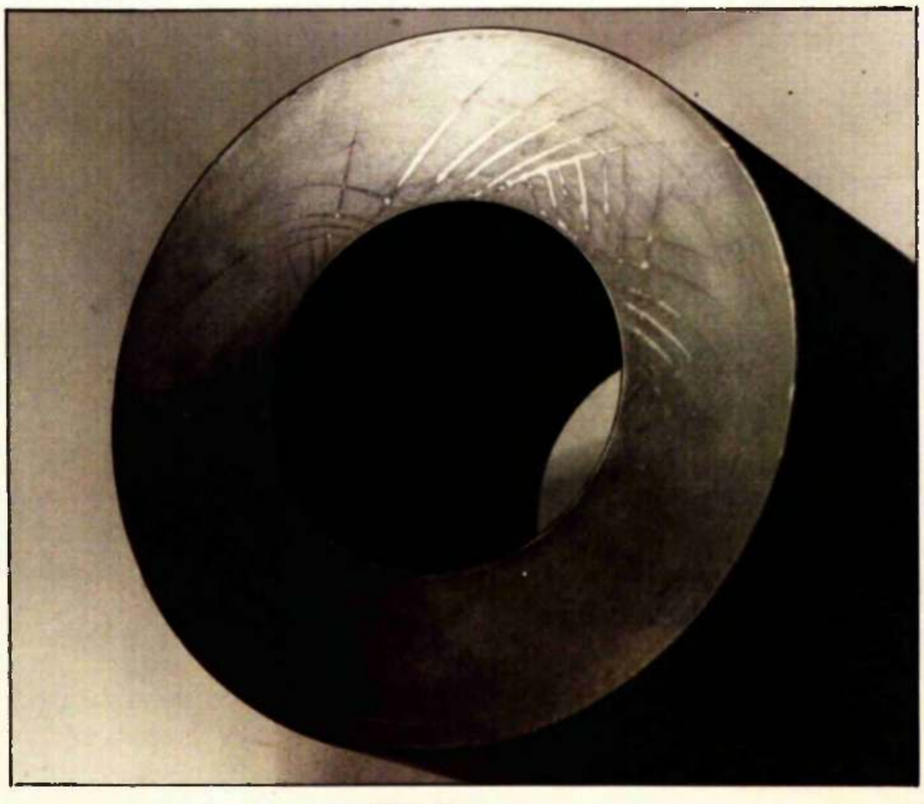

FIG. 23

LÜDERS LINES ~ FULLY PLASTIC

These axial lines which have their origin at the sleeve face spread from the ends of lines on the face which have reached the outside edge.

Although the technique of line observation was not developed to any extent in the present test series, it is suggested that some interesting results would arise from a more exhaustive study, using perhaps brittle resins or white-washed oxides to make the line development and observation more critical.

6. FATIGUE TESTS

6.1 INTRODUCTION

Following the static work of the previous section, it was decided to conduct a short series of fatigue tests on a similar type of shrink-fitted assembly. It was hoped thereby to apply some of the ideas gained on the transfer of moment from shaft to sleeve to the dynamic case. Although the primary interest of the tests was in the nature and development of bellmouthing resulting in a loss of grip, some conclusions drawn from previous investigations are of interest.

A considerable amount of research has been carried out on the fatigue of shrink and press fitted assemblies and a few only are briefly discussed.

Peterson and Wahl(33) believe that the press fit fatigue problem involves essentially a high stress concentration acting on a material weakened by rubbing corrosion. They state that it has been shown that the reduction in strength due to corrosion alone can be of the order of 25 - 30%. They showed that the fatigue strength of a shaft was reduced to about half when it carries a press fit hub. Mention is made of tests carried out in Darmstadt which showed that above a certain value the endurance strength was independent of pressure over a wide range. This was probably because a condition of yield had been reached at the collar bore, in which case the maximum peak stress no longer increases with fit allowance.

Cornelius(11) concluded that the reduction in fatigue strength due to fretting corrosion is negligible compared to that due to the clamping stresses. However Beale(31) indicated that fretting does accelerate fatigue with clamping stresses present and that relief of the bore at one or both ends has generally proved effective. Care has to be taken as it

has been observed that this results in an increased bending moment and failure farther within the grip. In the discussion of this paper it is mentioned that the effective area between wheel seats and hubs in press-fitted axle assemblies continuously diminishes with service so that the effective edge of the hub continuously progresses inward. This may result in an increased clamping stress and a lower fatigue strength which is not due to an increased bending moment. It is concluded however that the advantage to be gained from a reduction of static stress concentration can be outweighed in some circumstances by an increase in dynamic stressing.

On the subject of loss of fit, Horger and Cantley(23) show cases where all the original wheel fit near the outside hub face was lost during test due to bellmouthing of the wheel bore and rubbing corrosion; this being particularly noticeable at high crankpin stresses. The authors show further that hardening and rolling of the shaft portion within the seat considerably improved the life but found that fatigue cracks developed when running well below the endurance limit.

6.2 THEORY

Bellmouthing being the result of excessive crushing stresses on the web bore material, it is realised that the tendency should increase as the web thickness is reduced. If working loose in the sleeve is taken as the criterion of bellmouthing, there must be some length of sleeve which would as readily bellmouth as the shaft fatigue, when subjected to a fluctuating bending moment. This critical length is of considerable value since it gives the minimum web thickness without reducing the shaft strength.

A theoretical approach will not be presented, based on the Friction Moment proposed in the previous section.

Determination of L/D ratio to give equal strengths of fatigue and sleeve grip for a built-up shaft assembly (see fig. 1)

In the previous section (art. 4.4) it was proposed that the friction forces in the grip carried all (or nearly all) the applied moment up to some limiting value when slip takes place. Following slip, the moment is taken by a distribution of crushing stress on the sleeve and it is suggested that these stresses, being high for small moment increase above slip, would quickly produce bellmouthing. The high crushing stresses would naturally cause bellmouthing more readily on a sleeve which was already in a condition of yield due to a large shrinkage allowance. An elastic grip should be capable of withstanding some further moment after slip without bellmouthing. The contact stresses, however, are large for a small value of moment increase, especially with small L/D values and yield resulting in loss of grip would soon take place.

For the present analysis this difference between elastic and plastic grips is neglected, although further mention of this point is made later in the discussion of the results.

A form is therefore derived which assumes that a shaft will work loose in its sleeve when the friction moment given by

$$M_f = DL\,\mu P_s\left(D + L/2\right) \qquad \ldots\ldots (9)$$

has been exceeded.

The fatigue strength of the assembly is given by $M = Z f_s$ where Z is the shaft section modulus $= \pi/32 D^3$ and F is the fatigue limit stress for the type of assembly and material. This value can only be determined experimentally.

Hence equating:

$$M_f = M$$

$$DL\,uP_s\left(D + L/2\right) = \pi/32\,D^3$$

This gives:

$$L/D^2 + 2\,L/D - \frac{\pi f_s}{16\,P_s\,\mu} = 0 \qquad \ldots\ldots (23)$$

The solution of this expression shows:

$$L/D = -1 \pm \sqrt{1 + \frac{\pi f_s}{16 P_s\,\mu}} \qquad \ldots\ldots (24)$$

L/D is the critical ratio for equal strengths and by substituting appropriate values for f_s, P_s and μ it can be evaluated.

P_s is determined by the shrinkage allowance.

f_s was determined by experiment (fig. 24) and has a value of about 8 Tons/in.^{2}

The value of μ is somewhat more difficult to determine. Static values of coefficient are not thought to be reliable and it has been found (REF. 22) that a lower assembly force for press fits is obtained with pulsating press-in loads. It is also recorded that press-in loads are reduced proportionately with increase of velocity of assembly.

Lack of experimental figures and the considerable fluctuation of

friction coefficients in general leads to the assumption that μ will lie between .1 and .3.

Table 6. has been drawn up for two values of Ps and a range of friction coefficients.

TABLE 6

L/D RATIOS FOR EQUAL STRENGTHS

FIT ↓	P_s ↓	μ →	.1	.15	.2	.25	.3
.001"/in D	5 t/in²		1.03	.76	.6	.5	.43
.002"/in D	10 t/in²		.61	.43	.33	.275	.24

Before applying the derived expression to the present series of test results it is of interest to consider a recent paper "The fatigue of large shafts by fretting corrosion" by O. J. Horger(46).

Horger states that at bending stresses of 19.000-22,000 lb./in.^{2} difficulty was experienced in preventing a test specimen from working loose in its press fit. It was also noted that the holding ability of a press fitted assembly was less than or approached the endurance limit of a shaft having adequate residual stresses, whereas the reverse was generally true without the proper residual stresses. This was the result of the increase in fatigue resistance produced by favourable residual thermal compressive stresses.

Using the test data available in this paper it was possible to determine a friction coefficient (μ) from equation (9) for the stress range of 19,000-22,000 lb./in.^{2} quoted. Assuming slip at 19,000 lb./in.^{2} $\mu = .118$ and at 22,000 lb./in.^{2} $\mu = .136$. A radial pressure of 7 Tons/in from the .0014 in./in. diameter fit allowance was used in the derivation of those values.

Huggenberger(26) when pressing similar sized steel shafts into cast-steel rings (the materials used by Horger) with a lubricant of linseed oil

and tallow found for elastic grips that $\mu = .12$ to break the grip and $\mu = .10$ for motion in assembly or disassembly. Horger's lubricant was white lead and linseed oil.

Baugher's(3) coefficients for pressing steel shafts into cast steel spiders had an average value of .115, varying between .10 and .14.

The remarkably close agreement in these friction coefficient values would certainly indicate that the proceeding analysis involving friction moment strength is substantially correct. Its accuracy will be further tested in the results of the test series which follow.

6.3 SPECIMEN PREPARATION

A Sonderika test machine was the only type available and this restricted the specimen size to a ½ inch diameter shaft.

The specimens were built-up in exactly the same fashion as the split type of static bend specimens (art.5.2)i.e. two shafts joined by a shrunk-on sleeve with a slight gap left between the shaft ends. The gap was achieved by drilling a very small hole in the middle of the sleeve and inserting a wire which separated the shaft ends during shrinking. The wire was later removed.

Initial specimens did not run true in the test machine. Eventually a technique was developed by which the specimens were assembled between centres in a lathe. This gave the necessary degree of alignment for smooth running.

6.4 TEST SERIES

The first test series F.1 was designed to find the critical l/D ratio analysed in the preceding theory for an unlubricated shrinkage allowance of .001 in./in. diameter. Starting with an l/D ratio of .75 the specimen was loaded at a stress value which would probably cause fatigue. Testing several specimens at each stage the grip length was gradually reduced until an assembly failed by the shaft working loose in the sleeve. Various loads were tried at each stage and in general the method was one of trial and error.

Having fixed the critical l/D ratio at .4 Test Series F.2 was carried at this value of grip/diameter ratio and with the same fit allowance. It was hoped in this series to determine the exact load which would produce gradual bellmouthing of the sleeve and eventually failure by working loose.

Despite the utmost care this was found impossible. All failures took place just after the machine was started when the critical load had been reached or exceeded. Below the critical load no failure took place and the specimen ran on indefinitely. One specimen only broke this general rule and failed after a period of running.

This sudden failure is now known to be a property of the friction grip but at the time of testing the friction theory had not been developed. In some of the later tests the load was increased every .5 x 10^6 cycles until the grip loosened or a load sufficient to produce fatigue was reached.

Series F.3 and F.4 were also carried out with an L/D ratio of .4, but with an unlubricated fit of .002 in./in. diameter and a sperm oil lubricated fit of .004 in./in. diameter respectively. These series were also designed to find a critical bellmouthing load.

In these two latter series an effort was made to measure any progressiv bellmouthing. A micrometer head was fixed over the centre of the running specimen and readings of deflection were taken at intervals. No success was gained with this simple rig, the deflections not changing during any test.

Series F.5 was carried out with a varying L/D ratio and a lubricated fit of .002 in./in. diameter. The loads to produce fatigue or grip failure were determined in each case.

All the test series results are recorded in the Tables which follow.

FATIGUE

6.5 RESULTS AND DISCUSSION

From the results of those assemblies which gave fatigue of the shaft, the S-N curve (fig.24.) has been drawn. This shows that for a mild steel shaft (yield stress 16 tons/in.^{2}) with a shrink fitted sleeve, the fatigue yield limit is approximately 8 tons/in.^{2}. This figure is in line with similar work carried out on press and shrink fitted assemblies.

Figures 26A and 26B show typical fractures of the shafts. It is noticeable that fracture occurs just inside the grip and not just outside as has been reported(31). There was considerable evidence of fretting at the entry to the sleeve and the fretting cracks can clearly be seen spread round the shaft circumference. Specimens which did not fail also showed signs of fretting corrosion and confirmed the idea that although the fretting by itself may not cause failure it weakens the shaft and fatigue occurs at a lower stress than would normally occur without its presence.

The first series of tests (Table 7) showed that with a .001 in./in. fit allowance and unlubricated shrinkage the I/D ratio which gave equal strength of shaft and grip lay between .4 and .5. These figures are very similar to those obtained by the theoretical analysis with assumed values of μ, the coefficient of friction. With an unlubricated fit it is quite usual for μ to be between .25 and .3, these values being derived from push out tests(42).

It is interesting to compare the curves drawn by Dorey(13) (fig.25) relating the axial thickness of a web and radial thickness of metal round the bore with conditions of (1) constant strength of grip and constant shrink allowance, and (2) constant strength of grip and constant hoop

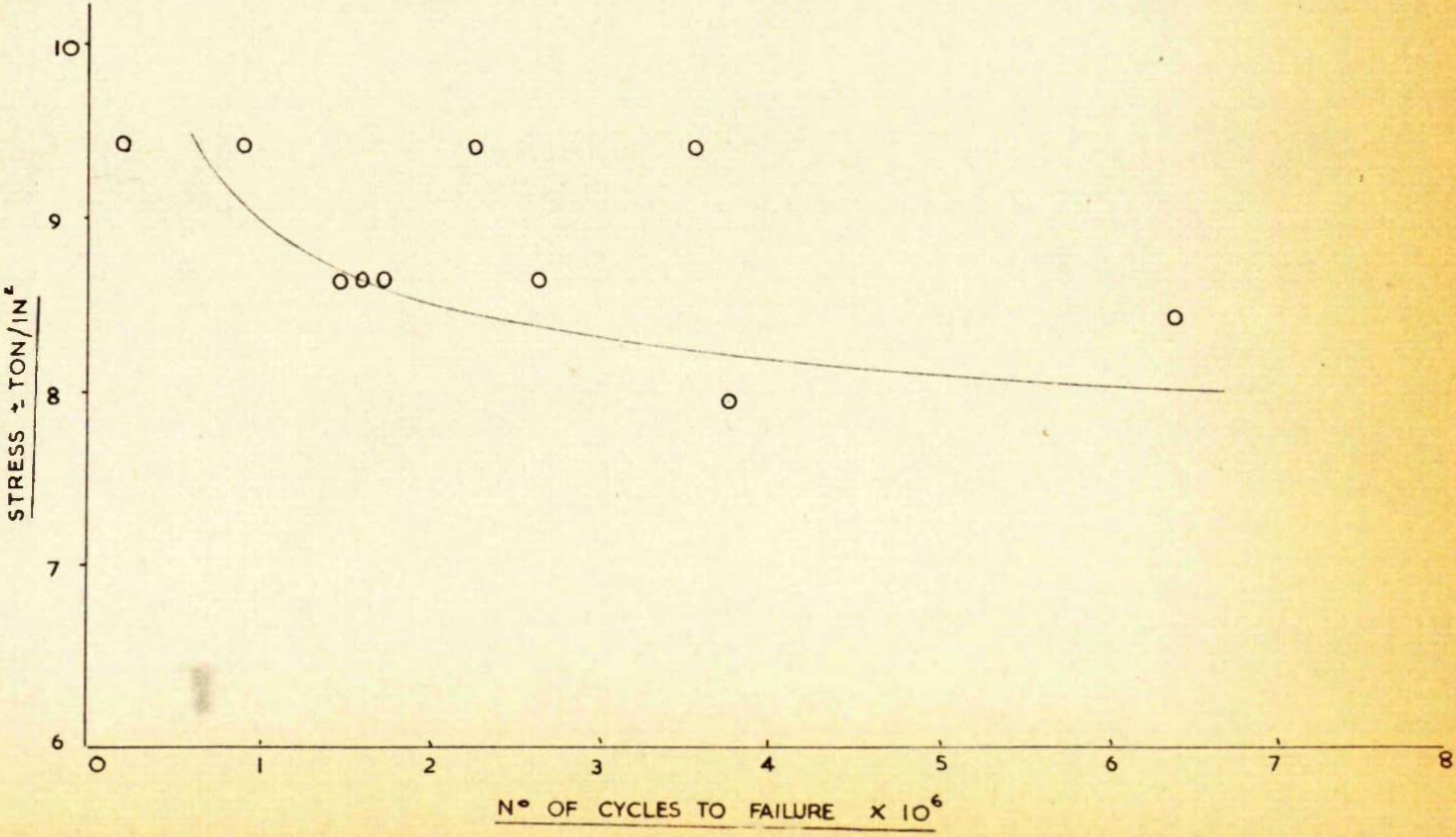

FIG. **24**. FATIGUE OF SHRINK FITTED MEMBERS

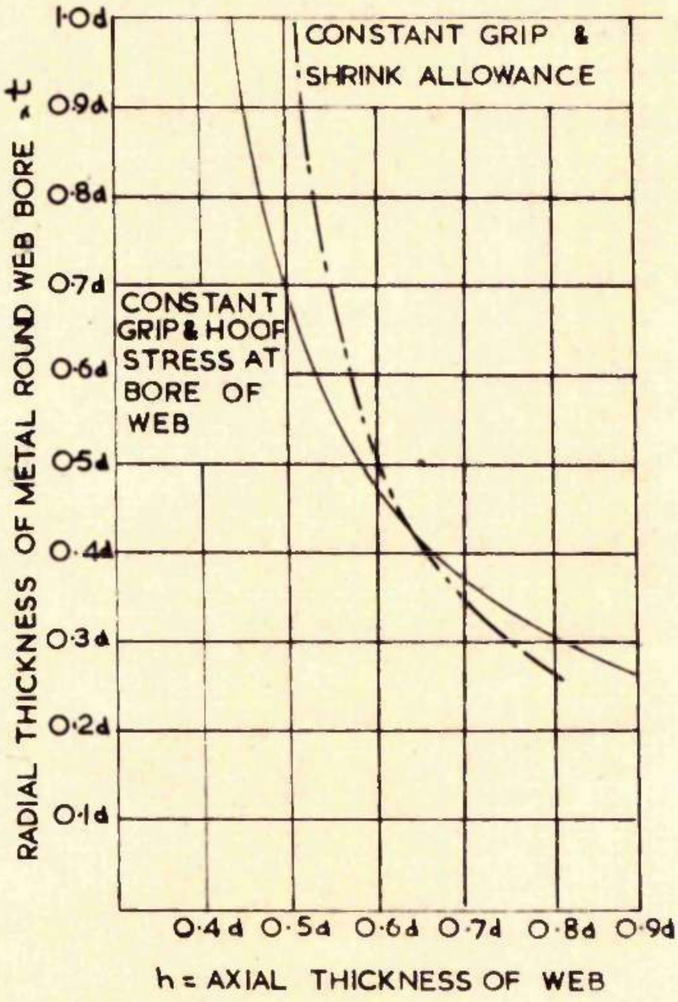

FIG.25.

FROM S.F. DOREY'S 'STRENGTH OF MARINE SHAFTING' stress at the bore. The grip strength is based on the friction grip when subjected to torque with web proportions given by Lloyd's Rules. The curves show that below a value of web thickness given by T/D = .45 to .51, the strength cannot be increased by increasing the metal thickness round the bore. Although these graphs do not bear a direct relationship to the fatigue work reported here, it is of interest to note that similar limiting proportions have been found analytically and experimentally with a shaft assembly subjected to fluctuating bending moments.

Tables 8, 9, 10 and 11 show the results for various conditions of fit and grip length. The column of friction coefficients is based on the results and calculated from equation 9, art. 4.4.

It is seen that the unlubricated fits of series F.2 and F.3 give μ values between .14 and .36. This range of μ value is similar to that generally obtained with static push out tests on unlubricated shrinkage fits. In general, the coefficient values of series F.2 with elastic grip conditions are somewhat higher than the F.3 figures with plastic grip conditions. This may be because no account has been taken of the possible fact, mentioned previously, that the elastic grip can withstand further moment loading after slip until the crushing stresses cause plastic flow. The differences, however, are small when one considers the inaccuracies which could arise in the assessment of the shrinkage pressure in such small specimens.

The lubricated .004 in./in. diameter fit tests recorded in Table 10 show a μ range of .115 to .165 which once again is in agreement with static push out tests for lubricated conditions.

Table 11 shows that with a lubricated fit of .002 in./in. diameter grip failure occurs at an L/D ratio of .6. This is consistent with the

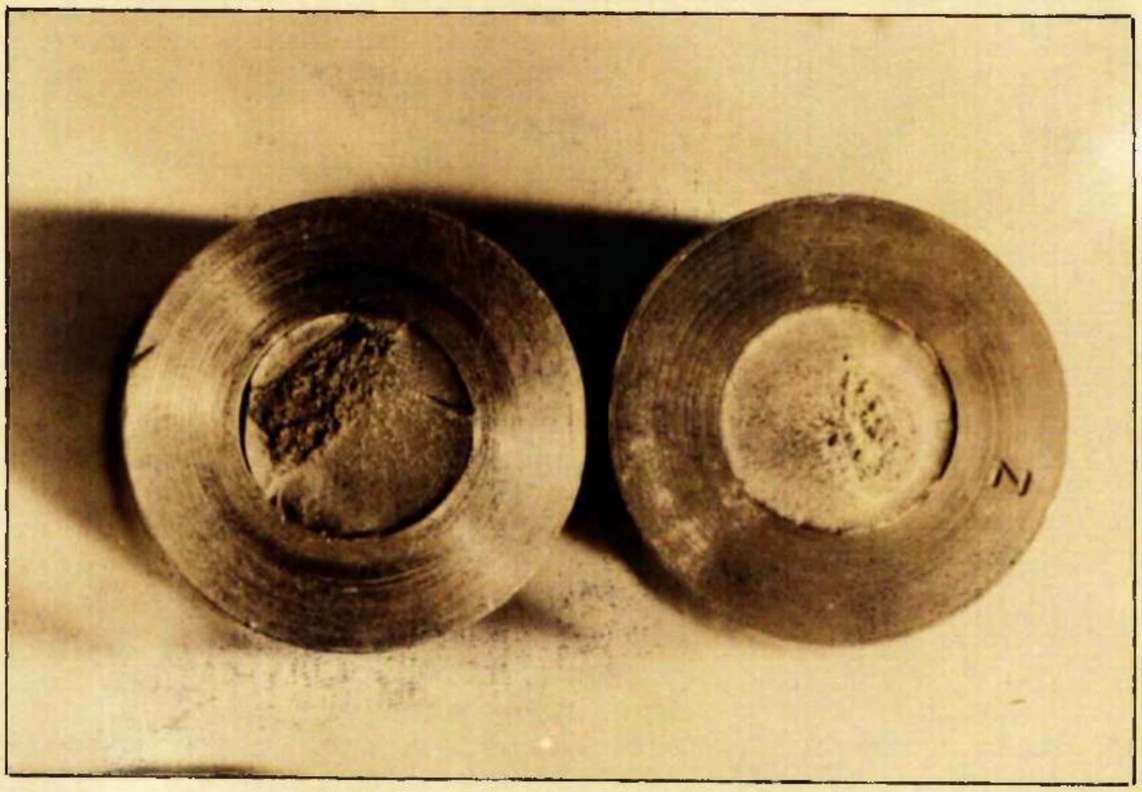

FIG. 26A

FIG. 26B.

BROKEN SHRINK-FIT FATIGUE SPECIMENS

theoretical analysis using an assumed value of $\mu = .10$ (see Table 6, art. 6.2). The μ values obtained are similar to the previous lubricated series.

All the tests have shown that friction μ values are obtained from the theoretical analysis which agree in general with accepted statically obtained figures. Werth(44) however, showed that lower values of press-in loads were obtained using pulsating loads and showed that the rate of pushing in considerably affected the load required. The scope of the present fatigue series however does not offer any conclusive evidence in this problem.

In the tests where the shaft worked loose in the grip, the nature of the failure gave some indication of the mechanism of failure. As previously recorded, despite the utmost care, it was only possible in one test to apply a load which gave failure of the grip after a period of running. In all other tests where the grip failed, failure occurred within 10,000 reversals of the critical load having been applied, and in most cases, within 100 reversals. This would seem to indicate that slip of some nature occurred in the grip in a similar fashion to that recorded in the static bend tests. It is emphasised, therefore, that once slip does occur, the applied moment, no longer carried by friction forces alone, is transferred from shaft to sleeve by a radial pressure distribution. This quickly causes the sleeve to open up and the shaft to work loose. Although a grip which was elastic under shrinkage forces might take a larger load to work loose after slip than a plastic grip, this additional "post-slip" strength is of little value since in most of the cases considered the plastic grip had a higher slip load. The elastic strength to resist bellmouthing is considerably less than the additional strength due to the presence of higher friction forces,

since it takes a very small load to convert an elastic grip to a plastic one.

The one specimen (No. 7 Series F.4) which worked loose after a considerable period of running (1.4 x 10^6 reversals) was examined closely. Much fretting was evident and it is suggested that this fretting caused a reduction in grip length, with a corresponding reduction in friction forces.

One further reason for the sudden failure mechanism experienced in the tests is the possible reduction in μ, the friction coefficient, after slip. Static push out tests show that after the initial load to produce movement or slip is reached a lower load is sufficient for the next slip, indicating a reduction in μ.

A similar reduction in μ in the present series would mean that a sudden load, previously carried by the friction forces, is thrown on to the sleeve by way of high crushing stresses which soon destroy the grip.

It is perhaps of interest to compare the accepted theory for the working loose of a shrink or press fitted assembly. The A.S.M.E. Handbook (p.184) quotes ".. the crushing stress should not exceed the unit pressure due to the fit allowance if the joint is not to loosen." On this basis the specimens tested should have worked loose at much lower loads, the actual values being some two or three times greater than the theoretical.

Some general conclusions to be drawn from the complete Fatigue Series are as follows:

(1) Grip failure would appear to be the result of high contact stresses, following the slip of the frictional forces set-up by shrinking. Bellmouthing to any serious degree was not observed where a grip had not failed completely and indications are that bellmouthing will not take place unless the friction grip has been overcome.

(2) Fretting corrosion was observed in all the tests which produced shaft fatigue and the nature of the failure emphasised the serious effect which fretting has on the endurance limit of the assembly.

(3) The recommended conditions for a strong shrinkage grip undergoing bending actions are high shrinkage pressure and high coefficient of friction. High shrinkage stresses (even in plastic range) do not seem to harm the grip strength although their effect on the fatigue strength may be detrimental.

TABLE. 7.

SERIES F.1.

TEST RESULTS

FIT ·001 IN/IN DIA. NOT LUBRICATED P=5 TONS/IN^2

SPECIMEN N°.	L/D RATIO	LOAD LBS.	SHAFT STRESS TON / IN^2	N° OF CYCLES TO FAILURE	TYPE OF FAILURE	REMARKS
1	·75	130	9·45	$\cdot 2 \times 10^6$	SHAFT FATIGUE	BREAK AT FACE OF SLEEVE
2	·75	120	8·7	$1{\cdot}76 \times 10^6$	"	BREAK AWAY FROM SLEEVE FACE
3	·625	120	8·7	$1{\cdot}64 \times 10^6$	"	"
4	·625	120	8·7	$1{\cdot}5 \times 10^6$	"	BREAK AT FACE OF SLEEVE
5	·625	130	9·45	$3{\cdot}59 \times 10^6$	"	"
6	·5	110	8·0	$3{\cdot}77 \times 10^6$	"	"
7	·5	130	9·45	60	GRIP FAILED	
8	·5	130	9·45	$\cdot 99 \times 10^6$	SHAFT FATIGUE	BREAK AT FACE OF SLEEVE
9	·5	130	9·45	$2{\cdot}29 \times 10^6$	"	"
10	·5	120	8·7	$2{\cdot}65 \times 10^6$	"	"
11	·4	120	8·7	0	GRIP FAILED	

TABLE.8.

SERIES F.2.

TEST RESULTS

$L/_D = \cdot 4$

FIT = ·001 IN/IN DIA. NOT LUBRICATED P = 5 TON/IN^2

SPECIMEN N°	LOAD LBS.	SHAFT STRESS TONS/IN^2	N° OF CYCLES TO FAILURE	FRICTION COEF^T	REMARKS
1	50	3·65	–	–	NO FAILURE AFTER 10^7
2	70·55	5·42	–	–	"
3	80·6	5·86	–	–	"
4	82	597	–	–	"
5	84·75	6·16	50	·25	
6.	84·95	6·18	–	–	NO FAILURE AFTER 10^7
7	89·85	6·52	200	27	
8	109 65	7·98	50	·325	
9	120	8·7	0	36	

TABLE 9

SERIES F.3.

TEST RESULTS

$L/D = \cdot 4$

FIT = ·002 IN/IN DIA. NOT LUBRICATED $P = 9$ TON/IN^2

SPECIMEN Nº.	LOAD LBS.	SHAFT STRESS TONS/IN^2	Nº OF CYCLES TO FAILURE	FRICTION COEFT	REMARKS
1	60	4·35	–	–	NO FAILURE AFTER 10^7
2	75	5·43	–	–	"
3	85	6·16	0	·14	
4	117 85	8·54	0	·214	
5	124	9·0	7×10^4	·225	
6	114	8·26	0	·21	

TABLE.10.

SERIES F.4.

TEST RESULTS

$L/D = \cdot 4$

FIT ·004 IN/IN. DIA. LUBRICATED (SPERM OIL) P_s = 11 TON/IN²

SPECIMEN N°.	LOAD LBS	SHAFT STRESS ± TON/IN²	FRICTION COEFᵀ.	N°. OF CYCLES	REMARKS
1	73·5	5·32	·1	0	NOT RUNNING TRUE
2	84·15	6·1	·11	6480	
3	68·85	4·98	–	10×10^6	NO FAILURE
4	109·65	7·95	·15	0	
5	114·75	8·34	·154	3780	
6	99·45	7·2	·135	0	
7	122·35	8·9	·164	$1·4 \times 10^6$	FRETTING AT GRIP

TABLE.II.

SERIES F.5.

TEST RESULTS

FIT= ·002"/IN DIA. LUBRICATED (SPERM OIL) P_s = 9 TON / IN^2

SPECIMEN N°	L/D RATIO	LOAD LBS.	SHAFT STRESS TONS/IN^2	N° OF CYCLES TO FAILURE	FRICTION COEFᵀ	REMARKS
1	8	117	8·5	6·45×10^6	–	FATIGUE OF SHAFT
2	6	114·25	8·3	O	·135	GRIP WORKED LOOSE
3	5	88·25	6·4	O	·13	"
4	4	58·65	4·25	O	·11	"

NOTE:- LOAD INCREASED EVERY 5×10^6 CYCLES UNTIL GRIP LOOSENED OR LOAD SUFFICIENT TO PRODUCE FATIGUE REACHED

7. MODEL CRANK TESTING MACHINE

7.1 INTRODUCTION

Initial specifications of the crank testing machine showed that it should be capable of applying to a 3" diameter model Diesel Marine single throw crankpin, a loading cycle similar to that on an actual engine. The bearing pressures on the crankpin should be capable of being increased to 1 Ton/in² giving the maximum load range of the apparatus as 0 to 9 Tons approximately.

It was agreed that the machine was not intended for a fatigue investigation but rather as a means of studying any progressive changes which might occur at the shrink grip under combined torsional and bending loading.

These conditions demanded a set-up which was not in the usual run of testing machines and the final suggestions for a suitable design were restricted to two proposals.

The first scheme considered employed the inertia forces of a reciprocating mass, and is shown diagrammatically in fig.**27**. The driven crank actuates a mass connected at the crosshead and the range of loading can be controlled by varying the mass or the speed of the drive. The loading cycle obtained by this means is restricted to the form of the Inertia curve shown in fig.**32** under the heading Analysis of Loading, and would not cover the effects of the gas loading.

To simulate the conditions at the aft end of a crankshaft the test crank should transmit a torque. This torque is superimposed in the Inertia Machine by means of a closed gear train which could be prestrained to give any desired value of torque. Employing this system, the power required to

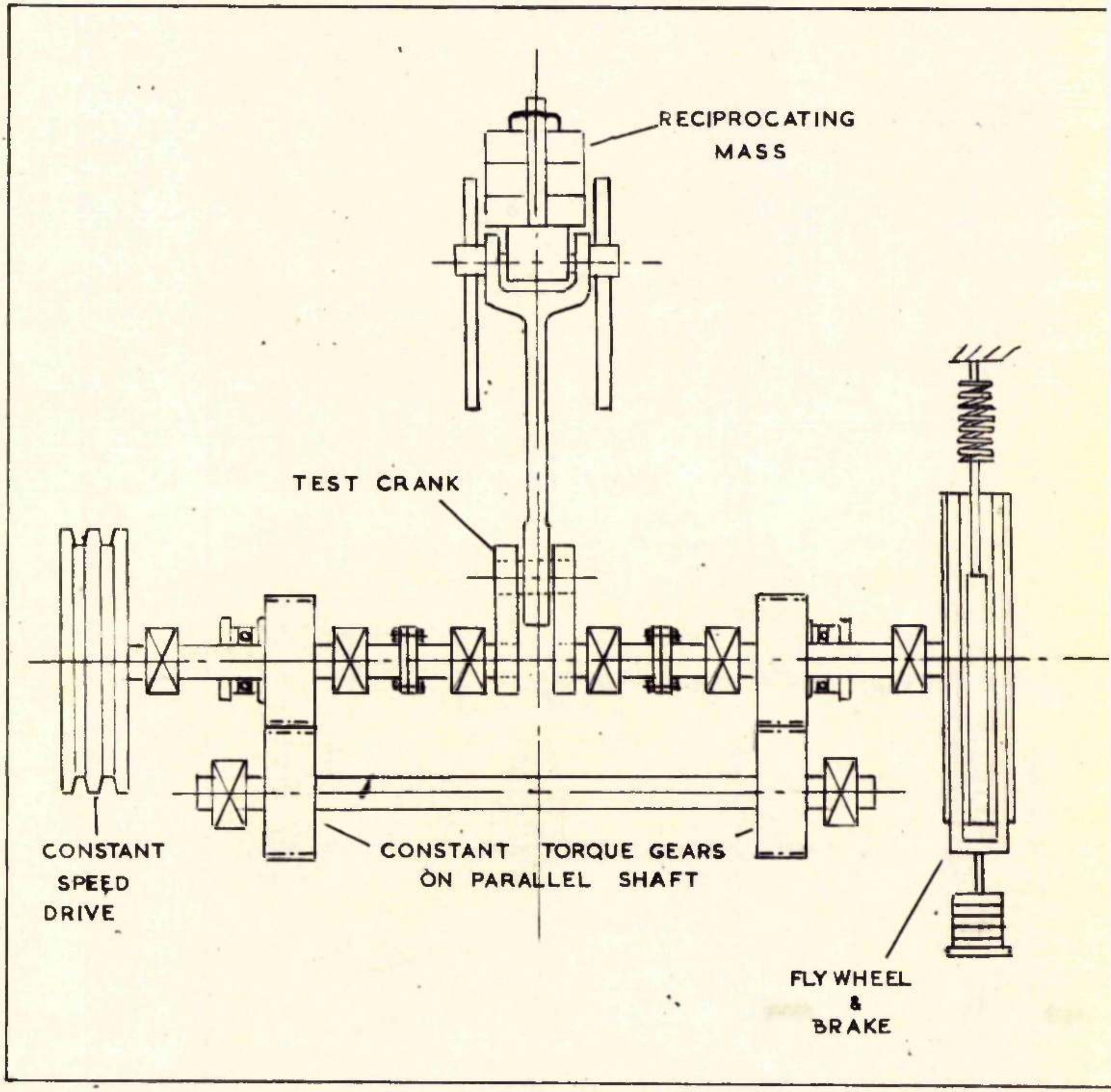

FIG 27

INERTIA TYPE CRANK TESTING MACHINE (DIAGRAMMATIC) run the test crank is simply that to overcome friction effects. It soon became evident that this arrangement would be somewhat inflexible and would involve large masses if the running speeds were to be as low as in practice. An alternative system using a stationary crank was then developed and this second proposal was the design accepted and built.

The principle of this machine is based on the fact that for any crank angle and connecting rod inclination the force in the connecting rod can always be replaced by a pair of component forces acting tangentially and radially at the crankpin (see fig.32). Hence the loading cycle on a rotating crank can always be reproduced on a stationary crank by applying the correct combination of cyclical component forces to the crankpin. This will be further explained later.

The fluctuating component forces are obtained by a hydraulic system. Four cam driven pumps or pulsators, the cam shape representing the loading cycle required, supply pulsating pressures to four hydraulic rams acting on a common loading block at the crankpin.

The loading range of each component can be controlled by the introduction to each hydraulic circuit of a variable elastic medium in the form of an air bag. Varying the initial air quantity controls the maximum cycle pressure.

A torque can be applied at one end of the crank by means of a lever arm and calibrated springs, and is taken off at the other end by a fixed arm. The use of springs ensures that the varying torque from the crankpin loading will be taken off at the fixed end of the crank as in actual practice.

Thus a system is produced which can simulate closely the loading cycle

of an actual crank and have the added advantage of a stationary model on which recordings such as strain values may be readily taken.

The complete design and building of the testing machine including the principles involved are now described in detail.

7.2 TEST RIG

Before building the complete test machine it was considered advisable to check the principles involved on a less extensive set-up. Several design features were new in character and likely to provide teething troubles which could possibly be overcome on the final machine in the light of the test-rig experience gained.

Accordingly a simple test-rig was built and proving tests carried out with it. The test-rig is shown in figs. 28 and 29. It consisted of a similar hydraulic system to that already described for the actual crank tester except that there was only one pulsating load. One cam driven pulsator supplied a fluctuating pressure to one loading capsule set up to strain a simple built-up frame.

The original pulsator design contained a small 1 cu.in. rubber air bag to provide the variable elasticity of the system. It was found, however that this bag did not supply a sufficiently large pressure range since the frame deflection was considerably more than the design figure. Unforeseen shear and web buckling effects on the short length of beam used were considered as likely causes of the excess deflection. It was decided, therefore, to use the air bag of a Greer Accumulator (volume 10 cu.in.) and this was found to give a more satisfactory range of loading. The maximum load of 11.2 tons was still somewhat less than the original design figure of 20 tons.

Two types of cam were tested: (1) A cam giving simple Harmonic variation of piston displacement, and (2) a cam with a sharp rise and fall over 180° and a dwell period of 180°.

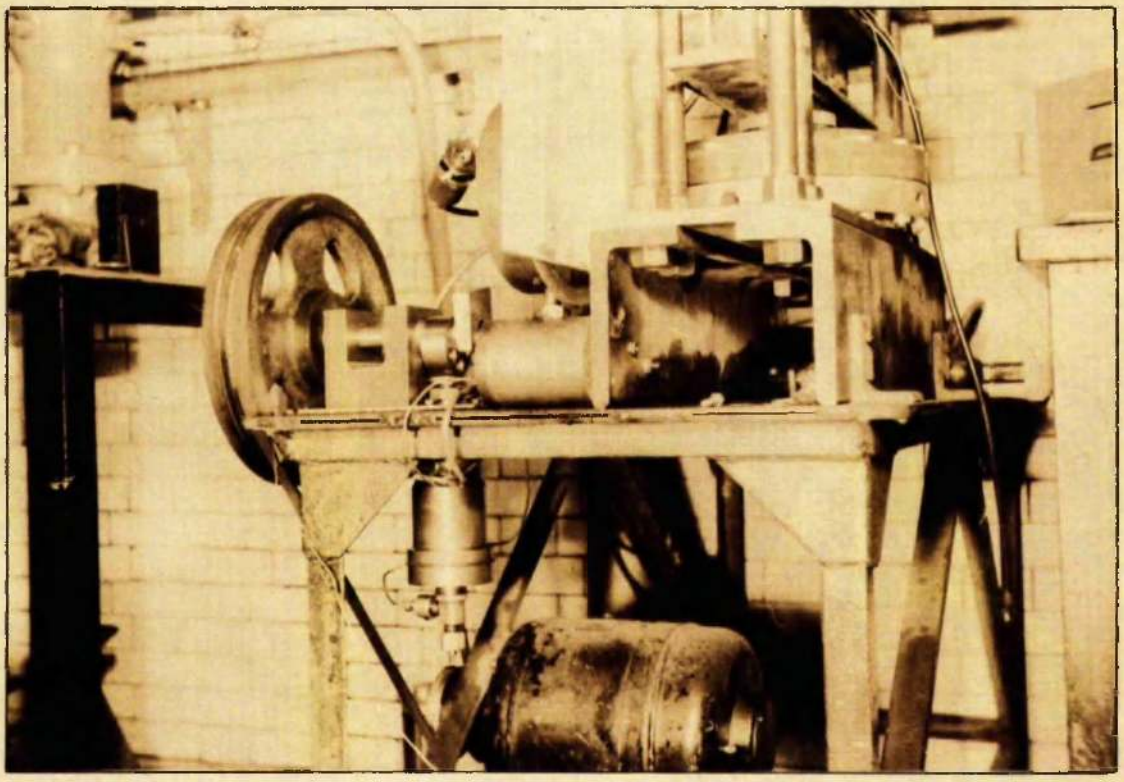

FIG.28.

TEST RIG ~ SHOWING CAM, PULSATOR & DRIVE

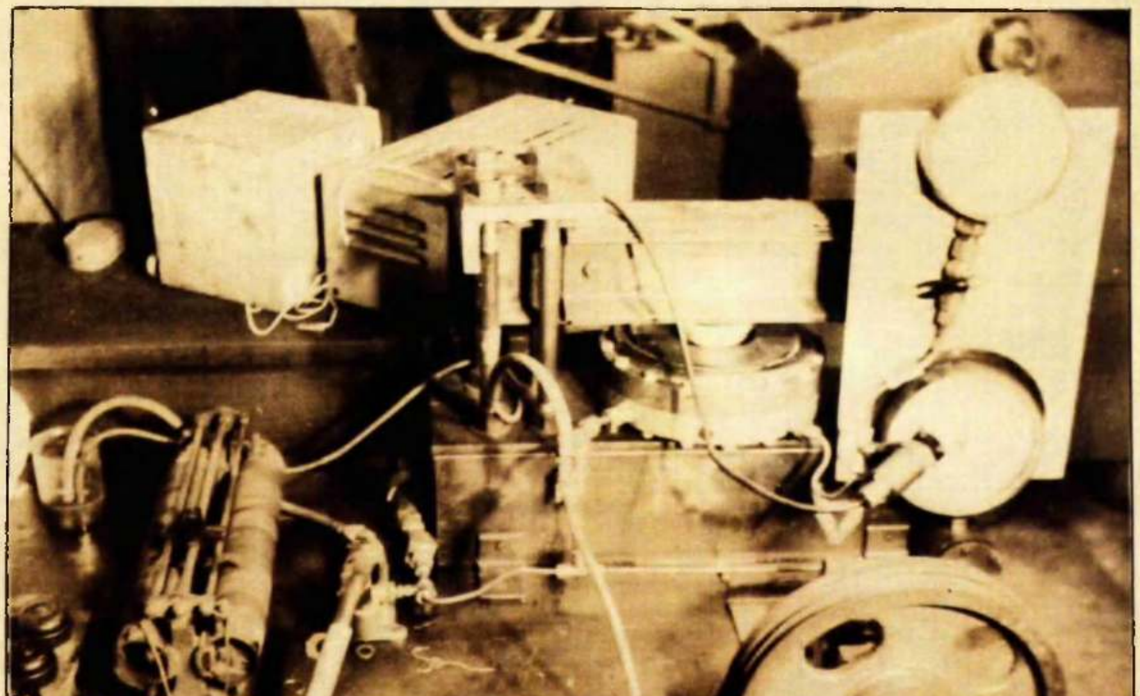

FIG. 29.

TEST RIG ~ SHOWING CAPSULE & LOADING FRAME

The following variables were noted for each test:-

(a) Base pressure and pressure range when the cam was turned over slowly by hand is given by a pressure gauge. This gauge, connected to the capsule, was previously calibrated by applying loads on a 50 Ton Avery machine and noting the corresponding pressure. The calibration curve is shown in fig.30.

(b) Speed of cam rotation - from a tachometer.

(c) Quantity of air in bag, i.e. full or empty. Intermediate tests were also carried out but are not recorded here as it is considered that these two conditions cover the extreme cases likely to be encountered.

(d) Circuits were set up to take oscilloscope recordings of beam strain and pressure in the capsule. It was found that only pressure readings could be taken with cam No.2 since the strain signal needed amplification and only an a.c. preamplifier was available. This amplifier gives satisfactory results with a constantly changing voltage signal as with the S.H.M. cam No.1 but does not in the case of cam No.2 where there is a dwell period, i.e. a period of constant voltage signal. The strain gauge recordings are not included in this report since the curves obtained were not well defined due to the unavoidable stray interference acting on the oscilloscope when it was operating at full gain. The general form of the curves, however, agreed with the pressure recordings.

These pressure signals were obtained from a C.A.V. photoelectric pick-up unit which gave a very satisfactory performance. An oscilloscope camera was used to obtain permanent records although some difficulty was experienced in holding the trace steady. This was a

FIG. 30.
CALIBRATION OF MACKLOW-SMITH HYDRAULIC CAPSULE

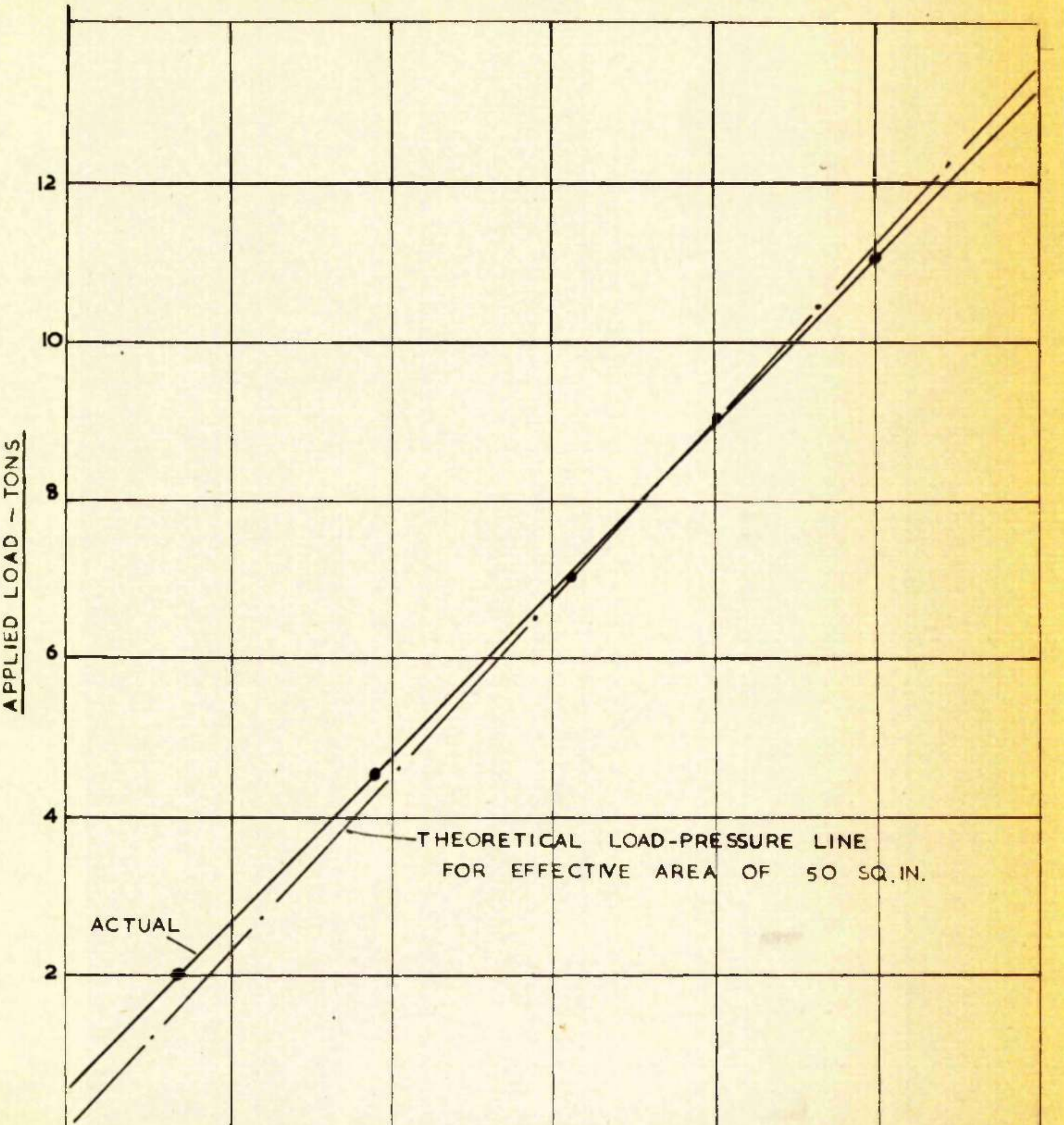

result of the oscilloscope being used at its minimum time base frequency while the pulsator was operating at its maximum speed of about 500 r.p.m.

A top dead centre marker signal was arranged to indicate any lag or lead effects in the pressure wave signal.

RESULTS

Fig.31A shows the traces for the S.H.M. cam (No.1) operating with air bag full and empty. The curves are clearly of S.H.M. form. The effect of the air quantity on the maximum load is evident, in addition to the fact that it seems to produce a greater lag (84° of cam rotation as against 52° when there is no air in bag).

Fig.31B shows the traces for the cam No.2 together with the theoretical form drawn to the same scale. The lag effects are not illustrated by displacing the actual and theoretical traces the required amount, since it was the shape differences which were considered most important.

With no air in the bag the trace is seen to follow the theoretical form quite well despite the lag of about 25°. Some loss of form is evident at the end of the loading stroke and the beginning of the dwell period. This rounding off effect is more evident with the air bag full where there is once again an increased lag. The general form, however, still follows the theoretical as well as could be anticipated.

The difference in loading ranges with the two cams is due to the cam displacements being inequal. No.2 cam had a greater stroke.

CONCLUSIONS AND SOME RECOMMENDATIONS FOR COMPLETE TEST MACHINE

The need of a very rigid frame was emphasised by the tests. Higher loads could be obtained by increased piston displacements but a more rigid structure would help towards the same end in addition to making the major

TEST RIG RESULTS FIG.31.

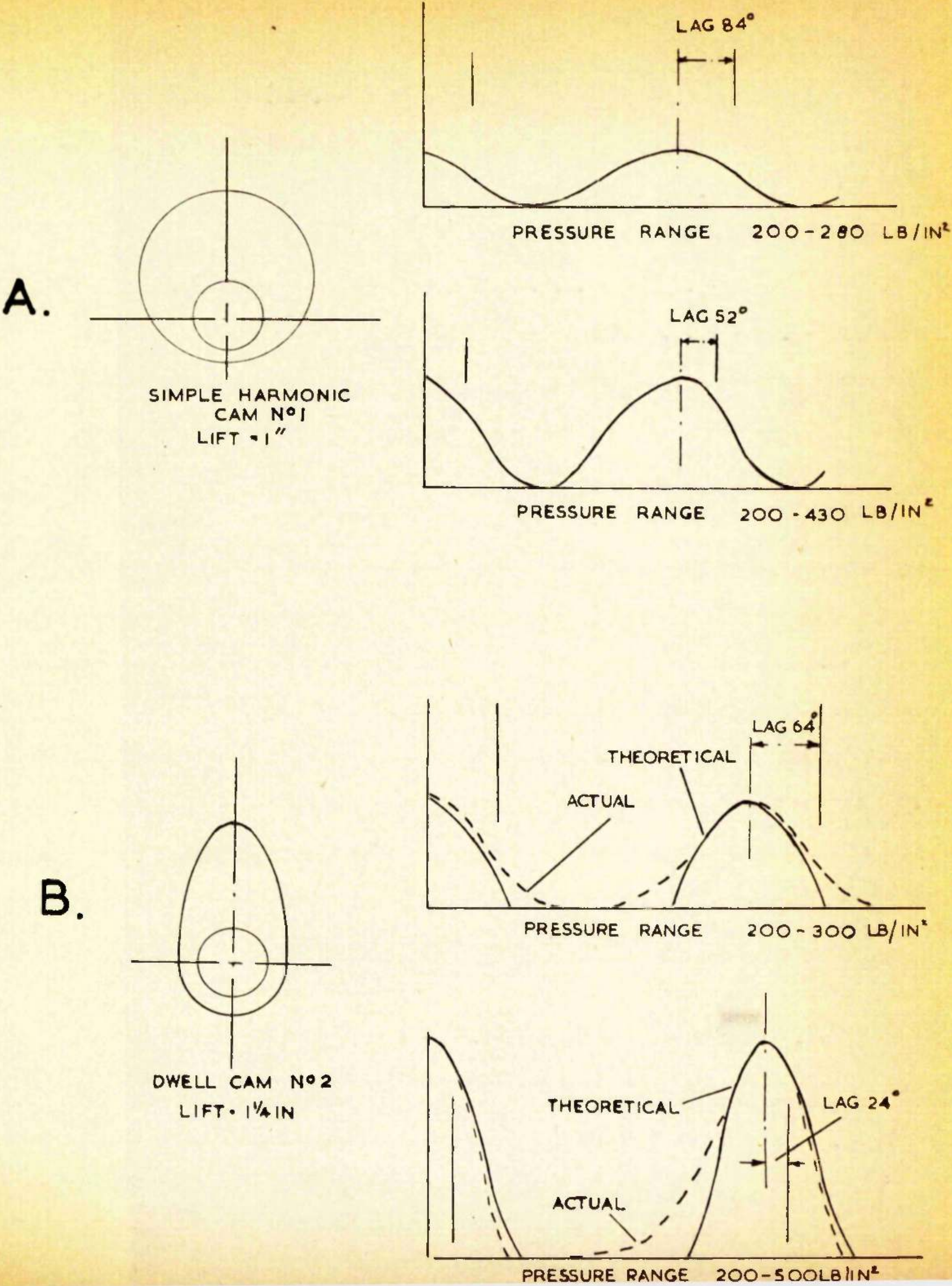

part of the system elasticity controllable by the quantity of air in the bag.

The greatest platen movement recorded was .018 inches. The makers quote a permissible static displacement of $\pm\frac{1}{8}$ in. or a dynamic displacement of $\pm1/32$ in. so there would appear to be no risk of damaging the rubber bonding with greater fluid displacements. Increases however are not recomended since they would result in greater hysteresis losses in the rubber and greater heat production in the oil from the increase of flow rate.

The Greer Accumulator was found to be an ideal unit for providing the variable system elasticity. It has the advantage that it cannot be overinflated.

At the speeds anticipated in the final test machine it is seen that the pressure variation follows the pulsator piston movement quite adequately. The S.H.M. cam made for much smoother running which was to be expected since the accelerations involved were much lower. Cam No.2 required a considerable base pressure to prevent the follower leaving the cam on the up stroke.

The difficulties of lag in the pressure curve could be overcome where necessary by an adjustable angle cam arrangement, the correct angle being obtained from a C.R.O. and pressure pick-up with phase marker. The C.A.V. pressure pick-up was found to give a quick, reliable, and easily recorded load reading. The capsule and pressure gauge may be easily calibrated and the pick-up quickly calibrated before a test.

One obvious source of trouble was in the overheating of the cam and follower, producing heating of the complete hydraulic system. The test-rig

lubrication was not adequate and it was thought that a liberal supply of lubricant to a roller bearing follower would help to minimise the heat production.

7.3 ANALYSIS OF LOADING

To illustrate the cyclic loading on a Marine Diesel Crankpin a set of weights, sizes, indicator diagrams, etc., was obtained from an actual engine. The following representative quantities per cylinder have been used in the loading analysis:

Reciprocating mass	4.5 Tons
Rotation mass	2 Tons at 29.5" radius
Maximum gas load on piston	210 Tons

Speed 120 r.p.m. Con rod/crank radius = 4 : 1

Fig.32A shows the individual gas and inertia loads over one cycle referred to the engine crosshead. Fig.32B gives the combined gas and inertia loading diagram. This diagram is now referred to the crankpin by considering the load P coming through the connecting rod. Load P has been divided into perpendicular component loads V, in a radial direction, and H, at right angles, and termed "tangential load". Load H is the "torque" or "working" component.

Fig.32C shows the component loads to a base of crank angle. It is seen that could these cyclic component loads be applied to a stationary crankpin with the same load profile and phasing, normal running engine con-rod loading conditions would result.

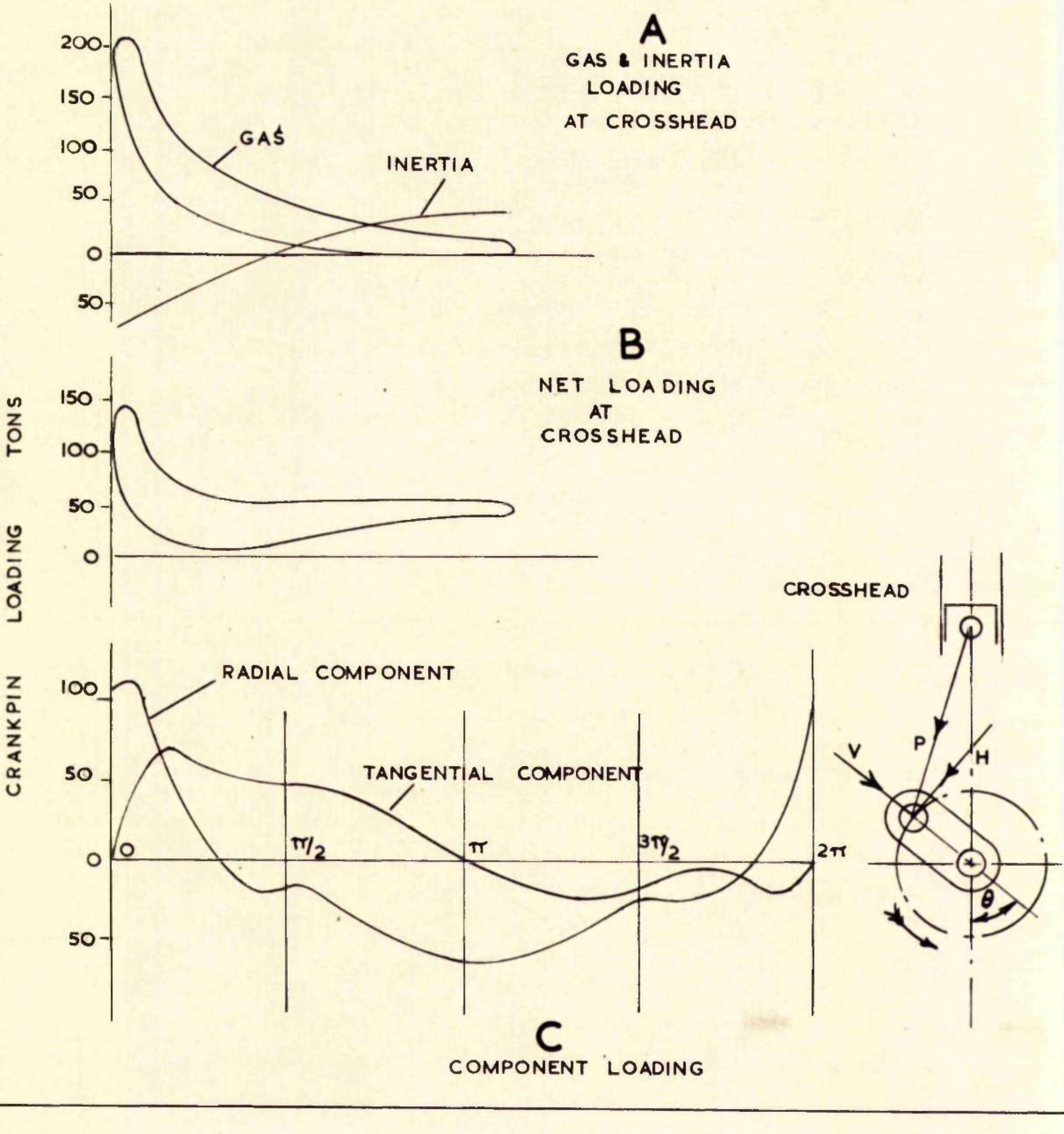

FIG.32.

ANALYSIS OF LOADING

7.4 PRINCIPLES AND GENERAL DESCRIPTION

It has already been stated that the testing machine operation is based on the fact that for any crank angle and connecting rod inclination, the force in the connecting rod can always be replaced by a pair of component forces acting tangentially and radially at the crankpin. The loading analysis has shown the type of cyclical component loading that must be applied to a stationary crank.

A hydraulic system was devised to apply these component loads and is shown diagrammatically in fig.33. Four small pumps or pulsators, driven off a common shaft, supply pulsating pressures to four loading capsules or hydraulic pistons. A capsule is in effect a cylinder with its piston bonded to its walls by a flexible rubber joint. Thus a pulsator and capsule connected together form a completely closed hydraulic system. When the piston moves downwards, fluid flows to the capsule whose piston, with a relatively large area, 50 sq. in., applies a load proportional to the system pressure set-up. Any deflection produced by this load allows the piston to move under the control of the rubber bonding.

If the system fluid is considered incompressible and the deflection of the member to which the load is applied remains elastic under the loading range, it is seen that the capsule load will be proportional to the displacement of the piston in the pulsator. Thus a cam-driven piston will apply loads represented by the displacement profile of the cam. This essentially is the system employed, with four cams shaped and phased to give the correct loading in four directions. Four capsules are required since a capsule can only supply unidirectional loading, and each component of the loading analysis has both positive and negative values.

HYDRAULIC SYSTEM - DIAGRAMMATIC FIG.3

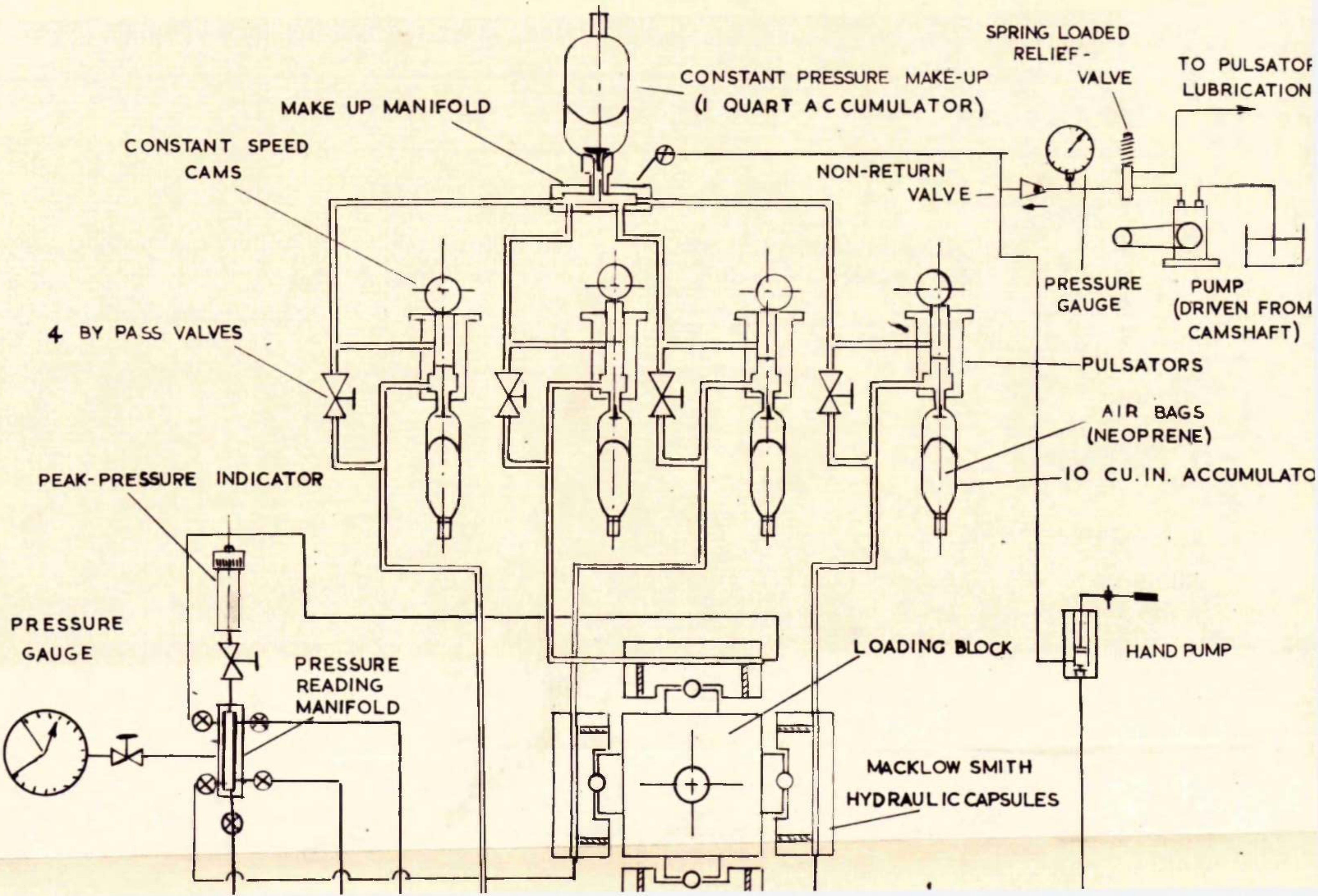

The system as it stands can only supply one range of loading for each set of cams, the maximum value reached depending on the cam lift and the capsule deflection. This would make the system somewhat inflexible since a new set of cams would be required to vary the range of loading. To overcome this handicap a variable elastic medium in the form of a rubber air bag has been placed in each pulsator-capsule system. By controlling the amount of air in the bag, a control is placed on the maximum pressure attained in the system. Thus for the same cam profile the maximum cycle load can be controlled by the amount of air in the bag - a small amount for large loads and a large amount for small loads. One difficulty is the fact that a rubber bag filled with air will not contract or expand elastically under the varying cycle pressure but according to some law $PV^N = C$. This has been overcome to some extent by imposing a base pressure of 200 lb./in.^{2} on the system which means that for the range of the $PV^N = C$ curve over which it is operating, the air in the bag is nearly behaving as an elastic medium, the curve being practically a straight line. This base pressure has the additional advantage of supplying a return load for the pulsator pistons, thus reducing the strength of return spring required.

It has been stated that each capsule and pulsator form one separate sealed unit. This is not quite correct since it is inevitable that there will be some leakage past the pulsator pistons. To compensate for this loss and to maintain the base pressure, each piston at the top of its stroke uncloses a port in the pulsator wall connected to a constant pressure supply. This port is also necessary for the return flow of fluid when a capsule piston or platen is compressed by the movement of the loading block

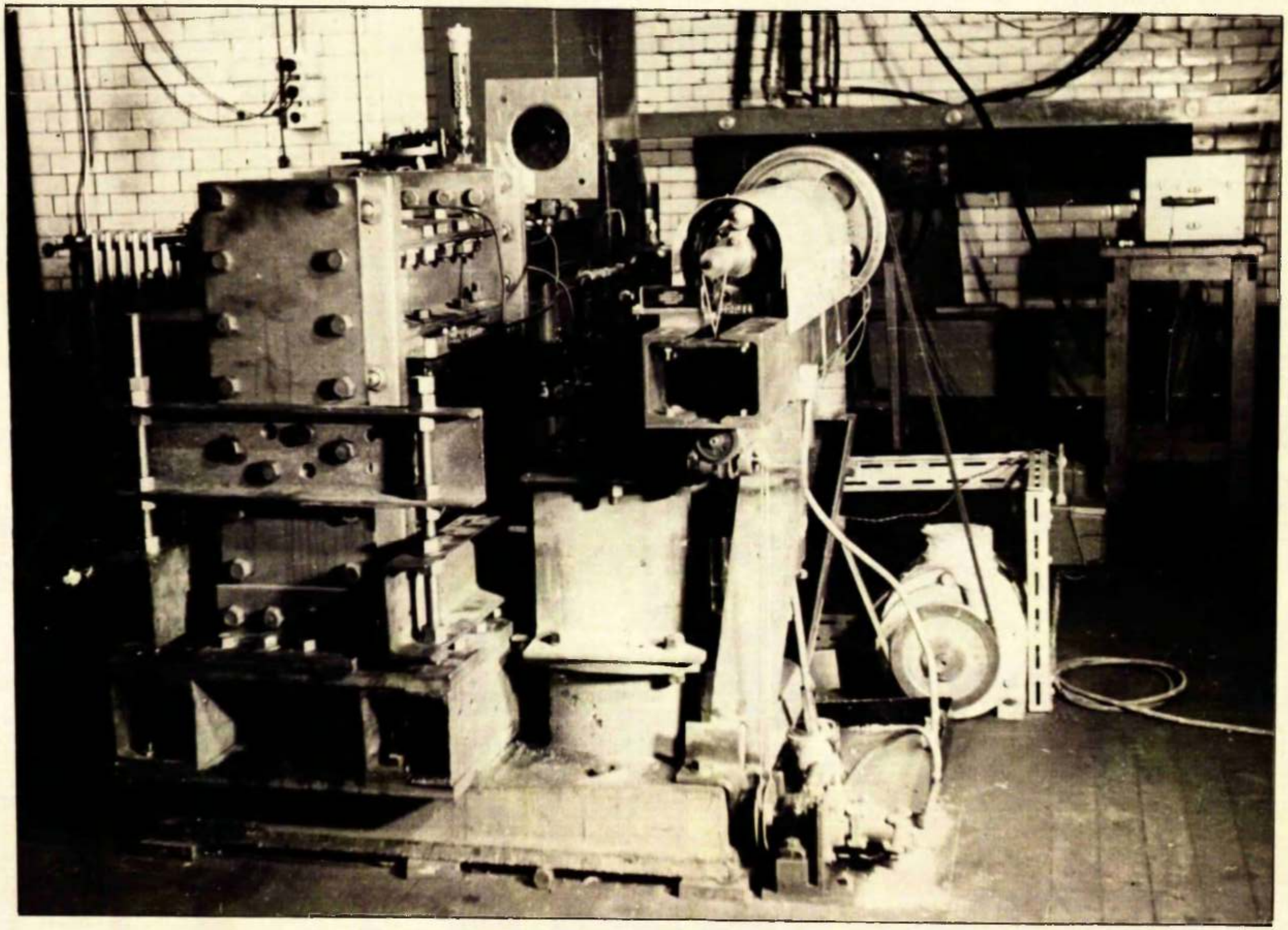

FIG. 34.

GENERAL VIEW OF TEST MACHINE

under the action of the opposite capsule. If the port were not present, the cam profile would have to be shaped to allow the pulsator piston to move to accommodate this inflow of fluid. As it is, a period of dwell can be made in the cam when the opposite cam is applying a load.

The make-up system consists of a quart size Greer Hydraulic Accumulator which is a larger size than the air bag unit used in the pulsator-capsule circuits as a loading control. This unit is described in detail later, and it is sufficient to say that it consists of a steel cylinder in which an air bag can be filled with air or nitrogen. When used as a leak make-up, the cylinder is half filled with fluid and half with air. As the fluid leaks from the system, the air bag expands, maintaining the pressure, since small volume changes do not affect the air pressure substantially. It was found that under long testing conditions the leakage was such that the base pressure did fall and an additional make-up system had to be fitted.

This consisted of a small pump driven off the cam shaft with a relief valve on the outlet feed which was connected to the Accumulator or base pressure manifold. The relief valve was set to maintain the base pressure, while the overflow which was not considerable as the pump was driven very slowly, was used for lubrication of the pulsator cams and guides. A non-return valve in the supply line of the make-up ensured that no pressure was lost in the system should the pump fail for any reason. The pulsator leakage and lubricant are led back through a filter to the pump providing constant no-loss circulation.

A small hand pump was used for priming and bleeding the system, while a foot pump with a special adaptor supplied by the makers was employed for

filling the accumulator air bags.

The pressure supply line from each pulsator has a connection to the make-up or base pressure with a screw down valve control. This is provided in order that the machine may be run without loading the test crank, the large accumulator damping out the pressures when the valves are open. The valves are also opened when starting in order that the initial torque on the motor is reduced.

Each capsule has a connection to a valve manifold from which all pressure recordings are taken. A pressure gauge gives static pressure values and a Dobbie McInnes Peak Pressure Indicator (see page 136) records the maximum cycle pressure in each capsule. Also connected to the manifold is a C.A.V. Photoelectric pick up unit for use in conjunction with an oscilloscope to show the pressure wave forms. The test crank is supported in two bearings with the webs vertical and the crankpin uppermost. Built round the crank is the loading frame supporting the loading capsules.

Both crank ends can be fixed to prevent rotation or one end can be fixed while a torque is applied at the other end by means of a torque arm and springs. The spring stiffness is such that all the torque from the capsule tangential component loads is taken off only at the fixed end, the small deflection having practically no effect on the spring load.

Safety devices include two cut-outs. One (page 139) operates in the base pressure system and cuts out the motor when the pressure falls below a predetermined value. The other (page 139) consists of four limit switches arranged at right angles, set to cut the motor when the crank shaft deflection exceeds a certain value.

Both the pulsator arrangement and the loading frame are built compactly on a cast iron base plate, the piping lengths thus being kept to a minimum.

A general picture of the testing machine has just been given, and all the components will now be described in much greater detail, with particular reference to the machining and building where the component design is original.

7.5 LOADING FRAME

The loading frame which supports the specimen and the loading capsules is shown in fig.35&36.

It is completely built up of mild steel plate, channel, I beam and angle. The base is of box form made up of two 1" thick plates and four 6" x 3" channel sections.

The uprights and crosspiece are of box form made with 6" x 5" I beam and ½" plates, all bolted together with 4" x 4" and 3" x 3" angle at the corners. The whole frame is bolted to a cast iron base plate which is mounted on four vibration damping rubber blocks.

The test crank specimen is supported in two bearing blocks fixed rigidly to machined pads on the top plate of the frame base, the set screws passing through pads and plate. The blocks are made in halves and spiggoted with a grease cap supplying grease to the grooves cut in the bearing surfaces.

The first test carried out caused considerable fretting damage to the bearing surfaces despite the use of various anti-seize compounds such as molydenum desulphide and harded bushes are now being fitted to the blocks in a further attempt to reduce the fretting.

The load on the crankpin is applied through a large block halved diagonally and spiggoted. This block is also now being fitted with a hardened bush.

The four loading capsules are set at right angles round the loading block. Three are bolted to the uprights and crosspiece, while the fourth is supported on the lower plate of the box section base and applies its load through a hole cut in the upper plate between the bearing blocks.

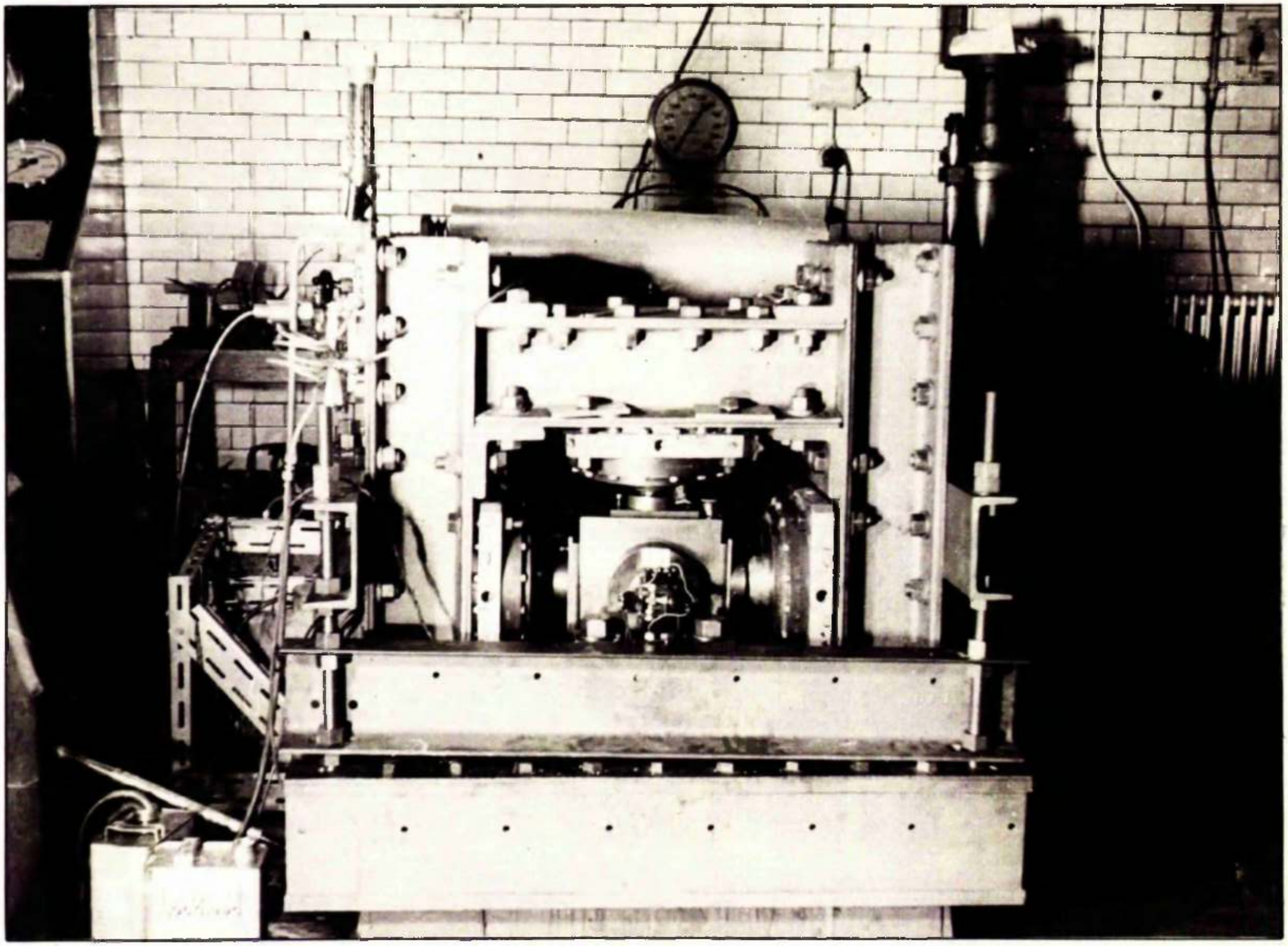

FIG. 35.

GENERAL VIEW OF LOADING FRAME

LOADING FRAME FIG.36.

SCALE ÷ 1:10

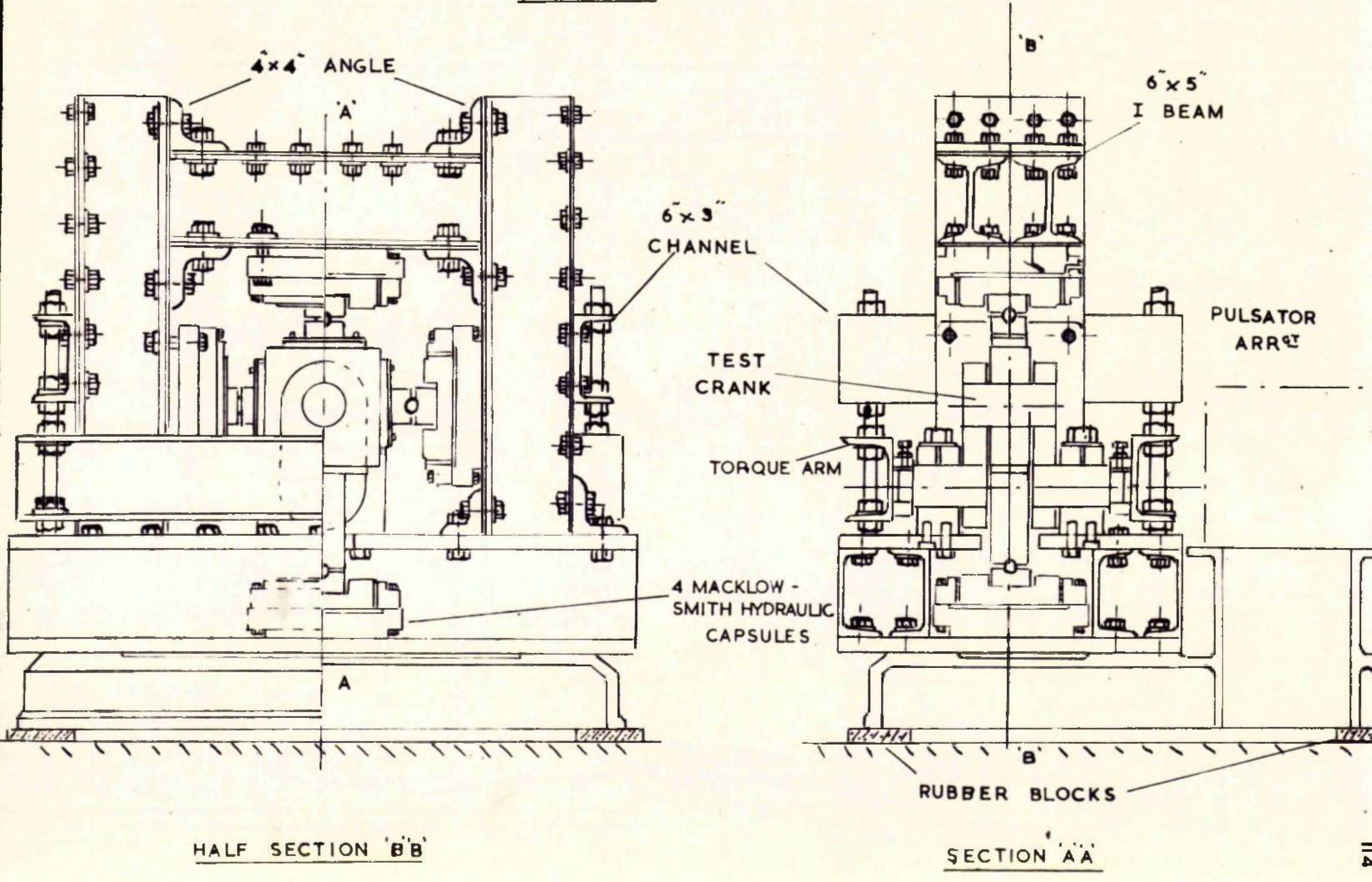

All loads are transmitted from capsule to block through a cup and ball joint and fitted distance pieces. The cup and ball ensures that no transverse load is carried by the rubber bonding of the capsule.

The 6" x 3" channel torque take-off arms are bolted at each end to the base and uprights by means of a 1" screwed rod and nuts, which permit adjustment of the arm should the specimen not be sitting squarely in position.

A square boss with a square hole machined in it is welded to the centre of each torque arm. The square ends of the specimen fit into these holes and are held rigidly by set screws screwed on to clamping plates. The set screws can be locked as they tend to work loose under the vibration loading.

7.6 TORQUE SPRINGS See fig. 39.

Two torque springs have been designed and made for the application of a fixed torque at one end on the test crank to simulate to some extent the torque coming from the other cylinders, assuming the test crank to be the aft throw.

The springs have not been used to date as it is thought that for the preliminary testing, conditions imposed on the crank should be as simple as possible. This is the case with both ends fixed when both journal and both pin shrink-fit grips receive a similar loading cycle. The journal fits are subjected to torque and bending while the pin fits only receive bending moment loading.

The springs are calibrated and give a loading rate of 200 lbs./in. They are arranged to give a pure torque and their loading rate is such

that all the torque from the crankpin loading is taken off at the fixed torque arm. The pure torque is obtained by an arrangement of the springs in which one presses down on one side of the torque arm and the other pulls up at the other. The springs are attached to the frame and torque arm by ¾" diameter screwed rods and adjusting bolts.

7.7 PULSATOR UNIT

There are four pulsator units each being the source of a pulsating pressure for a loading capsule. One complete unit is shown in detail in fig.37. It consists essentially of three sections:-

(1) Cam and follower.

(2) Plunger and cylinder.

(3) Hydro-pneumatic accumulator.

Each section will be described separately.

(1) Cam and follower

The four pulsators are driven by cams on a common $1\frac{1}{2}''$ diameter shaft supported in three self-aligning double roller bearings. Each cam is locked to a sleeve which is keyed to the shaft and prevented from moving axially by a locked grub screw, engaging in a dimple in the shaft. The cam is locked to the sleeve by a large locking piece or nut and adjustment plates. There are two such adjustment plates, one pinned to the cam and one to the sleeve. One face of these plates has radial teeth or serrations which engage when pressed together, producing in effect a type of clutch drive. Hence the cam can be rotated relative to the sleeve and locked in a different position altering the phasing of the pressure wave relative to the three other pressure waves.

The cams are of mild steel, case hardened after machining. The original set of cams is shown in fig.41 . These cams were rough milled and finished to the design profile by hand, the shapes not conforming to any easily machined form. As will be reported later more fully, these cams did not give the smooth running conditions hoped for and had to be changed later to ones giving a sinusoidal pressure cycle. The holes

PULSATOR DETAILS FIG. 37.

SCALE:- 1/4 SIZE

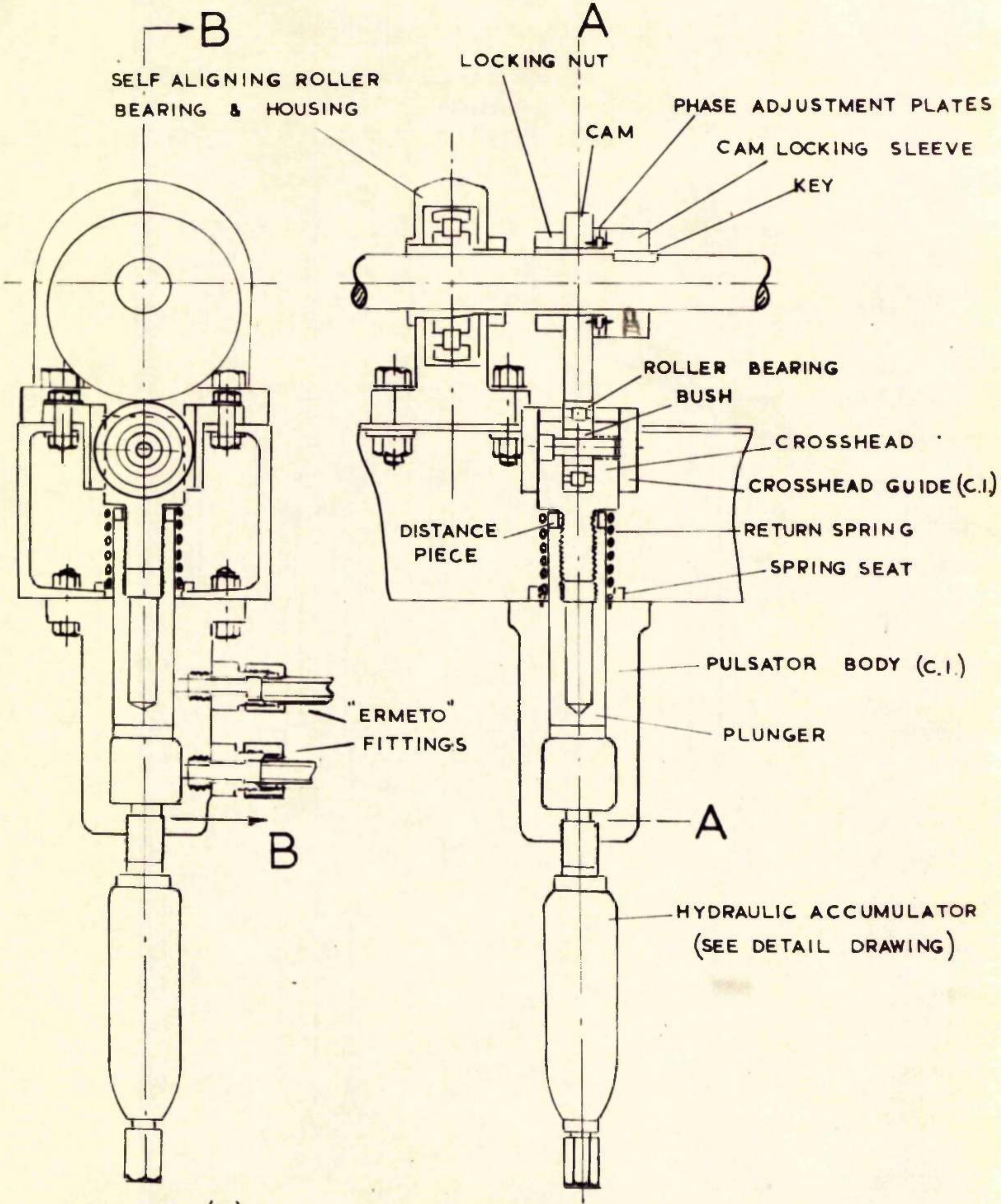

SECTION ON 'AA'

SECTION ON 'BB'

in the shown cams were for lightening.

The cam follower is formed by a $2\frac{1}{2}$" diameter double roller bearing set in a cylindrical crosshead which runs in a cast iron guide. The follower is prevented from rotating by means of slots in the guide in which the roller bearing sides engage. The fitting of the crosshead and guide presented some difficulty. The cylindrical crosshead and guide were first machined, honed and lapped to give a smooth running fit. The slot was then milled in the crosshead and the hole for the roller bearing holding set-screw drilled. The milled slot tends to produce a loss of fit in the guide and the bush on which the roller runs had to be accurately shimmed and fitted so that when the whole unit was tightened up by the set-screw a close running fit resulted. Any slackness in the guides would tend to defeat their purpose, which is to carry the side thrust from the cam ensuring that the plunger is axially loaded only. The guides are attached to the pulsator frame by two $\frac{3}{8}$" diameter bolts.

The lower portion of the crosshead is turned down and screwed to engage in the screwed bore of the pulsator plunger. A distance piece between the crosshead and plunger was fitted such that the make-up port in the pulsator body was just completely uncovered at the top of the stroke.

A return spring is set between the crosshead and the frame, being kept clear of the upper portion of the plunger by the distance piece and a seat screwed to the top of the pulsator body. The spring is light and is used principally to return the crosshead and plunger when lining up is being carried out. Normally the fluid pressure keeps the roller on the cam.

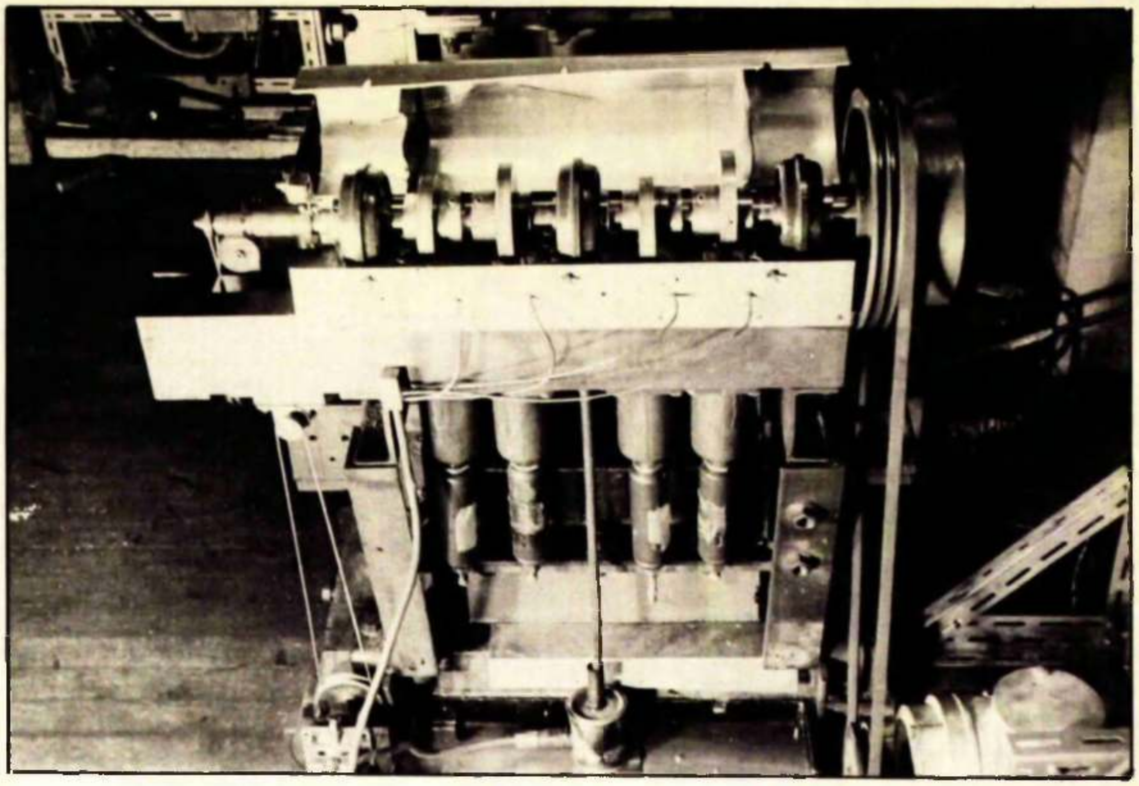

FIG. 38.

PULSATOR ARRANGEMENT

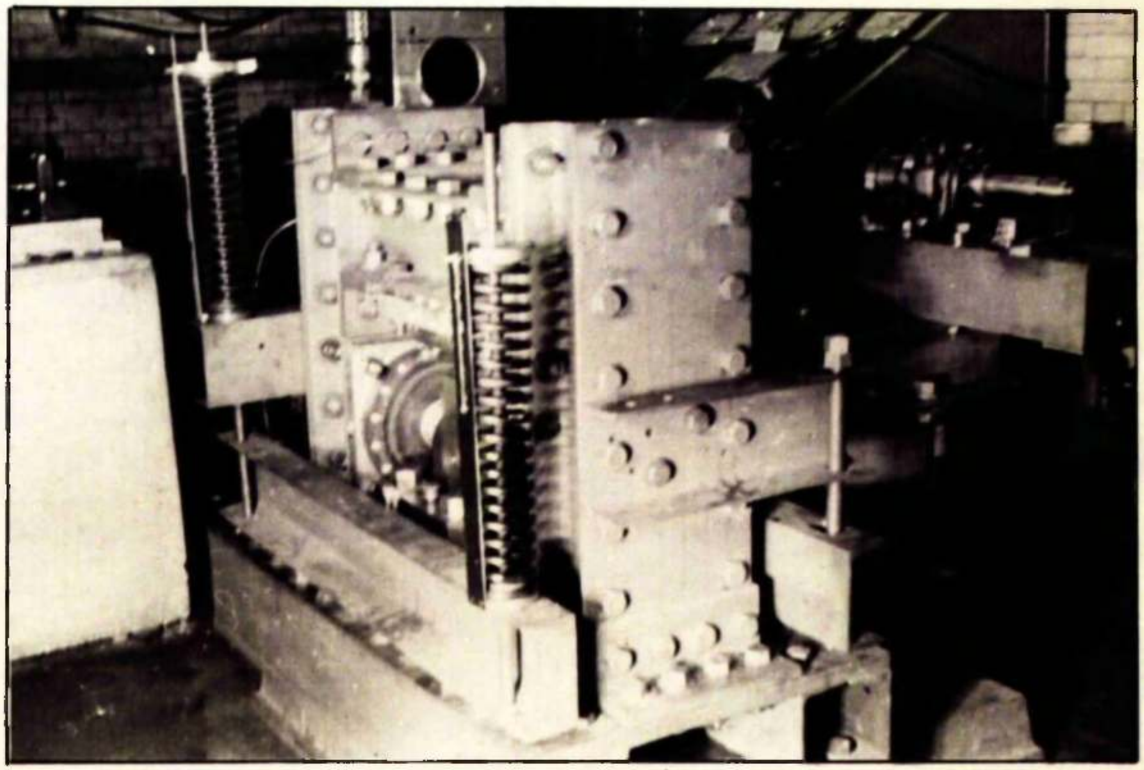

FIG. 39.

LOADING FRAME WITH TORQUE SPRINGS IN POSITION

FIG.40. PULSATOR ARRANGEMENT (SPLASH COVER REMOVED)

SCALE:- 1:10

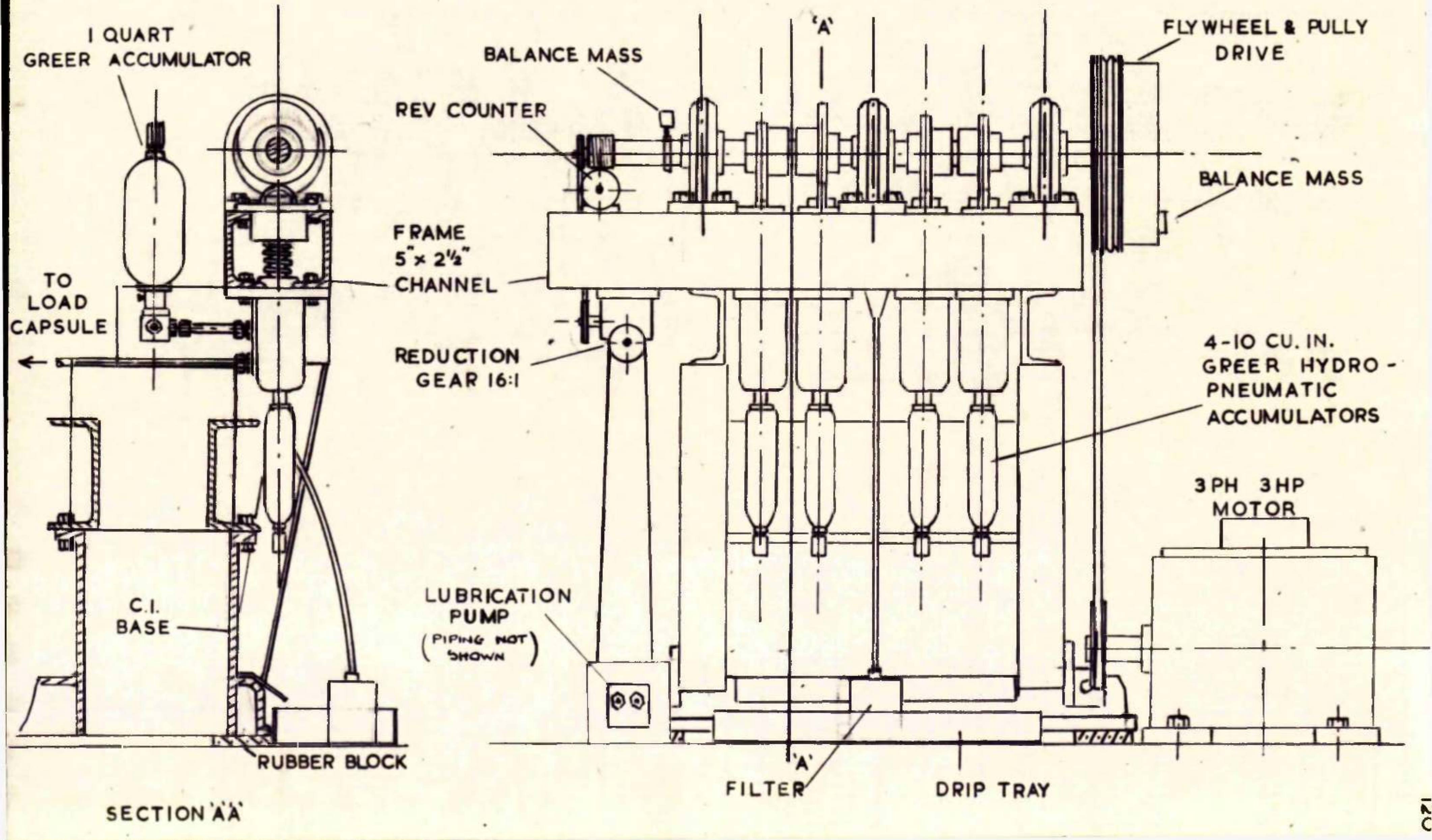

(2) Plunger and Cylinder

The plungers are of case hardened mild steel and were ground, honed and lapped to the bores of the mechanite cast-iron pulsator bodies. A good fit is essential to withstand the high pressures with a minimum of leakage past the plunger. The plungers are bored out to reduce the mass and internally screwed to fit the crosshead guide.

The pulsator body has two side ports, one a make-up supply at the top of the stroke, the other the pressure supply to the loading capsule. The pipes are connected to these ports by "Ermeto" high pressure fittings.

The pulsator is attached to the frame by four $\frac{5}{8}$" diameter bolts. Considerable care had to be taken with the lining-up of the pulsator cylinder and crosshead guide to ensure free running conditions. Although both sides of the box frame had been machined as accurately as possible, the channel section tended to distort when bolts were tightened up, throwing the machined faces out of truth. The pulsator body was first bolted firmly to the frame base and the crosshead guide bolts gradually tightened down using shims where necessary, until the guide was firmly fixed and the crosshead moved freely when pressed down, returning under the action of the light return spring. This procedure sometimes took a considerable period of time and it was soon realised that matters would have been made much easier had the frame been of cast-iron which would give a much more rigid structure.

(3) Hydro-pneumatic accumulator

To the end of each pulsator is screwed a Greer Hydro-Pneumatic Accumulator which acts as a pressure control device. This patent unit

is fully described on page 124 and it is not proposed to give any further details here. The male screwed end of the accumulator fits the tapered female thread in the pulsator body giving a high pressure seal.

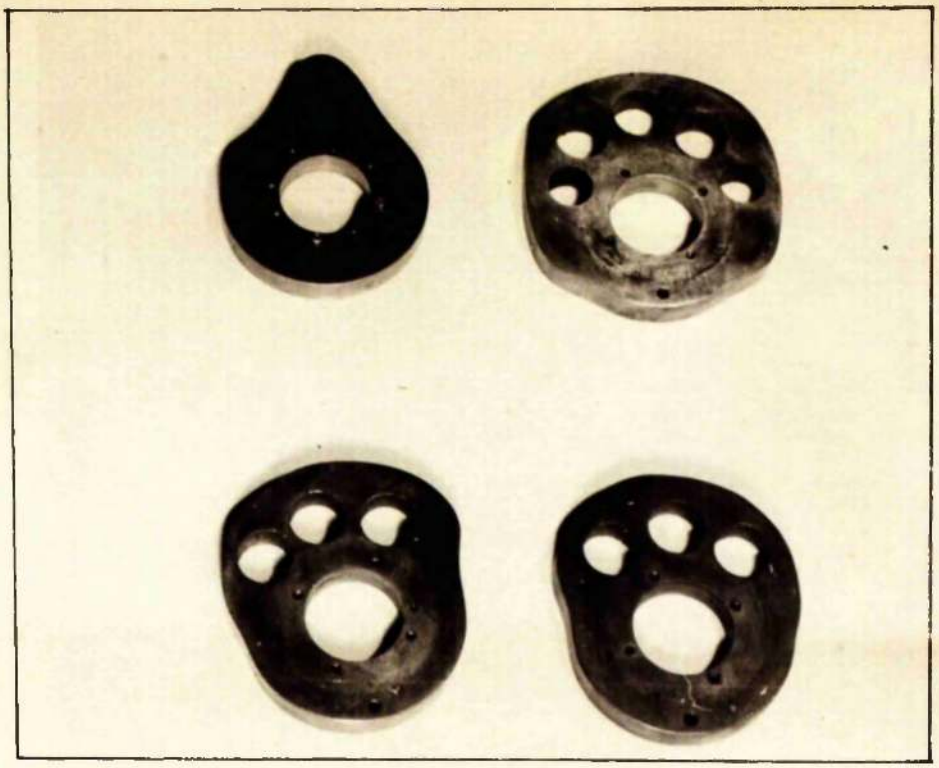

FIG. 41.

ORIGINAL TYPE CAMS

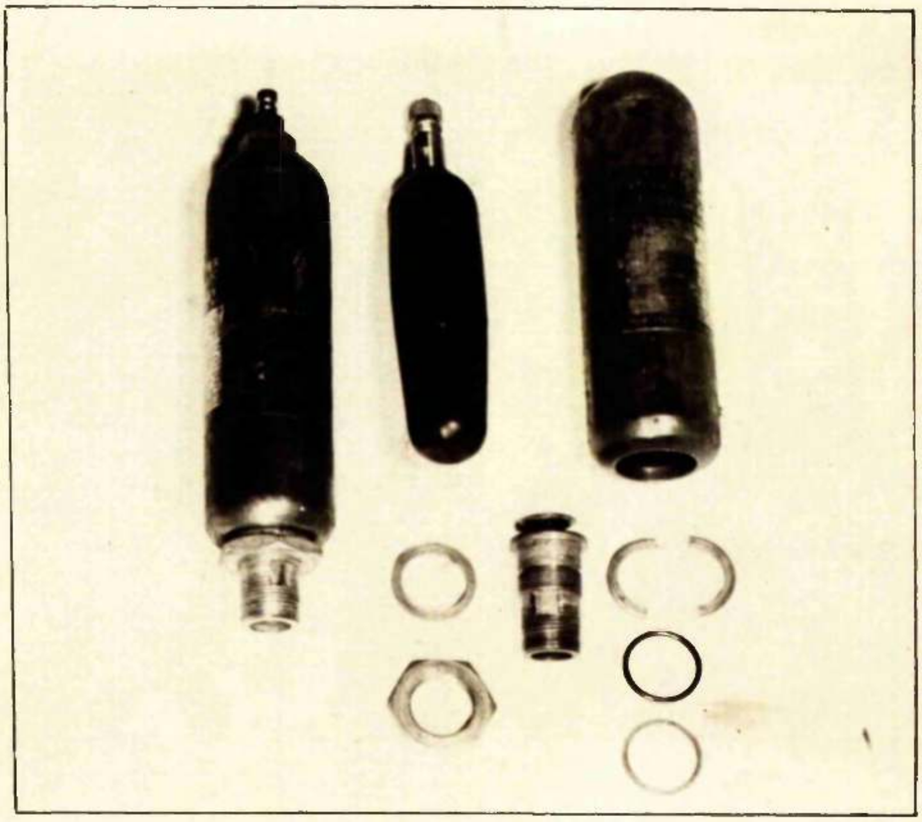

FIG. 42.

10 CU. IN. GREER ACCUMULATOR
& COMPONENT PARTS

7.8 GREER HYDRO-PNEUMATIC ACCUMULATOR

The test machine employs five Greer Hydro-pneumatic Accumulators; one quart size in the constant pressure make-up system, and four 10 cu.in. size, each forming part of a pulsator unit.

The component parts and operation of the accumulator are shown in fig.43, while a photograph of the 10 cu.in. size components and assembly is given in fig.42.

The accumulator body is made of a high quality steel seamless shell, capable of withstanding pressures up to 3000 lbs./in.^{2} with safety. Inside the shell is a neoprene rubber air or gas separator bag, with an integrally moulded valve which projects through one end of the shell. An efficient seal for the hole through which the valve projects is obtained by pulling the rubber and valve moulding hard against the internal surface of the shell, by means of a nut on the screwed outer body of the valve. The valve is of the Schraeder type usually found on the tubes of car wheels.

At the other end of the shell is a spring loaded poppet valve assembly, which, when open, provides a large area for unrestricted fluid flow.

The hole in the shell for the poppet valve body is sealed by a rubber O-ring assembly with split and pinned steel rings. In all sizes of accumulator above 10 cu.in. there is a small valve on the lower end of the poppet valve body for bleeding purposes. The lower end of this valve body is screwed female (1 quart size) or male (10 cu.in. size) for connection to a hydraulic system.

OPERATION

Consider the shell to be full of fluid and no air in the separator bag,

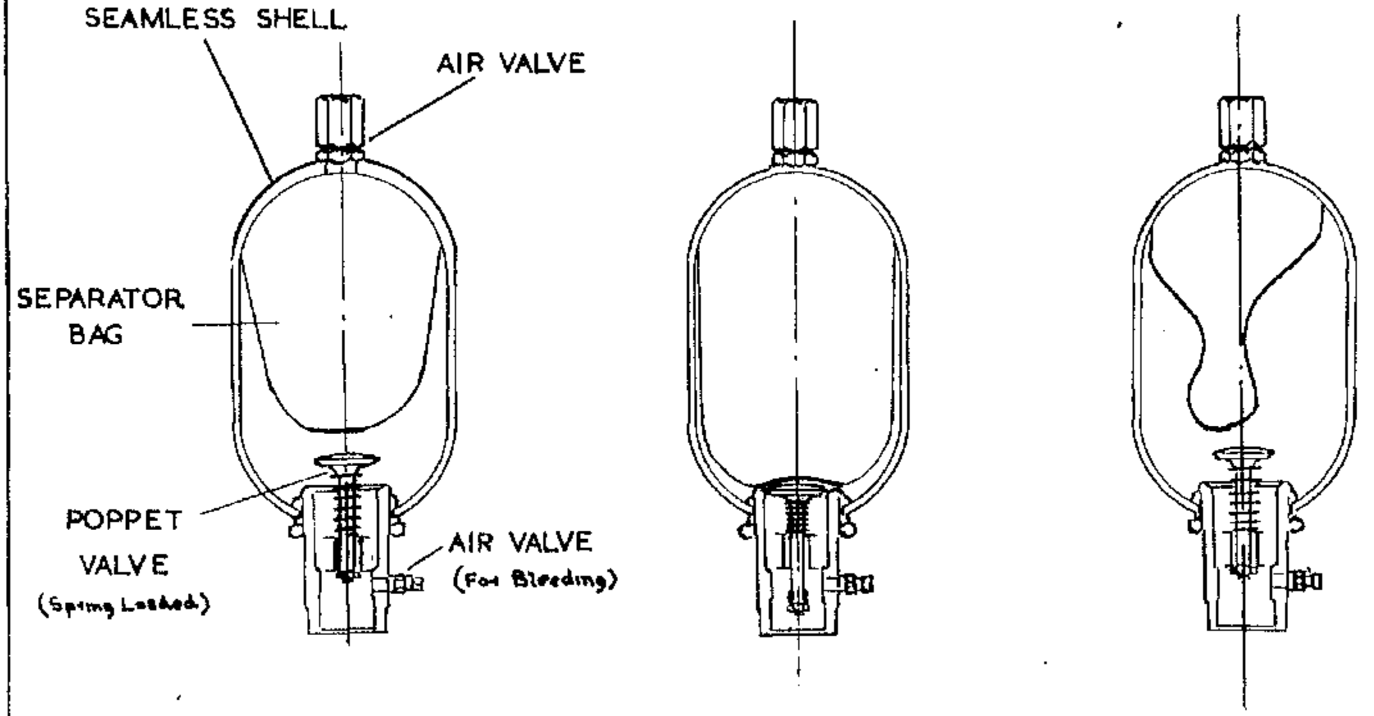

EMPTY ACCUMULATOR OPEN TO ATMOSPHERIC PRESSURE

ACCUMULATOR PRELOADED WITH GAS

GAS IN BAG COMRRESSED BY FLUID

FIG.43.

COMPONENT PARTS AND OPERATION OF GREER HYDRAULIC ACCUMULATOR so-called because it separates air from fluid. As air is pumped into the bag it expands and begins to fill the shell interior. The bag walls are specially moulded with varying thickness in order that as it expands it pushes the fluid out from one end, spreading along the shell wall and not permitting any fluid to become sealed between the bag and shell walls, except round the poppet valve seat. As it expands further, the bag pushes the spring loaded poppet valve into its seat, sealing off the flow of any fluid in or out of the accumulator.

As previously mentioned, some fluid is left in the shell between the lower end of the bag and the shell; this is termed "cushion fluid" since it acts as a cushion to the end of the bag, not permitting it to expand into the corners formed by the poppet valve and seal which could result in rupture.

The bag can now be pumped up to any desired pressure. If the pressure in the hydraulic system, into which the accumulator is connected, becomes greater than the preload pressure of the separator bag, the poppet valve opens, permitting fluid to enter and compress the bag.

7.9 PULSATOR ARRANGEMENT

The general arrangement of the four pulsators is shown in fig. 40.

The framework has been built up with mild steel channel and angle and is bolted to the main cast-iron base. An original arrangement gave too much overhang of the drive frame and stiffening angle has now been added.

The camshaft drive comes from a 3 H.P. 3-phase motor through a vee-belt drive to a flywheel and pulley on the shaft end. The motor is fitted with a starter and overload cut-out.

The shaft is supported in three Hoffman double roller self-aligning bearings, one of which is locked to prevent axial movement. At the opposite end to the drive a worm and wheel gives a 100 : 1 reduction drive for a revolution counter.

Balance weights have been calculated to give complete couple balance and equal vertical and horizontal force out-of-balance of the moving parts of the pulsators and these have been fixed at each end of the shaft.

The camshaft and bearings can be completely covered by a hinged aluminium splash cover while the motor and pulley drive has been fitted with a safety guard.

LUBRICATION

Early tests showed that the crosshead guides seized after a period of running if a constant supply of lubricant was not present. It had been hoped to run the guides in packed grease, but it soon became obvious that a drip lubrication was necessary.

Ordinary lubricating oil could not be used since this would fall down and contaminate the Lockheed brake fluid leakage from the pulsators. The high cost of this fluid made the collection of all leakage most desirable. Since the Lockheed fluid has a castor oil base it was decided to try using it as a lubricant and this has proved completely successful, there being no further seizure.

This drip lubrication has been combined with the constant pressure make-up supply system to give the arrangement now described.

7.10 MAKE-UP AND LUBRICATION ARRANGEMENT

A photograph of the arrangement is shown in fig.45 while it is shown diagrammatically in fig.46.

The small swash-plate pump is chain driven at slow speed from the camshaft through a reduction gear and pulley system. The pump pressure supply is fed to a modified three-way valve through a pressure gauge connection.

The three-way valve has two small spring loaded non-return valves fitted to two of the normal valve openings. One of these openings leads to the main system base pressure at the accumulator manifold, while the other, which has a screw control for the spring load on the ball, leads to four pipes supplying lubricant to the guides. The first valve requires a pressure load greater than the combined load of the base pressure and the spring to open it. When the system pressure falls this valve opens allowing fluid to flow and maintain the pressure. The second valve is in effect a relief valve and is adjusted to open at a pressure which is

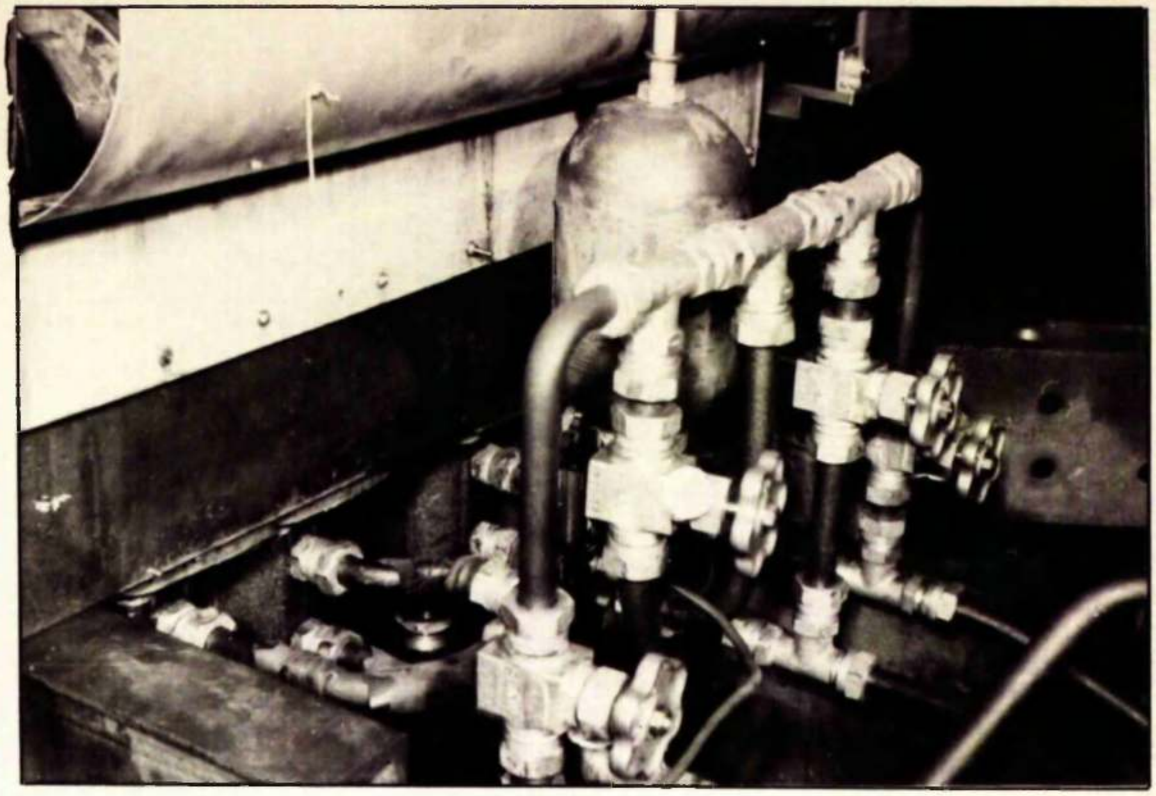

FIG. 44.

BY-PASS CONTROL VALVES & MAKE-UP ACCUMULATOR.

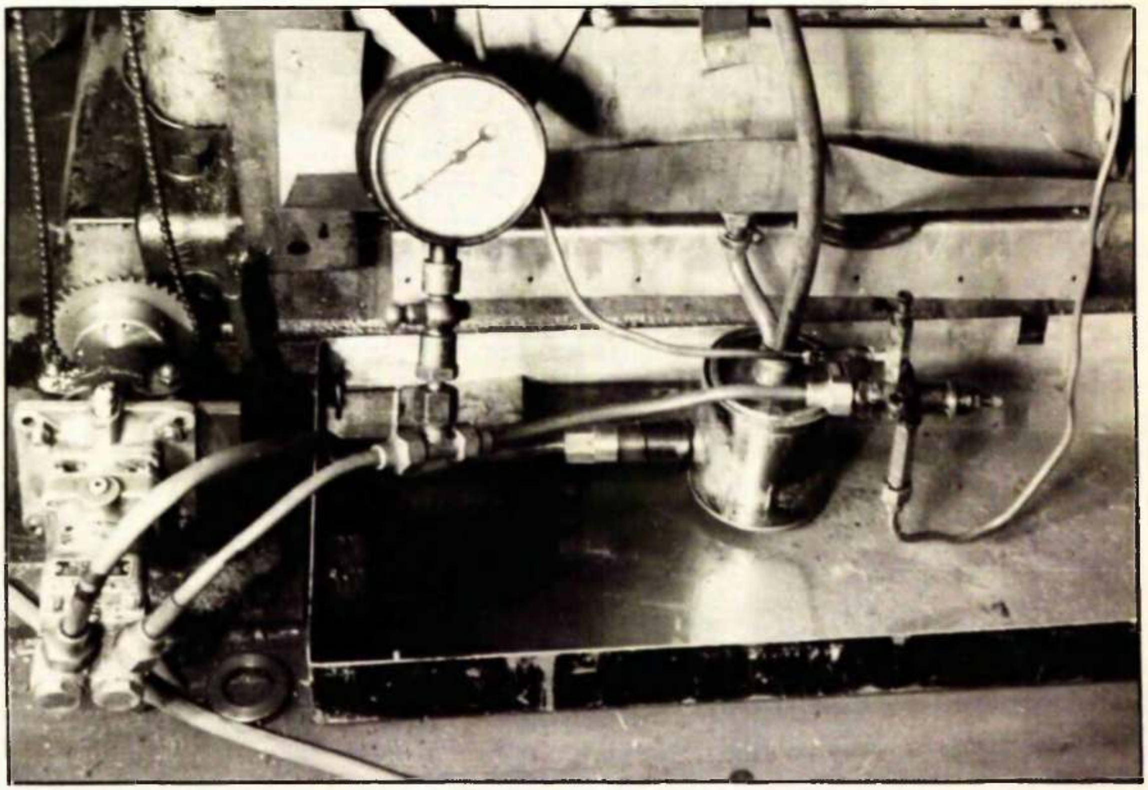

FIG. 45.

MAKE-UP & LUBRICATION ARRANGEMENT.

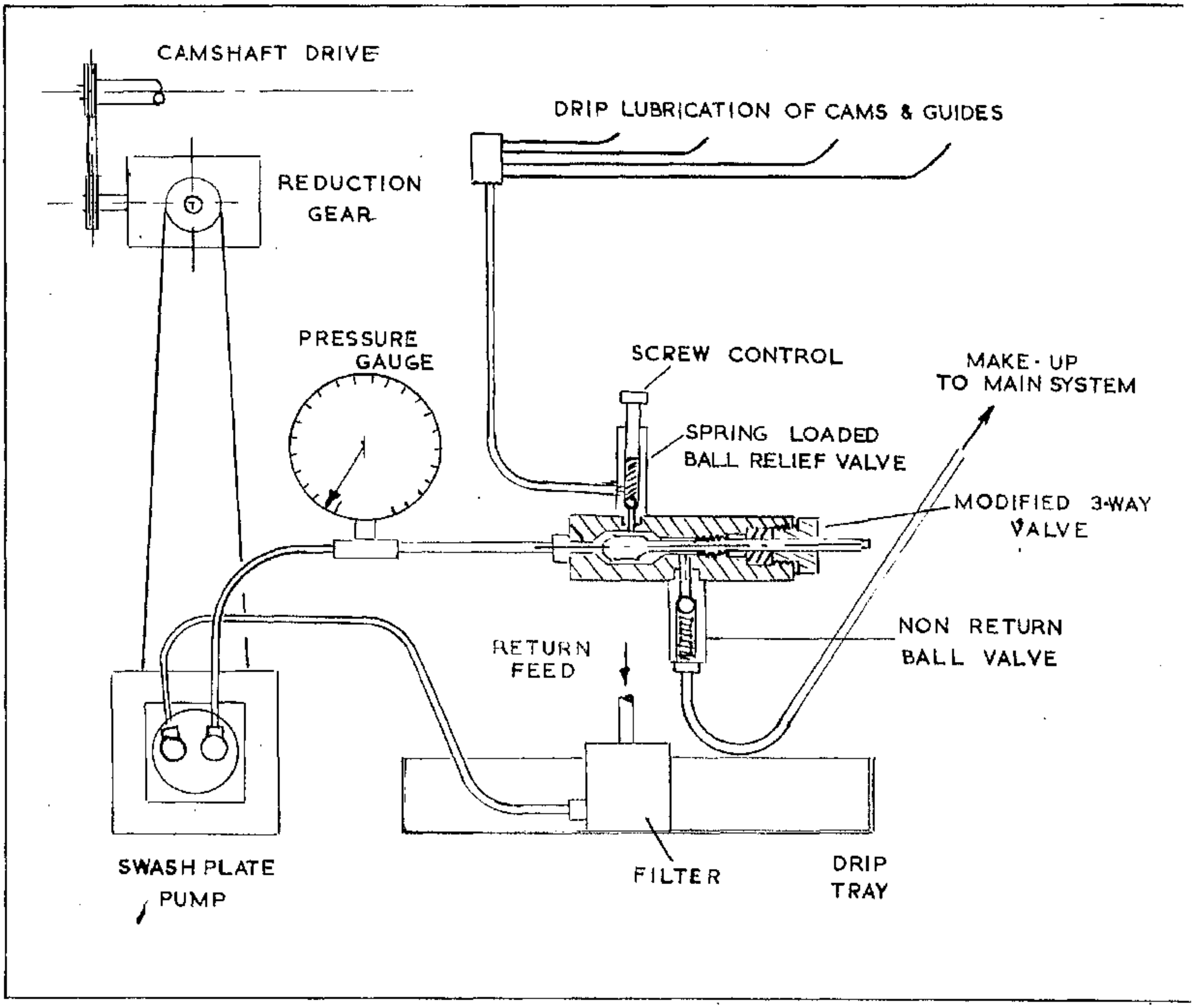

FIG. 46.

LUBRICATION AND MAKE-UP ARRANGEMENT
(DIAGRAMMATIC)

slightly less than that required to open the first valve when the system is at its normal base pressure. This relief valve is thus normally open supplying lubricant and only closes when the base pressure falls, opening the other valve. It can be adjusted to give any desired system base pressure and as the pump supply is always greater than the pulsator leakage a constant supply of lubricant is available at the cams and guides.

The original screw down control of the three way valve can be used to cut off the pump supply or the supply to the main system.

The lubricant from the cams and guides falls down into the pulsator box frame and is led through a return pipe and filter to the pump inlet. The box frame base has been sealed as far as possible by painting the joints of the pulsator bases and bolts with "Araldite" casting resin, with a hole left for the return pipe. A tray collects any leakage from the frame and is cleared periodically.

7.11 PIPING

All the pipes from the pulsators to capsules and make-up are of high pressure steel tubing 11/16 in. O.D. and approximately ⅝ in. diameter bore. The valves and connections for this piping are all "Ermeto" type.

All other piping is of ¼ in. O.D. high pressure copper tubing with "Simplifix" type connections and valves.

7.12 MACKLOW-SMITH CAPSULE

The Macklow-Smith Pressure Capsule or Hydraulic support has been designed to measure applied load, but in the test machine it has been adapted as a means of applying load.

Referring to fig. 47 the capsule is essentially a shallow cylinder having its piston or platen bonded to its walls by a flexible rubber joint. The space under the platen is filled by a fluid which, under pressure, applies a load to the platen and tends to make it move out under the control of the rubber bonding. If a restraint is provided such that practically no movement of the platen takes place, no load is taken by the rubber joint and the whole is transmitted by the platen.

The platen is virtually floating and tilts to accommodate eccentric loading which is resisted by a balanced shear in the joint on opposite sides, and in no way affects the application of the load.

The fluid space under the platen and the strength of the rubber in shear limits the amount of tilt which can be accommodated, and for larger values a cap and ball is used.

In the designed use of the capsule, the fluid cavity is connected to a pressure gauge and this closed system filled with fluid. When a load is applied to the platen, the fluid being practically incompressible, no movement takes place, and the joint takes no load. The pressure reading in the gauge gives a value which can be calibrated for known loads.

As the capsule is being employed as a load applying device, several modifications have been made. Two connections have been made to the fluid space:- one large diameter hole $\frac{5}{8}$" to permit free flow of fluid from the pulsator and one $\frac{1}{4}$" hole to measure the applied pressure

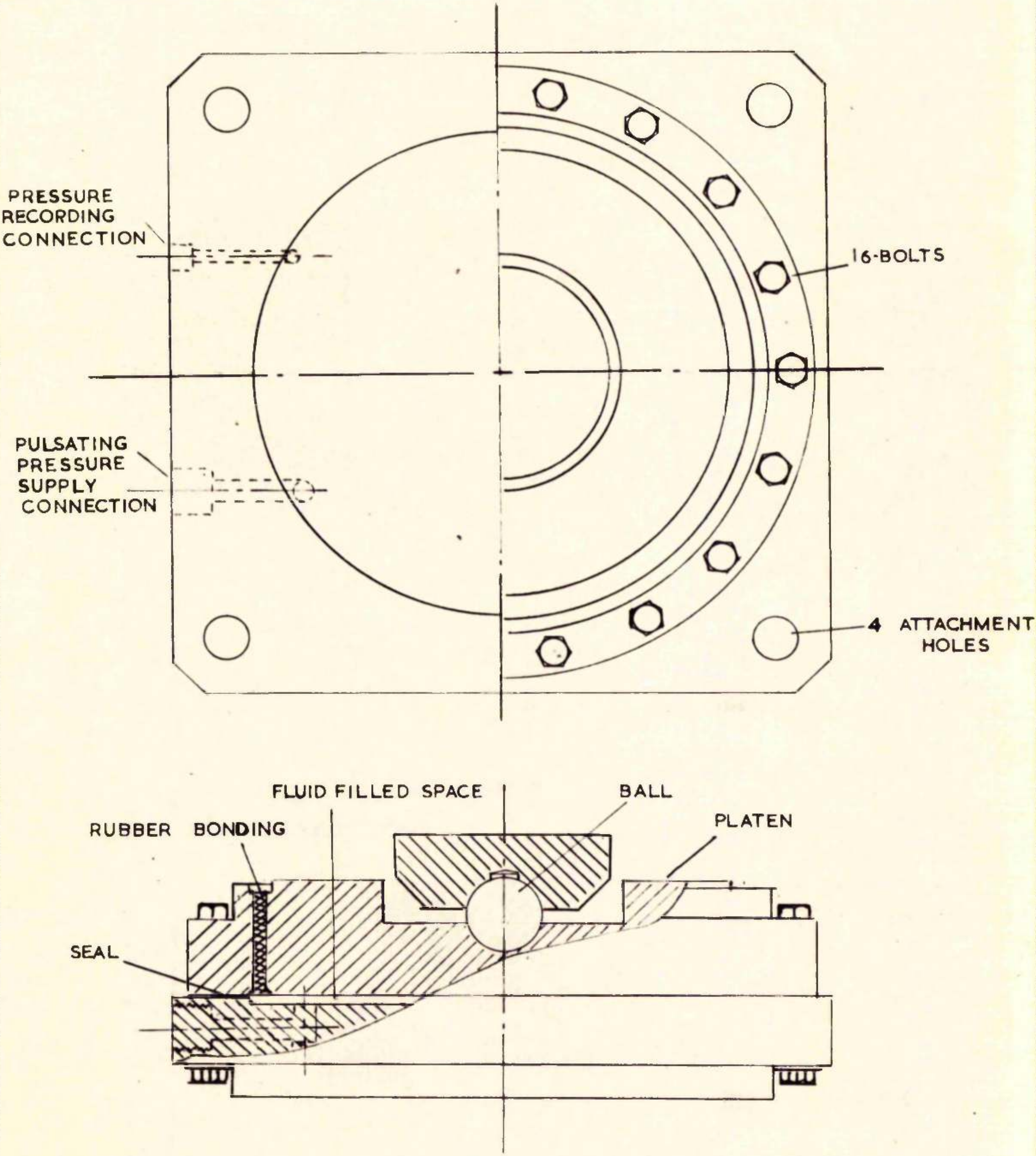

FIG.47.

MACKLOW-SMITH HYDRAULIC CAPSULE

SCALE — 1" = 2½"

via the pressure gauge, peak pressure indicator or pressure pick up.

Hence a pulsating pressure applied to the space supplies a pulsating load to the resisted platen and a calibrated pressure reading gives the value of this load.

The capsules may be supplied in all sizes from 500 lbs. up to 500 tons, and are of very rigid mild steel construction. The 4 capsules employed in the machine have an effective platen area of 50 sq.ins. and a rubber bonding giving a maximum permissible load of 20 tons at a pressure of about 900 lb./in.^{2} The depth of bonding governs the maximum pressure that is permissible.

The capsules have a specially designed square base with four $\frac{3}{4}$" holes for ease of mounting on the machine.

The natural rubber, which the makers prefer to use as a bonding material, necessitates the use of a non-harmful fluid such as Lockheed Brake Fluid which has a natural oil base.

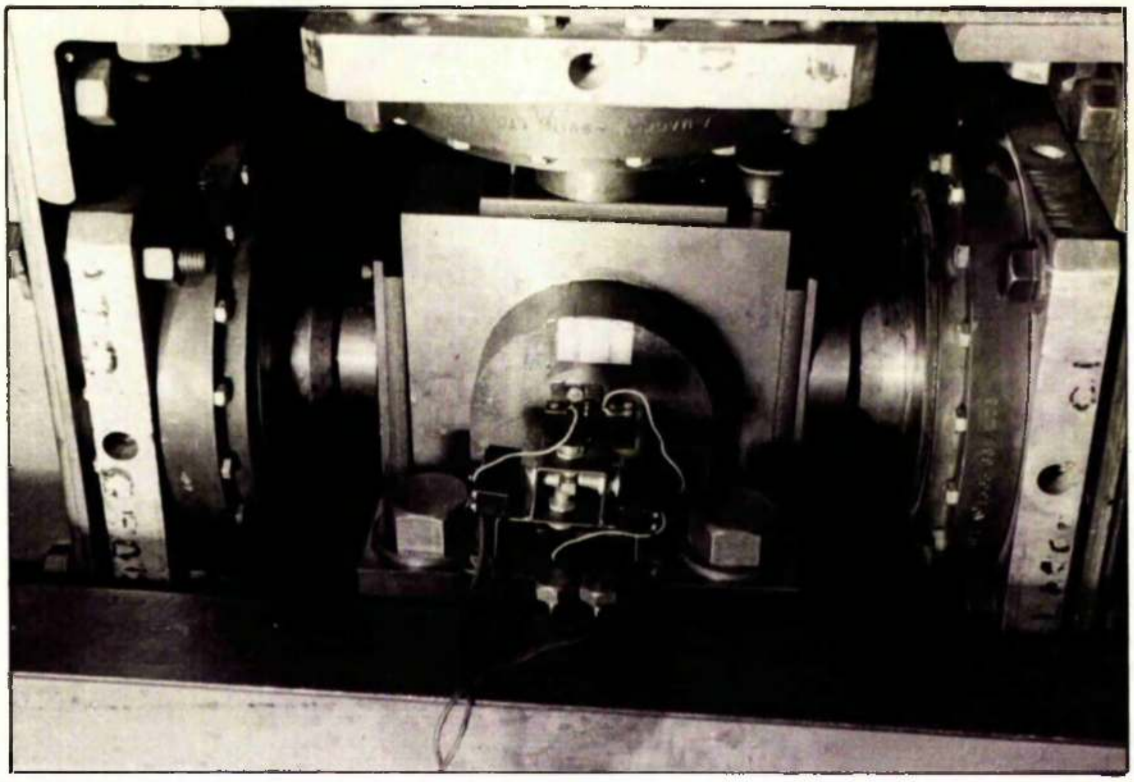

FIG. 48.
LOADING CAPSULES & BLOCK; ALSO DEFLECTION CUT-OUT.

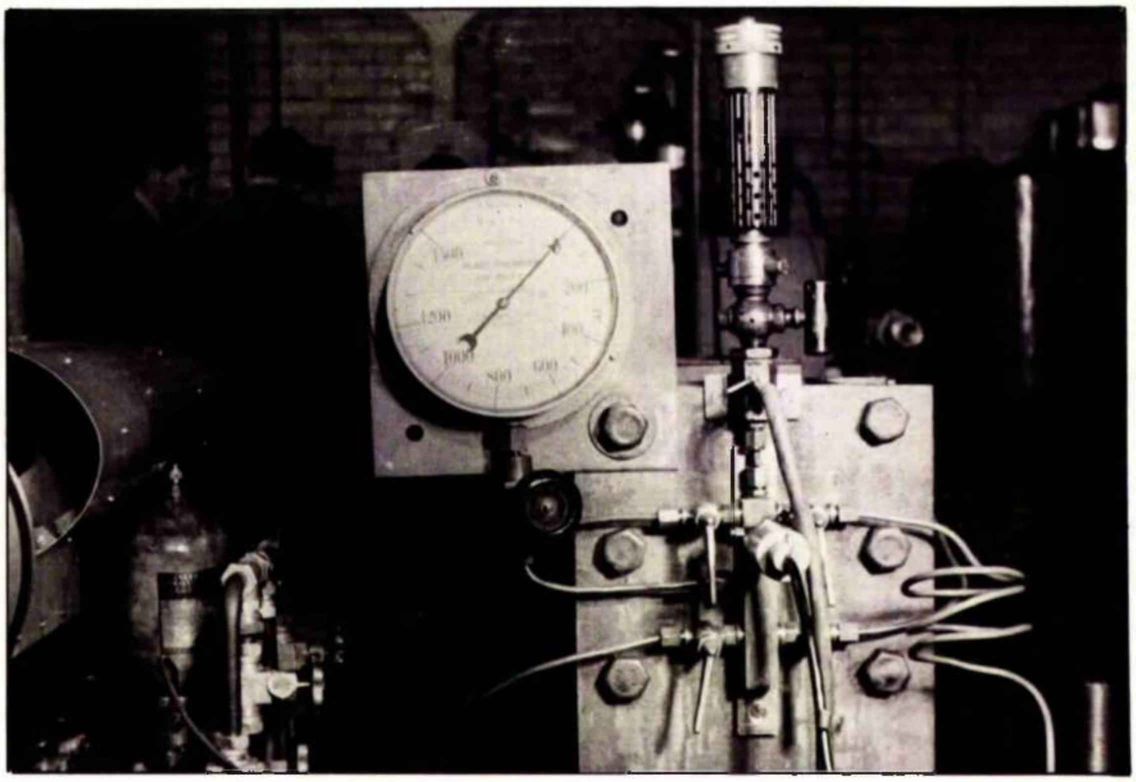

FIG. 49.
PRESSURE GAUGE, PEAK PRESSURE INDICATOR, C.A.V PICK UP & VALVE MANIFOLD.

7.13 DOBBIE-McINNES PEAK PRESSURE INDICATOR

This indicator is used in the hydraulic system to measure the maximum cycle pressures in each capsule and hence determine the maximum working load. The instrument has been designed essentially as an engine indicator but can be employed in hydraulic pressure measurement.

GENERAL DESCRIPTION

With reference to fig. 50, the upper end of the stainless steel bellows is screwed to the bellows unit and the lower end is fixed to the push rod. A system pressure compresses the bellows and raises the push rod and its spring seat against the resistance of the calibrated pressure spring so that the lift of the rod is a measure of the pressure. The top of the push rod has a left-hand thread carrying a conical nut which is urged to screw downwards on the rod by a clock spring. As the push rod rises, the nut is freed from its seat and is at once constrained by the clock spring to screw down again on to the seat, thus preventing the push rod from falling when the pressure falls. As the nut is part of the thimble unit, its rotation, which is a measure of the lift of the push rod, is read on pressure units on the graduated thimble. With normal pressure cycle speeds, there is not time for the nut and thimble to move the full distance in one cycle; hence the action is automatically repeated over the following cycles, each time getting nearer to the peak pressure. This accounts for the characteristic series of jumps of the thimble. In practice, the movement rapidly becomes so small as to be invisible after a few cycles, the number depending on cycle speed and rate of pressure rise.

DOBBIE - M^c INNES
PEAK PRESSURE INDICATOR

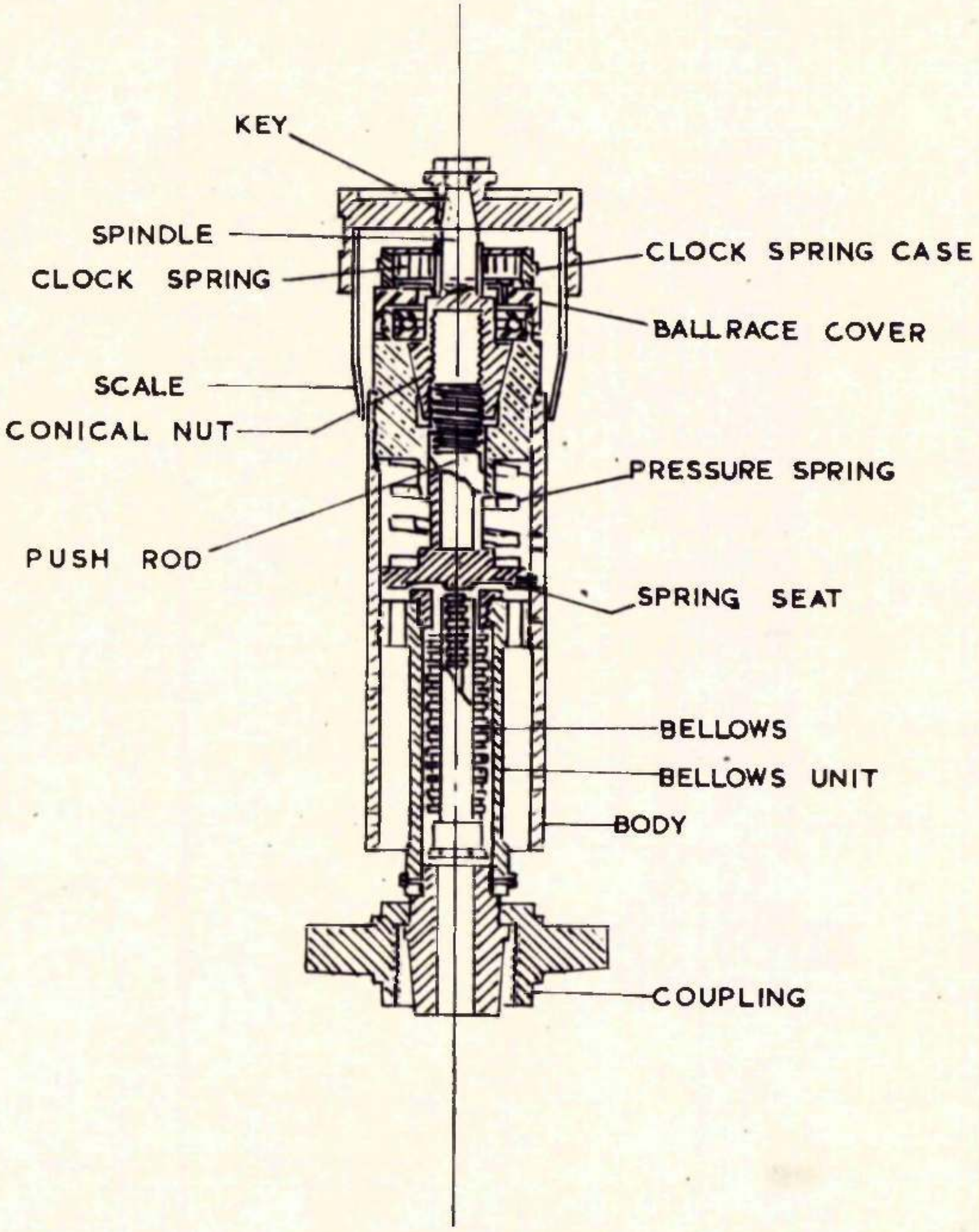

FIG.50.

The indicator is fitted to the pressure gauge manifold with a female core and coupling nut, through a normal engine indicator type of cock.

Complete satisfaction has been given by the operation of this instrument, although the pressure scale is much larger than is required with a corresponding loss of accuracy. The indicator calibration was checked statically, by turning the camshaft over slowly by hand and comparing the pressure gauge reading with the scale reading.

OPERATING INSTRUCTIONS

When using the indicator, the first step is to turn the thimble clockwise, to ensure that the instrument has been reset. The valve or cock is now opened SLOWLY and the thimble moves in small jumps to record the maximum pressure, opposite an index line on the body. A false reading may be obtained if the cock is opened suddenly and the thimble allowed to move in one or two big jumps.

The instrument should then be reset and the above procedure repeated to give a check. This is repeated for each loading capsule by using the corresponding valves on the manifold. When the recording is complete, the thimble should be reset in order that the spring is not left under load.

7.14 SAFETY CUT-OUTS

For long term testing of the type envisaged for the crank testing machine it is essential to have some safety device should any unforeseen failures occur, especially when it is unattended. Two devices, in addition to the motor overload cut-out, have been designed and fitted to the machine.

A. EXCESS MOVEMENT CUT-OUT (See fig.51)

This cut-out is designed to operate if the pressure in the hydraulic system should for any reason become excessive or should the crankshaft or any of the various members supporting it, fail.

The device is formed by four Burgess Micro-switches arranged at right angles to produce a limit of movement in four directions in the plane at right angles to the line of the crankshaft.

The switches are held in a sheet metal frame fixed to the top of one of the journal bearing blocks. A short length of square rod is fitted to the crank web and extends centrally through the space formed by the push-ends of the switches.

The micro-switches can be adjusted by means of lock nuts to operate at any desired movement of the square rod. The actual deflection to produce cut-out is measured by placing a feeler gauge between the rod and the push-end of the switch.

The four switches are wired in series with the hold-on coil of the motor starter. The switches do not make circuit again automatically and are fitted with a reset button.

B. LOW PRESSURE CUT-OUT (See fig.52)

There are many commercial minimum pressure cut-outs available but the

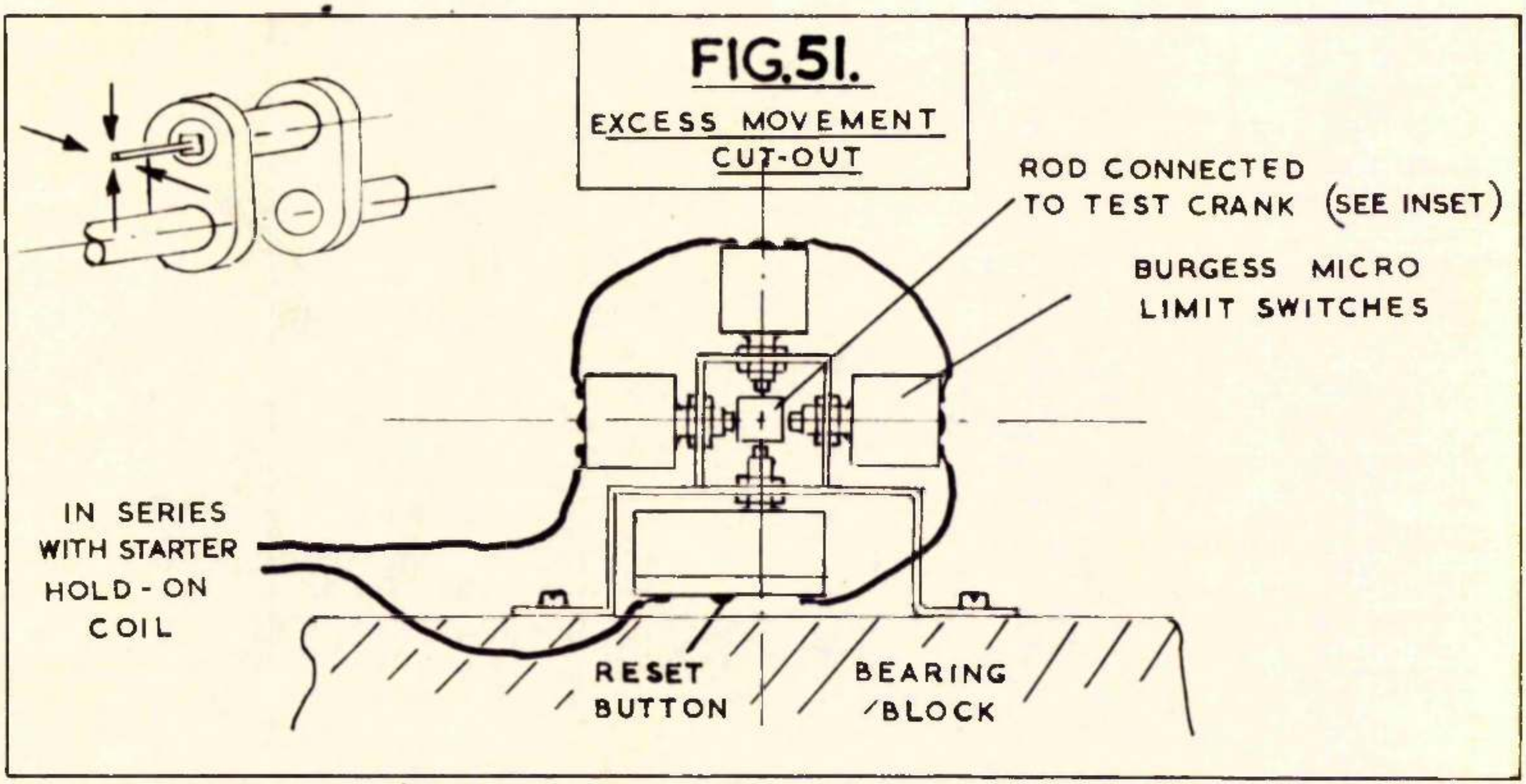

FIG. 51.

EXCESS MOVEMENT CUT-OUT

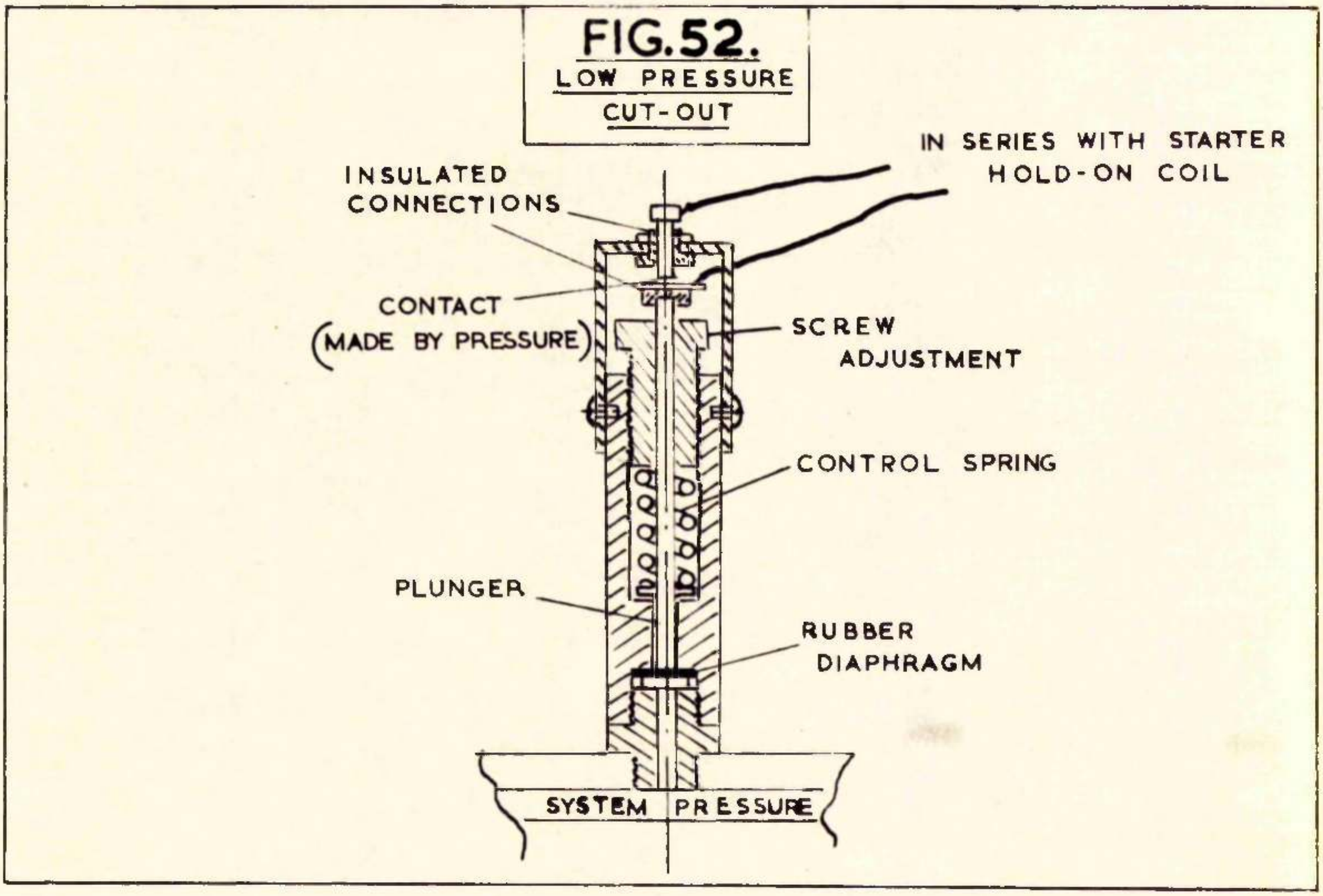

FIG. 52.

LOW PRESSURE CUT-OUT

SAFETY CUT-OUTS

FIGS 51 & 52.

one described here was made up quickly to enable a test to be completed and has proved satisfactory.

Referring to the diagram, when the system pressure is of such magnitude that it can overcome the spring load, the plunger moves upwards and makes contact at the insulated contacts, completing the series circuit with the motor starter hold-on coil.

The small rubber diaphragm is used to avoid leakage past the piston and provides sufficient movement to make and break the contacts. The small movement permitted by the contacts ensures that the diaphragm remains intact.

Should the system pressure for any reason fall below a predesigned value the spring load becomes greater than the pressure load on the plunger and contact is broken. The spring load can be controlled by a screw adjustment to give cut-out at any desired pressure.

SETTING

The cut-out was set to the correct cut-out pressure by putting the contact connections in series with a battery and light bulb with no spring load on the plunger. The system pressure was then pumped up to a value slightly below that required for the normal base pressure, noting the light go on. The spring adjustment was then screwed down until the light just went out. The system pressure was then increased until the light went on again. The cut-out pressure was checked by releasing the system pressure and noting at what value of pressure on the gauge the light went out on the way down. The cut-out was set to operate at a pressure some 20 lb./in^2 below the base pressure value.

7.15 BLEEDING THE HYDRAULIC SYSTEM

The presence of air in the hydraulic system of the test machine would introduce several difficulties and the complete system must be thoroughly bled. The air would have a similar effect to the air in the accumulator bags, reducing the maximum load capacity of the machine. In addition system air could readily find its way from one capsule circuit to another during a test, changing the loading cycle and giving non-uniform conditions.

The position of the ports in the capsules and the general configuration of the system makes bleeding somewhat difficult. Only the top capsule can be bled when connected up on the loading frame. The other three must be filled prior to fixing with the neighbouring piping connected. The pipe ends are sealed in order that the capsule may be lifted into position and, once bolted in position, the positioning of the pipes makes it possible to make the joints without any fluid escaping.

Assuming that there is no air in these capsules and immediate pipe connections, fluid can be pumped into the rest of the system with a joint cracked at the highest point in the by-pass valve assembly (see fig.44) to permit outflow of air. The pulsators are then turned over by hand letting fluid into every space and forcing air to flow to the cracked joint. When no further air bubbles appear from this joint the main section of the system can be assumed free of air and the joint made again. Finally the top capsule, being the highest port of the system, is bled. This is accomplished by pumping fluid through the supply pipe to the capsule and out through the pressure recording pipe to the valve manifold. A small glass section in the pressure release return pipe is observed until no further air bubbles are evident when the release valve can be closed.

Air may come out of solution during testing but this can mostly be made to collect in the high part of the by-pass piping by opening the by-pass valve occasionally. This part of the system is only connected to the make-up or base pressure manifold and any air in it will not affect the capsule loads when the by-pass valves are closed.

Air may come out of solution within the capsules and in the case of the lower three, could become locked. At present nothing short of removing these capsules and refilling will overcome this contingency. An additional bleeding port at an appropriate point in the capsule would overcome this difficulty and, indeed, considerably simplify all bleeding. At the time of building it was decided not to interfere with the sealing of the capsules by drilling an extra port but in view of the bleeding difficulties experienced it is now considered advisable.

7.16 MODEL CRANK SPECIMENS (See Fig. 53)

The dimensions of the model test crank for the first test have been scaled down from a single throw of a Marine Diesel crankshaft satisfying Lloyd's Rules. The shaft diameter is 3" and is completely built up, i.e. both journals and pins are shrunk in to the webs. The journals have a square section machined at fore and aft ends to permit the attachment of the torque take-off arms.

MACHINING

The webs were flame cut and rough milled to shape and the journal and pin holes rough bored in a lathe. The bores were finish bored on a mill with a boring head and then honed to size with a check on parallelism. The two webs were bored together making corresponding holes the same size and saving machining and setting-up time.

The pins and journals were turned and ground to size between centres with an allowance left on the part of the journals outside the web grip for trueing up after shrinking.

After shrinking the crank was set up in a lathe between centres and the journals machined to suit the bearing blocks. The journal ends were then milled to the square section required to fit the torque take-off arm boss.

SHRINKING

The webs were heated to a maximum temperature of 600°C (for the large fit allowance of 2.8×10^{-3}in. per inch) and allowed to soak for several hours. One journal and the pin were shrunk into the web and the assembly allowed to cool. The other journal was then shrunk in and the two webs placed on their side faces. While the second web was still hot the other end of the pin was shrunk in, the web sides providing a means of aligning

TEST CRANK SPECIMENS

FIG.53.

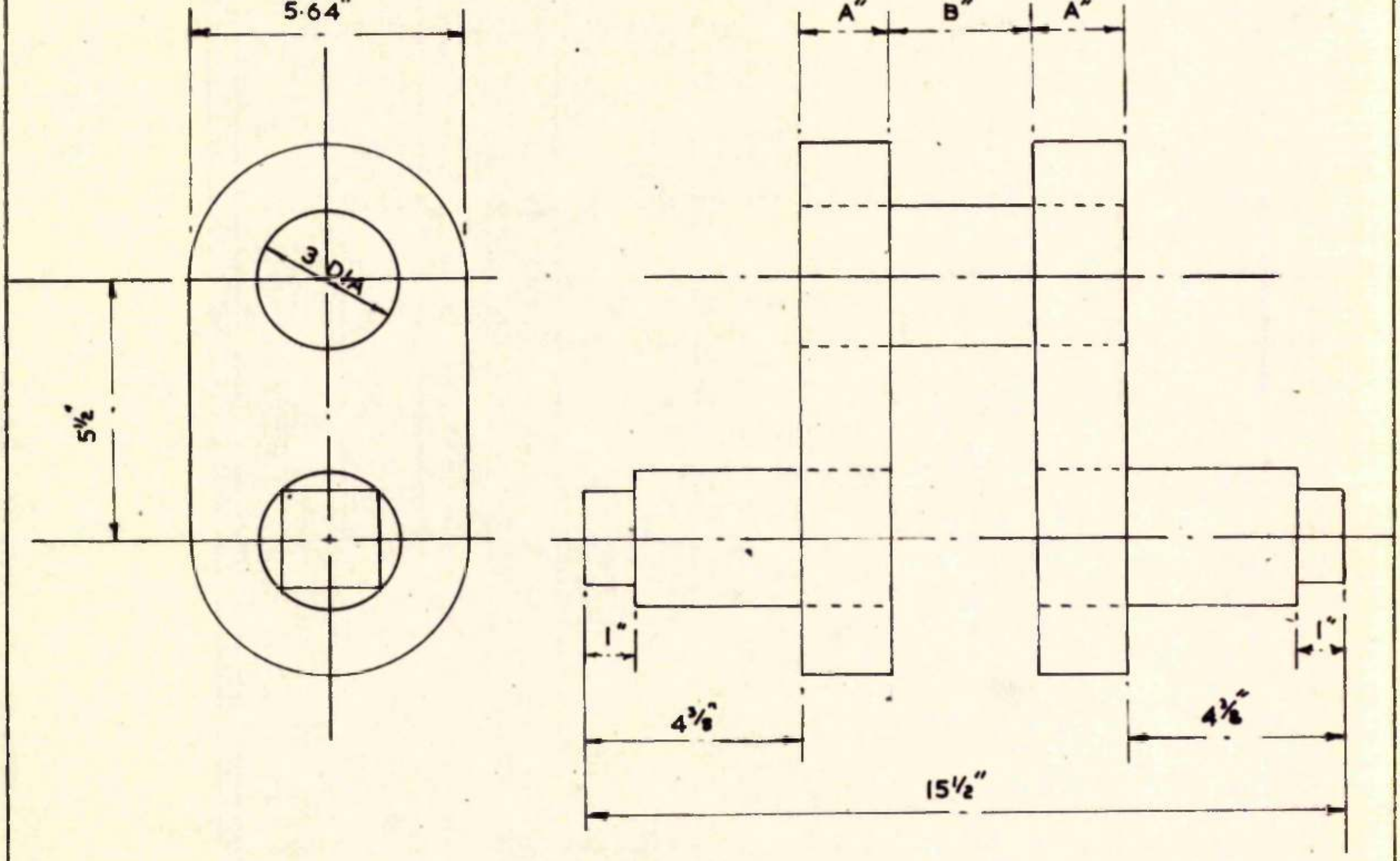

SPECIMEN Nº	NOMINAL FIT ALLOWANCE	DIMENSION		REMARKS
		A	B	
1	00028″/IN DIA	1·875″	3″	
2	0·0028/IN DIA	1·5″	3·75″	

the two journals. All shrinking was carried out with Sperm oil as a lubricant, being rubbed on the pin and journals with a soaked cloth just prior to shrinking.

7.17 TEST PROCEDURE

The well greased test specimen is placed in position in its bearings and the top halves bolted down making sure that the crank is free to move.

The two halves of the loading block are then bolted together on the crankpin. It may be necessary to rotate the crank slightly to get the block halves in position and bolted.

The torque arms are then attached at either end of the specimen, preventing any further rotation.

The cap, ball and distance pieces can now be placed between the capsules and the loading block. Some adjustment of the torque arms may be necessary, for the distance pieces on the side capsules to be fitted. In the case of the bottom capsule, it is important to note that the cap, ball, and long distance bar should be in position before the loading block is fitted.

The specimen is now ready in position and the torque arm connections can be given a final tighten up and the set screws on the square boss locked.

The excess movement cut-out (fig.51) is now fitted to the top of the bearing block and the four micro switches adjusted to give a suitable allowable movement before cut-out takes place. Feeler gauges may be used to achieve this position of adjustment.

Assuming the hydraulic system to have been filled and bled, air can then be pumped into the accumulators. The quart size make-up accumulator is filled with air at a pressure, half of that required for a base pressure, in order that there is a quantity of fluid in the accumulator.

The four pulsator accumulators are filled with a larger quantity of air

than will be eventually required during test, e.g. an initial pressure of 100 lb./in.^{2} might be given to the bags.

The system can now be pumped up to its base pressure by the hand pump, and the low pressure cut-out adjusted as already described.

With the by-pass valves open, the pulsators should be turned over by hand to ensure free movement of the pistons. Having shut off the pressure gauge, the motor can now be started.

The machine is then running under no load conditions. To apply pulsator loads to the capsules the by-pass valves are closed. The maximum pressure in each capsule can then be noted on the Peak Pressure Indicator, and the air quantity in the pulsator accumulator adjusted till the desired value is reached. All the air should not be expelled from the accumulator as this results in fracture of the neoprene bag.

Before loads are applied it should be noted that the make-up and lubrication pump is operating satisfactorily and the revolution counter has been zeroed.

During the test, readings of maximum pressure should be noted regularly and accumulator air quantities adjusted if necessary.

7.18 RUNNING-IN TESTS

Initial tests on the machine soon showed that the profiled cams, giving the theoretically correct gas and inertia loading cycle on the crank, were not satisfactory. Despite large spring and fluid pressure return loads on the cam follower loss of contact occurred at the design running speed of 500 r.p.m. giving heavy knocking.

In order that an adequate speed of testing might be obtained the cams were modified to a form giving a straight-forward sinusoidal pressure variation similar to that examined in the initial test-rig (see fig.31A). In this way maximum loads similar to those obtainable with the first set of cams, could be applied; the loading cycle was not, of course, of the true theoretical form. It was considered unlikely that shape of loading curve would affect the results, the maximum cycle load being thought the critical factor. The sinusoidal cams provided smooth running conditions which, with care, could be maintained for long periods.

The running-in trials showed that the original design figure of 9 Tons maximum loading could just be reached when the vector loads of two capsules were summed. The maximum loads in the torque producing capsules fell short of the expected figure although it had been anticipated that the specimen and resisting torque arm stiffnesses would limit these loads. In general it was realised that a solid construction loading frame would have led to much greater scope in loading.

7.19 MODEL CRANK TEST NO.1

Although the No.1 crank specimen had been used for the running-in trials at various loads it was decided that it should be subjected to a period of testing under maximum load conditions. Load readings from the Peak Pressure Indicator were taken at regular intervals and average values for the four directions are shown in the sketch above Table 12 .

On the completion of 1.5×10^6 reversals of loading the specimen was removed and examined. The crank was then dismantled by boring out the pin and journals to fine shells and pushing them out in a hand press. The web bores were carefully examined and remeasured.

7.20 NO.1 TEST RESULTS

Table 12 has been drawn up to summarise the test results.

It is at once obvious that there has been no bellmouthing tendency, the bores having remained perfectly parallel. There has been a loss of fit but this is consistent with the fit loss due to overstrain caused by the excessive shrinkage allowance of .0028 in/in. diameter.

The one striking feature of the web bores was the fretting which had occurred within the web grip. This fretting extends for 180° round the journal bores at the entry to each grip, extending to a maximum depth of ¼" at that part of the bore nearest the crankpin (see fig.56 and diagram Table 12). The fretting is exactly the same in both webs.

It is interesting to note that a similar effect occurring with the same pattern and in the same grip region was observed in a marine crank examined after 18 years' service(42). It was possible with this crank to push a feeler between the web bore and the pin for some depth at the fretted region. Although this was not possible with the test crank, it is thought that

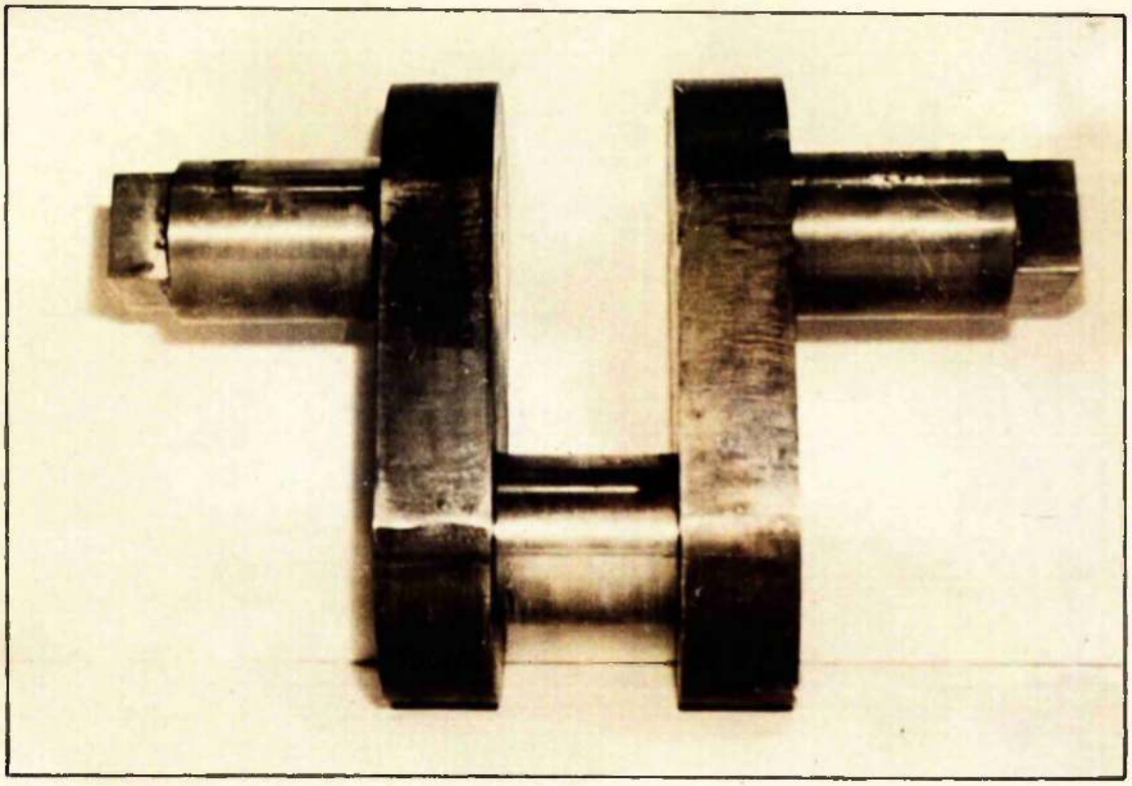

FIG. 54.

TEST CRANK SPECIMEN ~ BEFORE TESTING

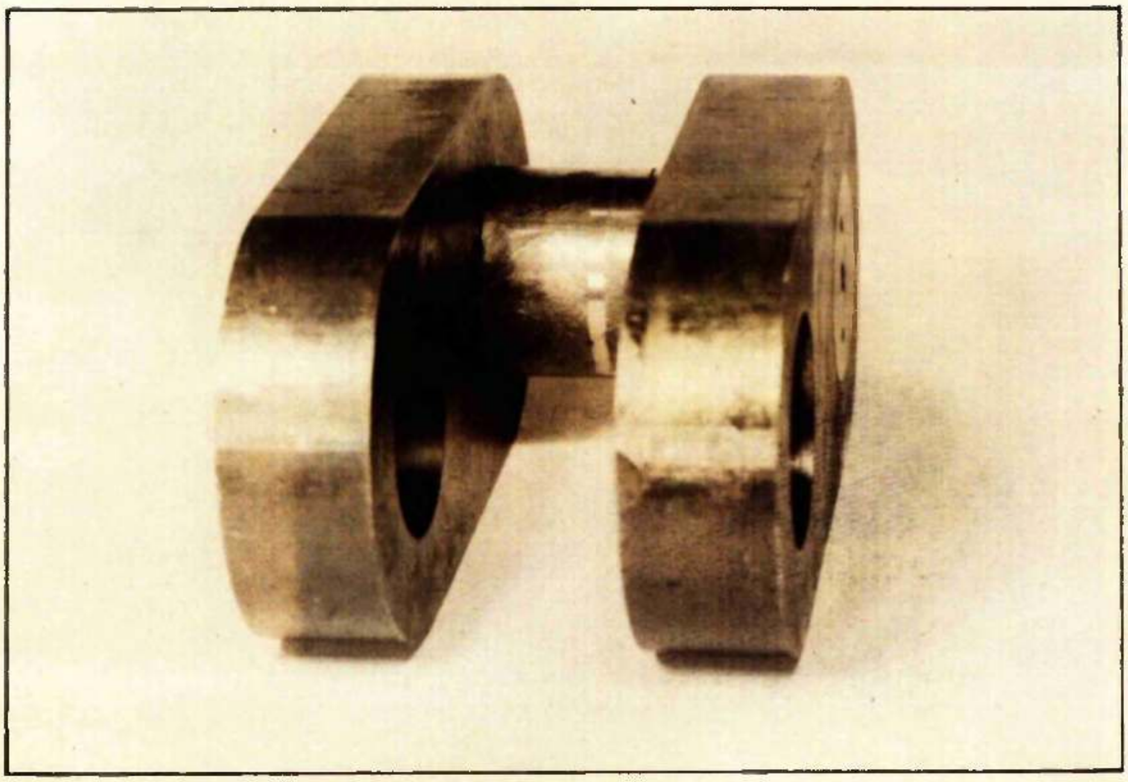

FIG. 55.

TEST CRANK SPECIMEN ~ AFTER TESTING

JOURNAL PINS REMOVED

continued loading would eventually produce a comparable loss of fit. Local measurement showed that over the fretted portion the diameter was on average some .0003" greater than the maximum web bore diameter. It is thought that this internal (i.e. within grip) fretting results from minute local slip which occurs at the entry to the web under the action of combined bending and torsional loading. The grip entry is a region of extreme stress concentration and slip is inevitable when the shear stress associated with the friction grip is exceeded. It is significant that the fretting occurred in the two grips under maximum torsional load, while the obvious directional effect is in the plane of the maximum bending load. It is thought likely that fretting occurs right round the grip but in some regions is too insignificant to be observed.

A further possible explanation of the fretting is that it is caused by the web flexture. Under pulsating bending loading the web flexes and produces a momentary reduction or elimination of the shrinkage pressure over the zone marked out by the fretting. This would permit slip to take place under the action of an applied torque giving rise to fretting conditions. This would explain the directional nature of the effect (i.e. the preference plane of flexture) and its evidence only being found in grips subjected to torque. Although the web flexture may also cause a reduction of shrinkage pressure on the inner (or crankpin) side of the journal grip, no torque action can reach through the grip to produce slip.

If the web flexture does, indeed, produce such a result it is anticipated that a thinner web would give even more pronounced fretting under the conditions of increased flexture. The results of the second test on the test machine with a reduced grip crank are anticipated with interest.

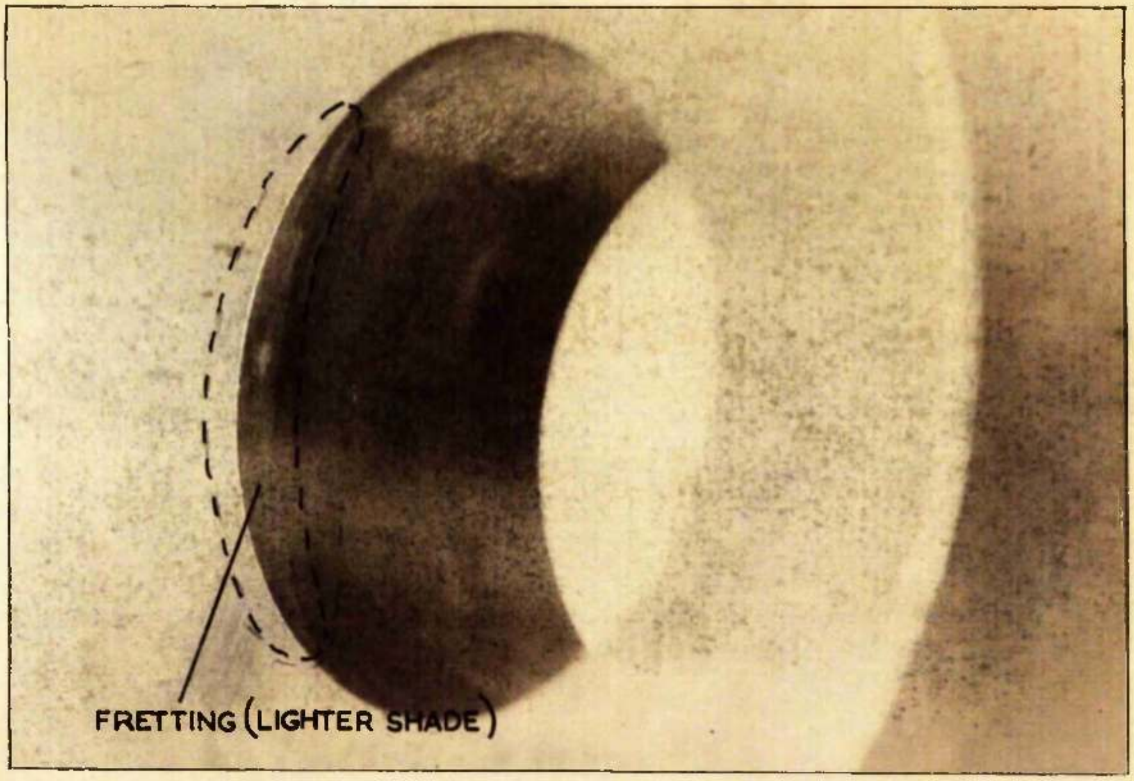

FIG. 56
INTERNAL GRIP FRETTING

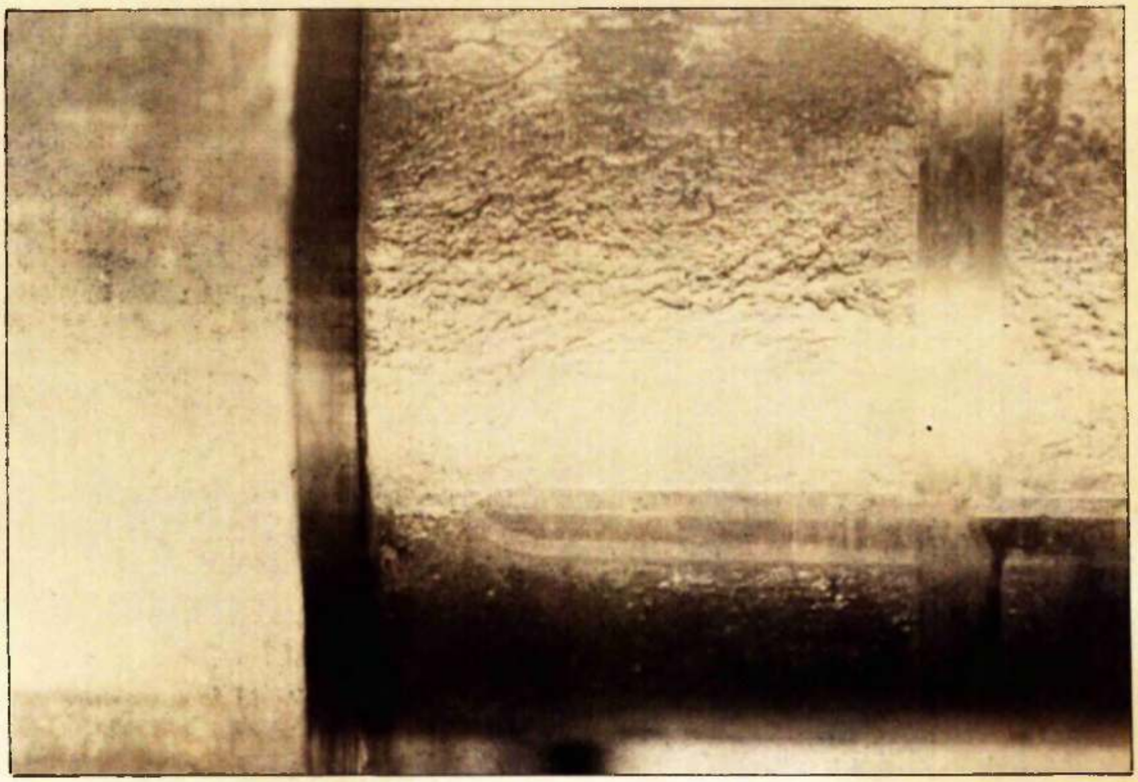

FIG. 57
EXTERNAL PIN FRETTING

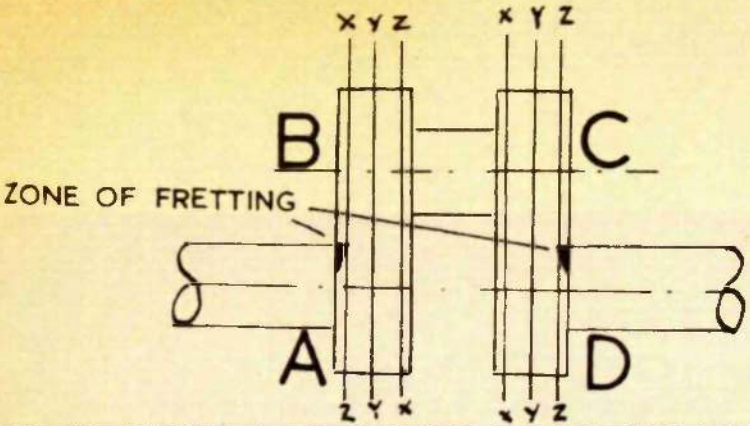

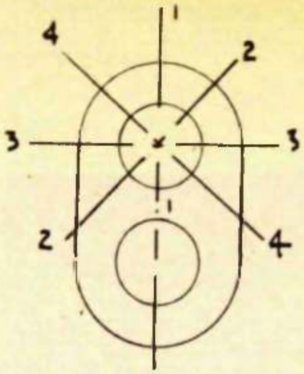

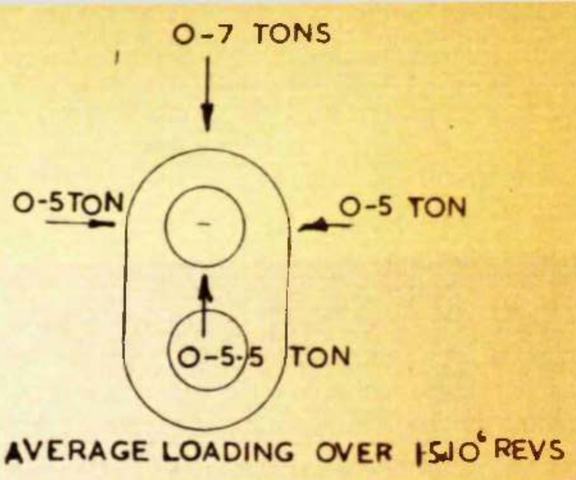

AVERAGE LOADING OVER $1{\cdot}5 \, 10^6$ REVS

WEB BORE	AXIAL PLANE	NOMINAL SIZE OF BORE 1-1 BEFORE	1-1 AFTER	2-2 BEFORE	2-2 AFTER	3-3 BEFORE	3-3 AFTER	4-4 BEFORE	4-4 AFTER	AVERAGE WEB BORE & PIN SIZE INCHES BORE BEFORE	BORE AFTER	PIN	INITIAL FIT ·001 IN./IN. DIA	FINAL FIT ·001 IN./IN. DIA	LOSS OF FIT ·001 IN./IN. DIA	REMARKS
A	X	-8·6	-3·8	-8·6	-4·0	-8·9	-3·7	-8·8	-3·7	2·9913	2·9958	2·9987	2·5	1·0	1·5	
	Y	-8·6	-4·4	-8·6	-4·4	-8·8	-4·0	-8·7	-4·1							
	Z	-8·6	-5·0	-8·6	-4·6	-8·8	-4·3	-8·8	-4·4							
B	X	-8·3	-6·1	-8·8	-62	-8·9	-6·1	-8·5	-6·4	2·9916	2·9946	2·9990	2·8	1·8	1·0	
	Y	-8·2	-6·4	-8·7	-65	-8·8	-6·3	-8·3	-6·5							
	Z	-8·1	-6·4	-8·5	-6·6	-8·2	-6·2	-8·0	-6·4							
C	X	-8·7	-6·2	-8·8	-6·4	-9·1	-6·0	-9·0	-6·2	2·9912	2·9940	2·9986	2·5	1·5	1·0	
	Y	-8·7	-6·3	-8·8	-6·3	-9·0	-5·8	-8·9	-6·3							
	Z	-8·7	-60	-8·8	-5·9	-8·9	-5·3	-8·8	-5·7							
D	X	-10·4	-7·3	-10·3	-7·2	-10·5	-6·8	-10·3	-7·0	2·9896	2·9926	2·9976	2·7	1·7	1·0	
	Y	-103	-7·6	-10·3	-7·6	-10·5	-7·2	-10·3	-7·5							
	Z	-10·6	-7·9	-10·6	-7·9	-10·6	-7·3	-10·6	-7·7							

TABLE 12.

MODEL N°1 TEST RESULTS

Fig. 57 shows that the pin and journals suffered considerably from overall fretting outside the grip, despite efforts to keep them well lubricated. Various anti-fretting compounds were tried, without much success, at various stages as the "creaking" associated with the fretting was heard.

This fretting was interesting as it illustrated very clearly the considerable damage which can take place in a comparatively short time when conditions of slip and high load are present.

A satisfactory solution to this problem was not found and it was found necessary to fit the test machine journal and pin blocks with replaceable hardened bushes to prolong the life of the rig.

A possible solution which came to mind later is that of wrapping the pin and journals with a thin layer of polytetrafluorethylene, a low friction material, which is recorded(45) as having proved successful in combatting fretting.

7.21 MODEL CRANK TEST NO.2

A second specimen was prepared with the same shrinkage allowance as the first (.0028 in/in.dia) but with a reduced web thickness. It was hoped thereby to initiate or accelerate any bellmouthing tendencies associated with the type of loading supplied by the machine.

Modifications to the test machine delayed the commencement of this second test and no results are available.

8. GENERAL DISCUSSION AND CONCLUSIONS

In this report some emphasis has been placed on a greater understanding of the mechanism of bellmouthing of built-up crank webs and it would appear that several factors have been brought to light that help to this end.

The investigation has shown that the following may be a possible pattern for the development of bellmouthing:-

Excessive combined bending and torsional loading on a grip results in bending "slip" taking place. The effect of this slip is to produce an increase in radial pressure, of cape and corner form, within the web grip. This cape and corner loading will act cyclically on the material of the web which can be in an elastic or an elastic-bounded plastic condition, depending on the shrinkage allowance.

The stresses involved are high and opening out at each side, or bellmouthing, of the web will result as the overstrained material develops a permanent loss of fit in the plane of the bending action. This gradual loss of fit leads to a reduction in friction grip and, ultimately, complete failure by torsional slip.

The fundamental quantity in the problem is clearly the friction grip which must be capable of withstanding combined torsional and bending loading without slip.

Perhaps the most interesting feature revealed by the investigation was that bending moment can impose a load on the friction grip; a value of moment can be applied, either alone or in combination with torsional loading, which will produce bending "slip" in the grip.

High stresses arising from torsional vibration have in the past been considered in many cases to be the cause of slipped pins. The study on combined torsional and bending loading has indicated that high bending

stresses could equally contribute to a failure-by-slip condition. A grip design should be based on an expression which caters for the combined effect of both types of loading.

Under conditions of combined bending and torsional loading it would seem possible that once bending slip took place the grip would immediately fail in torsion. This would make bellmouthing or the gradual opening out of the web impossible. This need not be the case, however, as the combined torsion and bending results have shown. The bending slip only produces a change over from friction to radial pressure loading conditions, without affecting the torsional grip strength.

The friction grip being a direct function of both friction coefficient and shrinkage pressure indicates that high values of both these quantities should be aimed at.

High friction coefficients are readily available if care is taken that the mating surfaces are dry and free from film. Chemically dry surfaces give coefficients as high as 0.8. It is recommended that crank builders should make every effort to prepare mating surfaces more thoroughly than the "shop-dry" condition of normal present-day shrinking practice. Even under the usual shop conditions of crank manufacture, some special care in this direction could show increases of 100% or more in the friction grip strength. Many crank manufacturers base their grip design on a safe value of coefficient of 0.2; with the special care mentioned this figure could be considered very conservative.

Length of grip, or web thickness, has been shown to be a critical factor in the cause or cure of bellmouthing. Grip lengths based on Lloyd's Rules would certainly seem to give adequate strength provided the shrinkage is good. On the question of whether web thicknesses could be reduced,

the small scale fatigue tests indicated that L/D ratios of 0.5 or even lower would be satisfactory, provided care was taken to obtain a high friction coefficient.

The effect of time on the friction coefficient of an operating crank web is not known although suggestions have been made that oil seapage within the grip could produce a reduction in its value. If in fact there are factors leading, through time, to a reduction in friction strength, bellmouthing could readily be associated with a duration effect when, in fact, the bellmouthing had just started as moment slip took place under the reduced friction coefficient conditions.

Regarding the choice of shrinkage pressure, it has been shown(42) that a shrinkage fit has a maximum grip strength under axial or torsional static loading when the fit allowance is in the region of .0015 - .002 in/in diameter. Present day marine practice favours an allowance between .0012 and .0017 in/in. diameter. The present test results suggest that the higher end of this range should be chosen.

It is of interest to note that assembly stiffness is not affected by excessive shrinkage allowances when subjected to bending; fits of .004 in/in. diameter showed no significant difference from those of .002 in/in. diameter.

Bearing wear-down is another factor which could readily lead to failure by bellmouthing. Increased bearing clearances will lead to increased bending stresses which automatically increases the likelihood of bending moment "slip". This association of bearing wear-down with web slip is one which is not unusual when service cranks have been examined.

The onset of bellmouthing must necessarily produce a change in stiffness of a crank member. This, in turn, will result in a change in

vibration characteristics affecting the original stresses and producing a re-orientation of force actions. This may well throw a greater strain on another part of the system, releasing the bellmouthed web from the hazard of immediate failure.

The model crank testing machine has shown itself capable of producing effects on a small scale crank similar to those found in an actual crank after many years service. From the findings of the complementary work on the small scale static and fatigue tests, however, it would seem unlikely that the test machine has the loading capacity to produce an example of bellmouthing. Future tests will be conducted on cranks with a reduced web thickness which will increase the possibility of its initiation.

The effect of fretting within the grips of the crank tested is interesting since it shows that slip does occur at the grip entry. Although this slip is extremely small and arises mainly from the torsional loading, it will leave the pin or journal free to flex within the grip, producing a form of bellmouthing at one side of the web only. This could be a progressive effect leading to complete bellmouthing but it would appear to be of a very long-term nature and of secondary importance to the serious loss in fatigue strength due to the fretting. This problem has been well covered by many researchers and it is generally agreed that, where possible, the geometry of the crank should be altered to prevent or limit the high stress concentration causing fretting at the entry to the grip. Such measures as relieving of the web at pin entry or a radiused shoulder or notch in the pin have all been found successful in increasing fatigue strength by limiting fretting.

Some main points for built-up crank design and manufacture may be summarised from the conclusions as follows:-

(1) To prevent bellmouthing and grip failure by slip in general, the friction grip design should be based on an expression which covers combined torsional and bending effects.

(2) A high value of friction coefficient should be aimed at - chemically cleaned mating surfaces provide the best value.

(3) The fit allowance should be chosen to provide high interface pressure; fits between .0015 and .002 in/in. diameter are considered suitable.

(4) Provided high friction coefficients are obtainable, web thicknesses could be reduced without affecting the strength of the crank.

(5) High stress concentrations, particularly those giving rise to fretting, should be limited, where possible, by suitable design.

9. BIBLIOGRAPHY

Several of the references in the alphabetically listed index given below are not mentioned in the text of the thesis. These are quoted as they contain much relevant information on the subject of the research and provide excellent background reading.

(1) Allen D. N. de G. and D. G. Sopwith:
The Stress and Strains in a Partly Plastic Tube under Internal Pressure and End-Load.
1951 Proc. Royal Soc. Series A. Vol. 205, p. 69.

(2) Barton 1931:
Circular Cylinder with a Band of Pressure on Finite Length of Surface.
Trans. A.S.M.E. Vol. 63.

(3) Baugher J. W.:
Transmission of Torque by Means of Press and Shrink Fits.
Trans. A.S.M.E. Vol. 53. Paper M.S.P. 53-10, pp. 85-92. 1931.

(4) Coker E. G. and R. Levi:
Contact Pressures and Stress Distributions in Cams, Rollers and Wheels.
Proc. Inst. Mech. Eng. Vol. 1, pp. 693-730. May 1930.

(5) Coker E. G. and R. Levi:
Force Fits and Shrinkage Fits in Crank Webs and Locomotive Driving Wheels.
Proc. Inst. Mech. Eng. Vol. 127, p. 249. 1934.

(6) Cook 1931:
Yield Point and Initial Stages of Plastic Strain in Mild Steel Subjected to Uniform and Non-Uniform Stress Distributions.
Phil. Trans. Royal Soc. A. Vol. 230.

(7) Cook 1934:
The Stresses in Thick-Walled Cylinders of Mild Steel Overstrained by Internal Pressure.
Proc. I. Mech. E. Vol. 126.

(8) Cook 1938:

Some Factors Affecting the Yield Point in Mild Steel.

Trans. Inst.Eng. & Ship. of Scotland. Vol. 81.

(9) Cook and Robertson 1911:

Strength of Thick Hollow Cylinders under Internal Pressure.

Engineering. Vol. 92, p. 786.

(10) Cook and Robertson 1913:

Transition from the Elastic to the Plastic State in Mild Steel.

Proc. Royal Soc. A. Vol. 88.

(11) Cornelius H:

Zeitschrift für Metallklinke.

Vol. 36, p. 101. 1944.

(12) Dorey 1931:

Some Factors Affecting the Size of Crankshafts for Double Acting Diesel Engines.

Trans. N.E.C. Eng. & Ship. Vol. 47, p. 229.

(13) Dorey D. S:

Strength of Marine Shafting.

N.E.Coast Inst. of Eng. & Ship. May-June 1935.

(14) Dorey D. S:

Large Scale Torsional Fatigue Testing of Marine Shafting.

Inst. of Mech. Eng. 1948.

(15) Dwight:

Tables of Integrals and Other Mathematical Data.

Elliptic Functions. P. 771.

(16) Goloff A:

Determination of Open Loads and Stresses in Crank Shafts.

Proc. Soc. Exp. Stress Analysis. Vol. 3, p. 132.

(17) Gadd C. W. and N. A. Ochiltree:

Full Scale Fatigue Testing of Crank Shafts.

Proc. Soc. Exp. Stress Analysis. Vol. 3, p. 150.

(18) Gleitz K:

Fatigue of Large Diesel Crankshafts.

Die Technik P.97. Berlin March 1952.

(19) Gough:

Engineering Steels under Combined Cyclic and Static Stress.

Presidential Address - Inst. Mech. Eng. 1949.

(20) Hetenyi M:

Handbook of Exp. Stress Analysis.

P. 643 and in general.

(21) Hirst G. W. C:

See Melbourne Symposium.

(22) Horger O. J:

A.S.M.E. Handbook - Metals Engineering Design.

P. 178 - Press fitted assembly. P. 123 - Cold working.

(23) Horger O. J. and W. I. Cantley:

Designs of Crankpins for Locomotives.

J. Applied Mech. Pp. A17-A33. March 1946.

(24) Horger O. J. and J. L. Maulbetsch:

Increasing the Fatigue Strength of Press Fitted Axle Assemblies by Surface Rolling.

J. Applied Mech. Vol. 58, p. A-91. Sept. 1936.

(25) Horger O. J. and C. W. Nelson:

Design of Press and Shrink Fitted Assemblies.

J. Applied Mech. Vol. 4, No. 4, pp. A183-A-187. Dec. 1937.
Vol. 5, No. 1, pp. A32-A36. March 1938.

(26) Huggengerger A:

Die Fesligkeit der Presselzverlundung mit Zylindrischer Sitzflache.

Lokomotiv und Maschinenfabrik Winterthur, Switzerland 1926.

(27) Lehr and Skiba:

Torsional Fatigue Testing Apparatus for Large Components.

Engrs. Digest 1945. Vol. 6, p. 85.

(28) Lehr & Ruef:

Fatigue Strength of Crankshafts of Large Diesels.

Engrs. Digest 1944. Vol. 5, p. 285.

(29) MacGill C. F:

A Record of Pressed Fits.

Trans. A.S.M.E. Vol. 35, p. 819. 1913.

(30) MacRae R:

Overstrain of Metals.

(31) Melbourne Symposium 1946:

Failure of Axles. Fatigue Failures in Steel Industry, etc.

In particular work of G.W.C. Hirst and discussion.

(32) Oldberg S. and C. Lipson:

Structural Evolution of the Crankshaft.

Proc. Soc. Exp. Stress Analysis Vol. 3, p. 118.

(33) Peterson R. E. and A. M. Wahl:

Fatigue of Shafts at Fitted Members with a Related Photoelastic Analysis.

J. App. Mech. Vol. 57. P.A.-1 March 1935.

(34) Rankin A. W.

Shrink-fit Stresses and Deformations.

J. App. Mech. Vol. 11, No. 2, pp. A77-A85. June 1944.

(35) Russell R:

Factors affecting the grip in Force, Shrink and Expansion Fits.

Proc. Inst.Mech.Eng. Vol. 125, p. 493 1933.

Abstracted in The Engineer Vol. 156, p. 604. 1933.

and in Engineering Vol. 136, p. 706. 1933.

(36) Russell R:

Contact Film Resistance in Rail Wheel Force Fits.

Journal of R.T.C. Vol. 3, Pt. 3. 1935.

(37) Russell R:

Influence of Film and Time on Force and Shrink Fits.

Trans. Inst. of Eng. & Shipbuilders in Scotland Vol. 80 1937.

[illegible]
[illegible]

([illegible]) [illegible]
[illegible]
[illegible]

([illegible]) [illegible]
[illegible]
[illegible]
[illegible]
[illegible]
[illegible]

([illegible]) [illegible]
[illegible]
[illegible]

([illegible]) [illegible]
[illegible]
[illegible]
[illegible]

([illegible]) [illegible]
[illegible]
[illegible]

([illegible]) [illegible]
[illegible]
[illegible]

([illegible]) [illegible]
[illegible]

([illegible]) [illegible]
[illegible]
[illegible]

([illegible]) [illegible]
[illegible]
[illegible]

([illegible]) [illegible]

(38) Russell R:

Experimental Studies on Crankshaft Stiffness.

Journal of R.T.C. Vol.4, Pt. 3. Jan. 1939. P. 467.

(39) Russell R. and Shannon:

The Limit of Grip due to Force Fits and its Increase by Cold Working.

Journal of R.T.C. Vol. 2, Pt. 2. 1930.

(40) Savin:

Research on Force Fits.

American Machinist. Vol. 68, p.889. 1928.

(41) Steele M. C. and Young J:

An Experimental Investigation of Overstraining in Mild Steel Thick-walled Cylinders by Internal Fluid Pressure.

Trans. A.S.M.E. Vol. 74, p. 355. 1952.

(42) Thomson A. St., Scott A. W. and Moir C. M:

Shrink-fit Investigations on Simple Rings and on Full-scale Crankshaft Webs.

Proc. Inst. Mech. Engrs. 1954. Vol. 168. No. 32.

(43) Waterhouse R. B:

Fretting Corrosion.

Proc. Inst. Mech. Eng. 1955. Vol. 169. No. 59.

(44) Werth:

Velocity of Pressing in Assembly and Effect of Fluctuating Loads.

Reported in A.S.M.E. Handbook. P. 187.

(45) Wood J. K:

Crankpin Design for Electric Locos.

American Machinist. Vol. 62, pp. 989-992. June 1925.
(American Edition).

(46) Recent Publications

International Conference on Fatigue of Metals.

Inst. of Mech. Eng. in co-operation with The American Soc. of Mech. Eng. London 1956.

10.

APPENDIX

APPENDIX

1. FRICTION COEFFICIENT CALCULATIONS

(A) PURE BENDING

EXAMPLE Series 1A Graph Page - 45

$L/D = .45$ Fit $\Delta = .001''$/in.dia. $D = 1\frac{1}{2}''$

CALCULATION

From graph, at friction moment slip, value of bending moment $M_f = 2.1$

From equation 9, Art. 4.4. -

$$M_f = \mu P_s DL\,(D + L/2)$$

$D = 1\frac{1}{2}''$ P_s (From Lame for $\Delta = .001''$/in.dia.) $= 5T/in^2$

Hence;

$$\mu = \frac{M_f}{P_s DL(D + L/2)}$$

$$= \frac{M_f}{P_s D^3 (L/D)(1 + \frac{1}{2}L/D)}$$

$$= \frac{2.1}{5 \times 1\frac{1}{2}^3 \times .45(1 + \frac{.45}{2})} = .226$$

(B) BENDING AND DIRECT LOAD

EXAMPLE Series D Graph Page - 58

$L/D = .71$ Fit $\Delta = .002''$/in.dia. $D = 1\frac{1}{2}''$ $d = 6''$.

CALCULATION

From graph, at friction moment slip, value of bending moment at hub face $M = 5.3$ in.Ton

Total slip moment $M_f = M + VL/2$ at grip centre

or, since $M = V \times d$ where d = moment arm to hub face

$$M_f = M + \frac{ML}{2d} = M\left(1 + L/2d\right)$$

$$\text{Thus } M_f = 5.3 \;\; 1 + \frac{.71}{2} \times \frac{1\frac{1}{2}}{6} = 5.6$$

From equation 9, Art. 4.4

$$M_f = \mu P_s DL (D + L/2)$$

$$P_s \text{ (for } \Delta = .002''\text{/in.dia)} = 9T\text{/in.}^2$$

Hence: $$\mu = \frac{M_f}{P_s DL\ (D + L/2)}$$

$$= \frac{5.6}{9 \times 1\tfrac{1}{2} \times .71 \times 1\tfrac{1}{2}\ (1\tfrac{1}{2} + \frac{.71 \times 1\frac{1}{2}}{2}\ )}$$

$$= .191$$

(c) BENDING - DIRECT AND TORSIONAL

EXAMPLE Series E Graph Page - 61

$L/D = .4$ Fit $\Delta = .001''$/in.dia. $M/T = 1$

$D = 1\tfrac{1}{2}''$ $d = 6''$

Calculations are based on bending slip or torsional slip.

At bending slip equation 22 is applied, i.e.

$$M_e = \sqrt{M^2f + T^2} = \mu P_s DL\left(D + L/2\right)$$

From graph $M = 1.3$ in. Ton

$$M_f = M + VL/2 = M\left(1 + L/2d\right)$$

$$= 1.3 \times 1.05 = 1.37$$

$$T = 1 \times M = 1.3$$

$$M_e = \sqrt{M_S^2 + T^2} = \sqrt{1.37^2 + 1.3^2} = 1.91 \text{ in.Ton}$$

$$\mu = \frac{M_e}{P_s DL\ \ D + L/2}$$

Ps (from Lamé for $\Delta = .001''$/in.dia.) = 5T/in.²

Hence: $$\mu = .236$$

At torsional slip equation 21, art. 4.9 is applied:

$$T_e = \sqrt{M_f^2 + T^2} = \mu \frac{P_s \pi D^2 L}{2}$$

M_s is assumed to remain as before since this value is the maximum bending moment which can be carried by friction forces, i.e. further moment is carried by radial pressure effect.

From graph torque T at torsional slip = 2.5 in.Ton

As before, M_f = 1.37 in.Ton

Hence: $T_e = \sqrt{M_f^2 + T^2} = \sqrt{2.5^2 + 1.37^2} = 2.84$ in.Ton

$$T_e = \mu \frac{P_s \pi D^2 L}{2}$$

$$\mu = \frac{2T_e}{P_s \pi D^2 L} = .259$$

2. <u>YIELD CONTACT PRESSURES</u>

(A) <u>NO-FIT TEST</u>

<u>EXAMPLE</u> Series 1A Graph Page - 45

L/D = .45 Fit $\Delta = 0$ $D = 1\frac{1}{2}''$

<u>CALCULATION</u>

From graph, M at yield = 3 in.Ton

From equation 17, art. 4.7 -

$$M = \frac{P_c DL}{24}\left[\pi L + \mu\left(\frac{3\pi D}{2} + 2L\right)\right]$$

Hence contact pressure at yield P_c

$$= \frac{24M}{DL\left[\pi L + \mu\left(\frac{3\pi D}{2} + 2L\right)\right]}$$

μ is assumed = .2, an average figure for this type of fit.

Thus: $$P_c = \frac{24 \times 3}{1\frac{1}{2} \times .45 \times 1\frac{1}{2}\left[\frac{\pi \times .45 \times 1\frac{1}{2}}{3} + .2\left(\frac{1\frac{1}{2}}{2}\pi + 1\frac{1}{2} \times .45\right.\right.}$$

$$= 18.7 \ T/in.^2$$

(B) ELASTIC SHRINKAGE TEST

EXAMPLE Series 1A Graph Page - 45

$L/D = .45$ Tb $\Delta = .001''$/in. dia.

When the fit allowance is such that yield of the bore material does not take place during shrinkage, the contact pressure due to applied bending is calculated in two stages. These two stages take place after bending moment friction slip has taken place as the friction forces are assumed to carry all the applied moment up to this point.

1st Stage Redistribution of shrinkage pressure according to equation 2, Art. 4.3.

$$P_c = \frac{12M_R}{DL^2} + P_s$$

Study of fig. 1 shows that this can only hold up to a value of applied moment when $P_c = 2P_s$. Thereafter there is no shrinkage pressure to redistribute.

The moment to produce this condition is calculated from equation where $P_s = 5T/\text{in.}^2$ (from Lamé) and

$P_c = 2P_s$

Hence: $M_R = \dfrac{5\pi DL^2}{12} = .9$ in.Ton

2nd Stage From the graph - friction moment slip takes place at 2.1 in.Ton and yield at 4. in.Ton. Hence, the moment, additional to the first stage, to produce yield is given by:

$$4.0 - (2.1 + .9) = 1.0 \text{ in.Ton.}$$

This moment is assumed to be resisted according to the No-fit equation 17, Art. 4.7.

$$M = \frac{P_c D L}{24} \left[\pi L + \mu \left(\frac{2\pi D}{2} + 2L \right) \right.$$

Putting $M = 1.0$ in.Ton and assuming $\mu = .2$

$$\text{in } P_c = \frac{24M}{DL \left[\pi L + \mu \left(\frac{2\pi D}{2} + 2L \right) \right]}$$

gives $P_c = 6.2$ T/in.^{2}

From 1st Stage $P_c = 2P_s = 10$ T/in.^{2}

Thus Total P_c $= 10 + 6.2$

$= 16.2$ T/in.^{2}